DISSERTATION

STABLE KINETOCHORE-MICROTUBULE ATTACHMENT IS SUFFICIENT TO SATISFY THE SPINDLE ASSEMBLY CHECKPOINT

Submitted by

Eric Cary Tauchman

Graduate Degree Program in Cellular and Molecular Biology

In partial fulfillment of the requirements

For the Degree of Doctor of Philosophy

Colorado State University

Fort Collins, Colorado

Summer 2016

Doctoral Committee:

Advisor: Jennifer G. DeLuca

Chaoping Chen
Eric Ross
Carol Wilusz

ABSTRACT

STABLE KINETOCHORE-MICROTUBULE ATTACHMENT IS SUFFICIENT TO SATISFY THE SPINDLE ASSEMBLY CHECKPOINT

During mitosis, duplicated sister chromatids attach to microtubules emanating from opposing sides of the bipolar spindle through large protein complexes called kinetochores. The kinetochore proteins that bind spindle microtubules are exquisitely regulated to ensure correct segregation of genetic material at mitotic exit. Aurora B Kinase (ABK) phosphorylates Hec1, a protein that directly binds microtubules. This is critical for enabling the release of incorrect kinetochore-microtubule attachments. Hec1 has nine ABK phosphorylation sites on its tail domain allowing for precise control over binding affinity. We find that at least 7 of these sites are required for wild-type kinetochore-microtubule (K-MT) attachment stability as evaluated by inter-kinetochore distance measures and chromosome alignment capability. We further observe that several sites may have more influence on K-MT attachment stability than others. Hec1 mutations preventing phosphorylation increase kinetochore-microtubule attachment stability.

In the absence of stable kinetochore–microtubule (K-MT) attachments, a cell surveillance mechanism known as the spindle assembly checkpoint (SAC) produces an inhibitory signal that prevents anaphase onset. Precisely how the inhibitory SAC signal is extinguished in response to microtubule attachment remains unresolved. To address this, we induced formation of hyper-stable kinetochore–microtubule attachments in

human cells using a non-phosphorylatable Hec1mutant, a core component of the attachment machinery. This mutant reduced the ability of ABK to cause release of erroneous K-MT so we could test the hypothesis that stable K-MT attachments satisfy the SAC even if those attachments deviate from the canonical bipolar form. We find that stable attachments are sufficient to satisfy the SAC in the absence of sister kinetochore bi-orientation and strikingly in the absence of detectable microtubule pulling forces or tension. Furthermore, we find that SAC satisfaction occurs despite the absence of large changes in intra-kinetochore distance, suggesting that substantial kinetochore stretching is not required for quenching the SAC signal. These results indicate a conformational change(s), within the kinetochore that occurs upon stable kinetochore-microtubule binding causes the eviction of SAC proteins. This advance in our understanding of SAC function offers insight into the mode of action and the variation in cellular response to mitotic arrest therapies often used in treatments of cancers.

ACKNOWLEGEMENTS

I won't ever be able to properly thank the DeLucas for all they have done for me thoughout my PhD work. My lab work began with an assurance from Jake and then Keith put felt pads on a microcope. That marked one of the first times that I thought it could be okay. The hard, quality work balanced with some fun times will remain forever instilled. All my lab mates deserve my gratitude. Those former students are an integral part of who I am professionally as well as personally. These current students who ask fascinating questions and are a reminder of why I love science. And Jeanne who helped us all get it done. I'm proud to call all of you my friends.

Outside of the lab, Carol Wilusz was my first advisor during lab rotations, and I never really let her off the hook. Thank you for your insight, and the directness of delivery of that insight. Jim Bamburg and Laurie Minamide taught me much throught these years about things science and things more important than science.

Finally, I am grateful for my family and friends. Grateful for your support, but also for your understanding. It was never that I didn't want to visit or spend more time, I was just busy, super busy…and poor.

And though Jenny certainly counts as family, you get a special paragraph. This would not, *would not*, have been completed without you. Thank you for all your help, all the ski trips missed, your encouragement, and your understanding. You spent a lot of time in lab waiting while I "quickly" got something done or I ran to work for "about an hour". I owe you big for this one.

TABLE OF CONTENTS

LIST OF FIGURES

Chapter 1: Introduction

1.1 Mitosis

The most dynamic phase of the cell cycle is mitosis. During this time, the microtubule cytoskeleton dramatically reorganizes to form the mitotic spindle. Microtubule-nucleating centrosomes are apparent as a pair of foci which separate from each other while emanating microtubules reach to capture newly condensed chromatin in the form of readily-observed, threadlike chromosomes for which Walther Flemming devised the word mitosis (Kops et al., 2005b). During mitosis in mammalian cells (Figure 1), exact copies of approximately 3 billion nucleotide base pairs, encoding over 20,000 genes are perfectly divided into two cells. Proper division is ensured by the Spindle Assembly Checkpoint (SAC), the mitotic surveillance mechanism. The SAC monitors attachment of the mitotic spindle to chromosomes, but precisely what aspect of that attachment that is evaluated is uncertain.

Chromosomes attach to the microtubules of the mitotic spindle at the primary constriction of sister chromatids. The proteins of the Constitutive Centromere Associated Network (CCAN) positioned at this site guide the assembly of kinetochores during mitosis (Figure 2). Kinetochores are macromolecular protein assemblages that attach to dynamic microtubules (Figure 3) in highly regulated fashion. We were able to determine the requirements of SAC satisfaction through the use of a non-phosphorylatable mutant version of Hec1. Experiments using this mutant allowed erroneous kinetochore-microtubule attachments to persist, enabling the identification of minimum requirements of SAC satisfaction. Through the following experiments, we furthered our understanding of the SAC, and how cells are able to exit mitosis.

Following chromosome replication in S-phase, cells enter the G2 phase of the cell cycle. During this period of cell growth, expression of Cyclin B is increased (Porter and Donoghue, 2003). Cyclin B accumulation and its binding and activation of Cdk1 is essential for cells' entry into mitosis (Nurse, 1990; Figure 4) and upon sufficient activation of Cdk1 by Cyclin B, mitosis begins (Lindqvist et al., 2009). Active Cdk1 phosphorylates several substrates enabling the dramatic structural changes characteristic to mitosis. Phosphorylation of nuclear lamins (Peter et al., 1990) and nuclear pore complexes (Lusk et al., 2007) enables nuclear envelope breakdown. Phosphorylation of Condensin II initiates chromosome condensation (Abe et al., 2011) and phosphorylation of microtubule associated proteins contributes to the massive reorganization of the cytoskeleton in mitosis (Fourest-Lieuvin et al., 2006). Further, Cyclin B-Cdk1 activates the Anaphase Promoting Complex (Wieser and Pines, 2015). Cyclin B levels remain high until Spindle Assembly Checkpoint satisfaction and mitotic exit when it is degraded by the proteasome (Gavet and Pines, 2010; Figure 4).

Mitotic entry is marked by prophase. This phase of mitosis is illustrative of the changes incurred within the cell due to Cyclin B activation of Cdk1. Chromosomes are fully condensed, the bipolar spindle forms as the two centrosomes separate, and nuclear envelope breakdown ensues (Figure 1). Chromosome condensation enables organization of genetic material such that it may be divided appropriately between daughter cells. The breakdown of the nuclear envelope permits association of chromosomes with microtubules that provide force for chromosome alignment and subsequent segregation.

1.2 Spindle Assembly

Newly devoid of the nuclear envelope, the chromosomes of prometaphase cells can associate with microtubules (Figure 1). Microtubules (MTs) are dynamic polymers comprised of α- and β-tubulin heterodimers. Both α- and β-tubulin monomers bind Guanosine Triphosphate (GTP) which is hydrolyzable in the β subunit, but not the α subunit (Nogales et al., 1998). Tubulin dimers bind to form elongated protofilaments which bind laterally to form the tubular microtubules. Subunit addition to a microtubule occurs at the β-capped, plus end preferentially to the α-capped, minus end (Nogales et al., 1999). Periods of microtubule growth and rescue events (defined as switches from shortening to growth) are supported by the addition of GTP-bound tubulin subunits. Microtubule shortening, initiated by catastrophe events (defined as switches from growth to shortening), occur when hydrolysis of GTP in the β-tubulin subunits from the minus-end of the microtubule catches up to the addition of new tubulin dimers at the plus-end (Alushin et al., 2014).

The characteristic catastrophe and rescue events of microtubules define their dynamic instability, and this dynamic nature provides MTs with the ability to power the movements of chromosomes. The polar nature of MTs enables precise coordination with several motor proteins to assemble and maintain the mitotic spindle. The minus ends of MTs are anchored to and grow from spindle poles (centrosomes in higher order eukaryotes). The kinesin motor protein Eg5 crosslinks antiparallel MTs, and forces spindle poles apart as it walks to respective microtubule plus ends (Kapitein et al., 2005). Inhibition of Eg5 results in failure to separate the two centrosomes, which renders spindles monopolar. Loss of the minus end directed motor, dynein, results in

spindles with unfocused poles and chromosome alignment perturbations (Mitchison et al., 2005). Interestingly, inhibition of both of these counteracting motors largely rescues defects (van Heesbeen et al., 2014). This partial rescue illustrates the careful coordination of these opposing motor activities in spindle assembly.

Dynamic MTs produce force as they grow and shrink. Elongating MTs are capable of pushing chromosome arms toward the spindle equator. Further, MT interaction with chromokinesins, chromosome-affiliated motor proteins, provide “polar ejection forces” (PEFs), which also help congress chromosomes to the spindle equator (Rieder and Salmon, 1994). These forces have been demonstrated as critical for timely chromosome attachment to MTs. Computer simulation data show that unbiased “search and capture”, whereby MTs grow from centrosomes in random directions until becoming stabilized through binding to chromosomes (Kirschner and Mitchison, 1986) would take much too long or not even be possible (Paul et al., 2009). However, PEFs and transient MT attachments to chromosomes position chromosomes in a ring shape near the center of the spindle (Magidson et al., 2011; Figure 5). The position of this prometaphase ring is further regulated and refined by chromokinesins (Stumpff et al., 2012) as well as transient lateral interactions of kinetochores with the MT lattice (Magidson et al., 2011). These activities move chromosome arms to the periphery of the ring leaving the centromeres/kinetochores exposed to the MTs in the center of the ring promoting the formation of stable MT attachments to chromosomes (Magidson et al., 2011).

1.3 The Centromere

The centromere is positioned at the primary constriction of chromosomes. It is a modified chromatin structure that demarcates the location of kinetochores (Fukagawa and Earnshaw, 2014) which serve as the attachment site for MTs to chromosomes. In humans, the centromere is built on highly repetitive DNA sequences, α-satellite DNA, that is not sufficient, or even necessary for centromere identity (Marshall et al., 2008; McKinley and Cheeseman, 2016). A more reliable marker of centromere position is the presence of histone protein H3 variant, CENP-A, instead of H3 in some centromeric nucleosomes (Black et al., 2007). Thus, rather than being specified by nucleotide sequence, centromere location is specified epigenetically.

CENP-A is very stable at centromeres and remains bound to centromeric chromatin throughout DNA synthesis. Unlike canonical histones which are replicated and immediately incorporated into DNA, newly synthesized CENP-A loads to centromeres in G1 phase of the cell cycle. These characteristics enable CENP-A to maintain centromere identity throughout the cell cycle (Jansen et al., 2007). Further, CENP-A is critical to the formation of kinetochores. It functions upstream of several pathways that are required for kinetochore assembly, but is not sufficient for kinetochore assembly in human cells (Van Hooser et al., 2001; Liu et al., 2006). However, when Holiday Junction Recognition Protein (HJURP), a CENP-A chaperone that guides its positioning (Foltz et al., 2009), was ectopically targeted using LacI-LacO array, the CENP-A that was recruited to HJURP was sufficient form a functional kinetochore (Barnhart et al., 2011). Thus, CENP-A plays a large role in reliably demarcating the centromere to initiate kinetochore assembly.

CENP-A was identified using antibodies produced in patients with CREST (Calcinosis, Raynaud's phenomenon, Esophageal dysmotility, Sclerodactyly, Telangiectasia) syndrome. Many of these patients produce anti-centromere antibodies, and their blood sera was used to immuno-stain HeLa cell centromeres. Also elucidated in this study were centromere proteins, CENP-B and CENP-C (Earnshaw and Rothfield, 1985). CENP-B and CENP-C recruit to CENP-A and begin a framework for the assembly of the rest of the 16 member Constitutive Centromere Associated Network (CCAN). The CCAN proteins reside at the centromere throughout the cell cycle (Cheeseman and Desai, 2008) and are the site of assembly for the kinetochore (Figure 2). CENP-B has been reported to assist in assembly of centromeric structures in yeast cells through its DNA binding ability (Kitagawa et al., 1995), but CENP-B null mice experienced very mild phenotypic effects (Hudson et al., 1998). In contrast, CENP-C has been shown to be integral in kinetochore formation. It directly recruits the microtubule binding KMN network (KNL1/MIS12/NDC80) (Screpanti et al., 2011). CENP-C also recruits CENP-T that also recruits KMN (Schleiffer et al., 2012; Tachiwana et al., 2015). CENP-C is also critical for centromere recruitment of the CCAN subcomplexes CENP-HIKM and CENP-TWSX that effectively form a bridge from the inner centromere to the kinetochore (Klare et al., 2015). As an additional contribution to outer kinetochore assembly, CENP-I was shown capable of recruiting Nuf2 (Liu et al., 2006) and KMN (Kim and Yu, 2015). In summary, the CCAN is constitutively poised at centromeres to guide the assembly of the outer kinetochore during mitosis. The kinetochore is essential for generating attachments to spindle microtubules to facilitate chromosome congression and segregation. (Przewloka and Glover, 2009).

1.4 The Kinetochore

Kinetochores are macromolecular protein assemblages consisting of over 100 proteins, and are the link between chromosomes and the mitotic spindle. Their ability to stably bind MTs enables chromosomes to harness the power of growing and shrinking MTs for alignment and segregation. Kinetochores also generate the “wait anaphase” signal which prevents premature segregation of sister chromatids (O’Connell et al., 2012). The key kinetochore proteins that bridge the centromere to MTs are members of the KMN network: KNL1, the MIS12 complex, and the NDC80 complex (Cheeseman et al., 2004; Figure 3).

The MIS12 complex (DSN1, NNF1, NSL1, and MIS12) (Euskirchen, 2002) directly binds CENP-C and provides a link between the inner and outer kinetochore (Screpanti et al., 2011). As such, MIS12 complex association with the centromere is critical for recruitment of outer kinetochore members. *C. elegans* cells depleted of MIS12 have reduced recruitment of outer kinetochore proteins KNL1 and NDC80 (Cheeseman et al., 2004). Further, HeLa cells depleted of MIS12 fail to align chromosomes and experienced prolonged mitosis ending with lagging chromosomes (Goshima et al., 2003).

The phenotypic result observed on MIS12 depletion is to be expected given the reduction in kinetochore-localized Ndc80 and KNL1. KNL1 is named for the *k*inetochore *n*ul*l* phenotype in *C. elegans* observed on its depletion (Desai et al., 2003). Desai et al. (2003) showed the phenotype following depletion of KNL1 closely mimicked that of CENP-C depletion including premature spindle pole separation and anaphase failure. Further, they demonstrated binding of *C. elegans* Hec1 and Nuf2 to KNL1, and a

reduction of the kinetochore localization of those proteins in the absence of KNL1. KNL1 was shown to directly bind MIS12 (Cheeseman et al., 2006), and it was confirmed as a critical component of the kinetochore in human cells (Cheeseman et al., 2008), serving as a link from the inner to the outer kinetochore.

KNL1 kinetochore association is additionally indispensable for K-MT attachment regulation and Spindle Assembly Checkpoint (SAC) function, as SAC proteins BUB1, BUB3, and BUBR1 are dependent on KNL1 for kinetochore localization (Kiyomitsu et al., 2007; Shepperd et al., 2012). This dependency explains the observed chromosome alignment defects and premature anaphase in cells depleted of KNL1 (Caldas and DeLuca, 2014). This is attributable in part to Bub1 phosphorylation of Histone 2A (H2A) which helps target the Chromosomal Passenger Complex (CPC: comprised of Aurora B kinase, INCENP, Survivin, and Borealin) to the centromere (Yamagishi et al., 2010). KNL1 is also required for the activity of Aurora B Kinase (ABK) at both centromeres and kinetochores. HeLa and RPE-1 cells depleted of KNL1 showed a decline in phosphorylation of an ABK substrate, Hec1, due to a decrease in the phosphorylated, active form of ABK at kinetochores and centromeres (Caldas et al., 2013). Finally, *in vitro*, it has been shown that KNL1 has MT binding capability (Cheeseman et al., 2006), and while this function may contribute to SAC satisfaction in *C. elegans*, it is not required for the generation of stable K-MT attachments in either *C. elegans* or human cells (Caldas and DeLuca, 2014; Espeut et al., 2012).

Direct attachment of the kinetochore to MTs relies primarily on Hec1 of the NDC80 complex (DeLuca et al., 2006; Figure 3). Hec1 is a subunit of the four-member NDC80 complex. This ~57 nm heterotetramer is roughly dog-bone shaped with globular

domains of Spc24 and Spc25 dimer proximal to the centromeric chromatin, and globular domains of Nuf2 and Hec1 dimer extend away from the chromosomes. Each protein of NDC80 contains a coiled-coil that reaches between globular domains of dimers and unite at a tetramerization domain forming the dog-bone shape (Ciferri et al., 2005; Wei et al., 2005; Figure 3). NDC80 complex assembly is reliant on initial dimerization of Spc24/Spc25 and Hec1/Nuf2. Neither Spc24 nor Spc25 will bind the kinetochore in the absence of the other (Wei et al., 2006), and they must be present in order for Hec1/Nuf2 to be recruited to the kinetochore (Bharadwaj et al., 2004; Cheeseman et al., 2006; Ciferri et al., 2005). NDC80 is likely tethered to the kinetochore by KNL1-MIS12 subcomplexes (Ciferri et al., 2007; Desai et al., 2003) and redundantly through interaction with CENP-T (Liu et al., 2006). Depletion of any member of NDC80 from cells results in K-MT attachment defects evidenced by: unaligned chromosomes, prolonged mitosis, decreased inter-kinetochore tension, and chromosome segregation errors. These phenotypes result because stable, end-on K-MT attachments are dependent on Hec1, which requires all NDC80 members (DeLuca et al., 2005; Kline-Smith et al., 2005; Maiato et al., 2004; McCleland et al., 2004; Sundin et al., 2011).

1.5 Kinetochore-Microtubule Attachments

Stable, end-on K-MT attachments enable chromosomes to harness the power of MT dynamics. Hec1 is able to stably bind MTs with sufficient strength to enable chromosome movements, but those attachments can also be released when necessary. The binding of Hec1 to MTs is thought to rely on electrostatic interactions between two unstructured domains: the basic, positively charged N-terminal “tails” of Hec1 and the

acidic, negatively charged C-terminal “E-hooks” on tubulin (DeLuca et al., 2006; Guimaraes et al., 2008; Miller et al., 2008; Figure 3). There are ~7-9 Hec1 molecules per MT (stoichiometric with the other NDC80 members) in chicken DT40 cells (Johnston et al., 2010) and around 14 in HeLa cells (Suzuki et al., 2015) enabling force-generating attachments that are highly regulatable. It has been further proposed these molecules oligomerize along MTs based on clustered NDC80-MT binding observed *in vitro* (Alushin et al., 2010; Wilson-Kubalek et al., 2008). This is certainly possible as a loop region in the coiled-coil domain of Hec1 provides flexibility to reach varying lengths along the MT lattice (Maure et al., 2011; Wang et al., 2008). However, oligomerization would certainly be limited in cells where NDC80 is physically bound to inner kinetochore proteins (Sundin and DeLuca, 2010) as that physical constraint would limit NDC80 positions along the microtubule.

In addition to interaction of the tail with MTs, a region on the CH (calponin homology) domain of Hec1, referred to as the “toe”, is also highly positively charged. This region is also critical for Hec1 MT binding (Tooley et al., 2011), and this interaction has been demonstrated through cryo-EM reconstructions (Alushin et al., 2010). Charge reversal mutations in this region indicate this binding may also rely on electrostatic interaction (Sundin et al., 2011). Through multiple binding motifs of Hec1, the kinetochore is able accomplish the task of maintaining attachments to MTs that are continually growing and shrinking (Cheeseman et al., 2006; Ciferri et al., 2007), and this enables chromosomes to use MT dynamics for congression and segregation.

Based on the idea that kinetochores bind MTs through multiple NDC80 complex contact points with weak affinities, a “biased diffusion” mechanism has been proposed

to explain the ability of kinetochores to maintain attachment to dynamic MTs. It is proposed that the free energy of the system is minimized by kinetochore components binding to the MT lattice. In this way, the movement of the kinetochore will be biased to remain bound to the MT regardless of growth or shortening (Hill, 1985). Observation of NDC80 components diffusing on the MT lattice *in vitro* lends support for this model as these data indicate that it is energetically more favorable for NDC80 complexes to diffuse along the MT than to completely release all attachment (Powers et al., 2009).

It is estimated that MT polymerization can generate upwards of 35 pN of pushing force, and a depolymerizing MT can pull with 65 pN of force (Desai and Mitchison, 1997). Importantly, forces in this range are sufficient to power chromosome movements. For example, in grasshopper spermatocytes, the forces necessary for anaphase chromosome segregation have been estimated at ~0.5 pN for anaphase chromosome separation and for chromosome congression, ~10 pN (Nicklas, 1988). Furthermore, NDC80-coated beads were able to remain attached to dynamic MTs while experiencing 2.5 pN of force (Joglekar and DeLuca, 2009; Powers et al., 2009). Together, these results suggest that MTs can generate the necessary forces for chromosome congression and segregation, and the outer kinetochore can remain bound to microtubule ends when placed under that force.

The many points of contact between the kinetochore and MTs also offer opportunity for precise control over binding. Hec1 CH domain binding can be influenced by the conformation of MTs. As GTP hydrolysis occurs in the depolymerizing MT, the affinity of the CH domain is reduced (Alushin et al., 2010) enabling the complex to diffuse down the MT. Further, Aurora B kinase (ABK), known as the “master regulator”

of kinetochore-microtubule attachment stability, is recruited to the centromere and kinetochore and has been shown to phosphorylate the Hec1 “tail” domain. Nine ABK sites on the Hec1 tail have been identified: Ser4, Ser5, Ser8, Ser15, Ser44, Thr49, Ser55, Ser62, and Ser69 (Ciferri et al., 2008; DeLuca et al., 2006; Nousiainen et al., 2006). Phosphorylation of these sites alters the charge of the Hec1 tail domain, and in turn, decrease the affinity of the NDC80 complex for microtubules (Miller et al., 2008).

The number of opportunities for kinetochore binding to MTs is quite large considering the number of MT binding proteins at the kinetochore, the number of copies of each of these proteins, and the varied nature of their binding. Kinetochores have been observed to bind neighboring MTs as well as to the kinetochore fiber they are conventionally shown to interact with (Dong et al., 2007). This unconstrained K-MT binding, where NDC80 molecules can additionally bind to nearby MTs (Zaytsev et al., 2014), enhances control of K-MT binding affinity. Further, some NDC80 molecules can remain bound to MTs while others are released. Partial binding maintains proximity of the kinetochore to MTs allowing use of disassembling MTs to power motion (O’Connell et al., 2012). NDC80 preferentially binds to straight MTs contributing to the poleward motion of chromosomes on a depolymerizing MT (Ciferri et al., 2008). The curvature of the filament that occurs upon GTP hydrolysis is what decreases the affinity between the Hec1 CH domain, ‘toe’, and the MT lattice. The ability of kinetochores to remain attached to depolymerizing MTs, despite the detachment of the Hec1 CH domain, is thought to rely on either interactions between the Hec1 tail and the MT lattice or contributions of other kinetochore-associated MT binding proteins such as the SKA

complex (Alushin et al., 2010; Park et al., 2016; Sacristan and Kops, 2015; Tooley et al., 2011).

The continued attachment between kinetochores and MTs during both MT growth and shortening is important for chromosome oscillations during mitosis. Chromosome oscillations involve chromosomes switching from poleward to anti-poleward movement, and these directed movements correspond to MT depolymerization and polymerization. These oscillations are part the process of chromosome congression and are thought to be important for faithful chromosome segregation during which stable K-MT attachments must be maintained (Skibbens et al., 1993).

In addition to maintaining attachments to growing and shortening MTs during chromosome oscillations, kinetochores must also be able to completely release MTs. This is particularly true early in mitosis when K-MT attachment errors are frequent. Deviations from bipolar K-MT attachments where each sister kinetochore is attached to MTs emanating from opposite spindle poles need release for correction. For instance, both sister chromatids can become attached to MTs emanating from the same spindle pole. Also, a single kinetochore may garner attachments from both spindle poles. The release of these incorrect attachments is due to high phosphorylation of the Hec1 tail by ABK. Hec1 tail phosphorylation increases K-MT turnover preventing these errors from persisting into anaphase where they would lead to chromosome mis-segregation. This process is known as error correction. The group of proteins responsible for error correction is the Chromosomal Passenger Complex (CPC) which is recruited to the centromere during mitosis.

The CPC, comprised of INCENP, Survivin, Borealin, and ABK (the enzymatic subunit of the complex), destabilizes incorrect K-MT attachments, which allows for the formation of new, correct attachments. Recruitment of the CPC to centromeres depends on the phosphorylation of at least two centromeric histones. Phosphorylation of Histone H2A by Bub1 kinase recruits Shugoshin (Sgo1), which in turn, has been suggested to bind Borealin and recruit the entire CPC to centromeres (Kelly et al., 2010). Histone H3 is phosphorylated by Haspin kinase which recruits Survivin and the CPC to centromeres (Yamagishi et al., 2010). In addition, ABK phosphorylates Haspin, which is necessary for its full activation. It has been proposed that phosphorylated H2A (pH2A) recruits ABK to the centromere (van der Waal et al., 2012) where it activates Haspin, locally implementing a positive feedback loop by initiating phosphorylated H3 (pH3)-mediated CPC recruitment. (Wang et al., 2011). Further evidence placing pH2A recruitment of Sgo1 (and subsequent CPC recruitment) upstream of pH3-mediated CPC recruitment is its dependence on Mps1, a kinase critical to SAC activity, which maximizes ABK activation (van der Waal et al., 2012). Precise control of ABK activity, both spatially and temporally, imparts exquisite control of K-MT attachment and release.

ABK phosphorylates multiple members of the KMN complex, resulting in reduced affinity of the complex for microtubules, but this effect is not through impaired assembly of the complex (Welburn et al., 2010). ABK activity is critical for the release of improper K-MT attachments as demonstrated by inhibition of the kinase or mutations limiting substrate availability; both result in chromosome segregation errors attributable to persistent, erroneous K-MT attachments. Inhibition of Ipl1 (yeast ABK) results in yeast cells that are able to form chromosome-MT linkages and separate sister chromatids at

anaphase, but these cells experience errors in chromosome segregation (Biggins et al., 1999). It was subsequently demonstrated in yeast that phosphorylation of Ndc80/Hec1 by ABK leads to increased turnover of K-MT attachments, which results in the release of incorrect attachments (Cheeseman et al., 2002; Tanaka et al., 2002). Reduction of K-MT binding affinity after ABK phosphorylation is conserved in *C. elegans* (Cheeseman et al., 2006). The role of ABK in proper K-MT attachment regulation was demonstrated in Ptk1 cells through microinjection of an antibody to the N-terminus of Hec1 (9G3). Increased inter-kinetochore distances, indicating hyperstable K-MT attachments were observed. Other indications of hyperstable K-MT attachments such as K-MT attachment errors, inability of chromosomes to align, and segregation errors were also observed. This phenotype was closely mimicked through alanine substitution of six ABK sites mapped to the Hec1 tail by mass spectrometry (DeLuca et al., 2006).

Errors in K-MT attachments occur most often early in mitosis. Initial K-MT interactions are largely stochastic providing opportunity for incurring incorrect K-MT attachments (Nicklas, 1997). Accordingly, ABK activity at the centromere is highest during prophase and prometaphase. Its activity is shown by the presence of the phosphorylated (active) form of ABK and levels of substrate phosphorylation (Andrews et al., 2003; DeLuca et al., 2011) facilitating turnover of these erroneous attachments (Cimini et al., 2006). Further, phosphorylation of MCAK (Mitotic Centromere-Associated Kinesin) by ABK recruits this microtubule depolymerase to the centromere. The microtubule depolymerase activity of MCAK is largely inhibited in early mitosis, but is active later to promote turnover of remaining erroneous K-MT attachments through its action on MTs (Andrews et al., 2004).

K-MT attachments in early phases of mitosis are relatively unstable (Zhai et al., 1995) because of the high ABK activity, but also because sister kinetochores have not achieved K-MT attachment-stabilizing bi-orientation. This occurs when each sister chromatid generates stable attachments to MTs emanating from each of the two opposite spindle poles. These amphitelic attachments create pulling forces resulting in tension at K-MT interface. This tension has been shown to stabilize attachments, resulting in a positive feedback that promotes the formation of further stable, force-producing attachments (Akiyoshi et al., 2010).

This tension also pulls the sister kinetochores away from each other and away from the centromere. In this fashion, kinetochores with stable and appropriate MT attachment are pulled beyond the reach of attachment destabilizing activity of ABK. In this 'Spatial Positioning Model', the physical separation of the KMN substrates from ABK reduces phosphorylation to stabilize correct attachments (Biggins and Murray, 2001; Liu et al., 2009). However, in addition to centromere localized ABK, populations at the kinetochore have also been observed (DeLuca et al., 2011) and it may be the regulation of this population of ABK that is critical for the regulation of K-MT attachment strength (Caldas et al., 2013). Regardless, a critical function of ABK is destabilizing incorrect K-MT attachments. The release of K-MT attachments is critical as it affords kinetochores the opportunity to make new, correct attachments essential for proper segregation of chromosomes.

1.6 Spindle Assembly Checkpoint

The Spindle Assembly Checkpoint (SAC) is the mitotic safety net. Its actions prevent exit from mitosis until equal segregation of chromosomes is assured. Mitotic exit

is delayed through sequestration of Cdc20, a cofactor necessary for the activity of the Anaphase Promoting Complex/Cyclosome (APC/C) (Figure 6). This E3 ubiquitin ligase targets Cyclin B and Securin for proteasomal degradation (Sudakin et al., 1995). Degradation of Cyclin B inactivates Cdk1, which leads to a sharp decrease in Cdk1-mediated, mitosis-promoting phosphorylation events and thereby promotes mitotic exit (Chang et al., 2003; Clute and Pines, 1999; Murray et al., 1989; Figure 4, 6). Activation of the APC/C also results in the proteolytic degradation of Securin, a protein that binds and inhibits Separase, a caspase-like protein. Destruction of Securin releases Separase which ultimately results in inactivation of the Cohesin complex and sister chromatid separation (Peters, 2006) (Figure 6). Cohesin is a four-member complex consisting of Smc1, Smc3, Scc1, and Scc3 (Ciosk et al., 2000; Onn et al., 2008) that joins sister chromatids at the centromere. The complex is necessary for obtaining and maintaining bipolar K-MT attachments; its depletion results in premature separation of sister chromatids (Sonoda et al., 2001). Ubiquitination of Cyclin B and Securin instigate the end of mitosis, and it is the role of kinetochores to maintain the mitotic state by holding the E3 ligase activity of the APC/C inactive until all kinetochores have established proper attachments to MTs.

APC/C inactivity is maintained by the Mitotic Checkpoint Complex (MCC) which binds to and inhibits Cdc20, the mitotic APC/C activator (Figure 6). The MCC is a four-protein complex comprised of Cdc20, Mad2, Bub3, and BubR1 whose formation and maintenance requires intact kinetochores. The kinetochore kinase Mps1 is thought to be the upstream initiator of MCC formation. Specifically, Mps1 phosphorylates the KMN component KNL1 which generates binding sites for Bub3 (London et al., 2012;

Shepperd et al., 2012; Yamagishi et al., 2012) that are essential to recruit Bub1, BubR1, Mad1, and Mad2 to unattached kinetochores. Additionally, the RZZ complex (Rod, ZW10, Zwilch) has been suggested to provide an alternate recruitment pathway for Mad1 and Mad2 to unattached kinetochores (Caldas et al., 2013; Kops et al., 2005a; Silió et al., 2015; Zhang et al., 2015). The assembly of the MCC at unattached kinetochores promotes SAC activation. Further, generation of closed Mad2 by the MCC provides a diffusible signal enabling a single unattached kinetochore to halt mitotic progression (Musacchio and Salmon, 2007; Rieder et al., 1995).

Mad2 is recruited to unattached kinetochores by association with Mad1. It exists in two conformations—open and closed. Upon Mad1 binding kinetochores, Mad2 is activated and transitions from an open to a closed conformation. Once in this form, Mad2 is able to bind and inhibit Cdc20. The proposed “Mad2 Template Model” suggests that Mad1/closed Mad2 catalyzes the formation of additional closed Mad2 (De Antoni et al., 2005), facilitating the formation and amplification of MCC complexes. In this manner, a single kinetochore can broadcast a diffusible ‘wait anaphase’ signal which delays mitotic exit (Rieder et al., 1995). Ultimately, the MCC binds to the APC/C which interferes with its ability to interact with and ubiquitinate its substrates (Cyclin B and Securin) (Herzog et al., 2009; Primorac and Musacchio, 2013; Sudakin et al., 2001).

The SAC is satisfied when all of the kinetochores in a cell cease their individual checkpoint signaling. Exactly what aspect of K-MT attachment provides satisfaction has provided interesting debate in field for some time. In one model, the physical attachment of microtubules to kinetochores signals for SAC satisfaction; in an opposing model, stable K-MT attachment produces tension between two sister kinetochores. This tension

thus provides the signal to silence the SAC. In 1995 it was demonstrated that laser-ablation of a single unattached kinetochore led to SAC silencing and mitotic exit in Ptk1 cells suggesting that stable K-MT attachment is the critical parameter read by the SAC (Rieder et al., 1995). That same year, it was demonstrated that pulling on an unattached kinetochore in grasshopper spermatocytes using a micromanipulator resulted in SAC satisfaction suggesting that tension between sister kinetochores is the key factor that induces SAC silencing (Li and Nicklas, 1995).

More recent research has suggested that stable K-MT attachment is the key to SAC satisfaction. In one study, researchers inhibited DNA replication enabling observation of mitosis without possibility of tension between sister kinetochores, as the sister wasn't formed. Mitotic exit indicated K-MT attachment was the parameter evaluated by the SAC (O'Connell et al., 2008). Additional support for SAC satisfaction dependent on K-MT attachment came from overexpression of the chromokinesin, NOD, in *Drosophila* cells. This produced additional polar ejection forces that stabilized K-MT attachments and cells were able to satisfy the SAC in the absence of tension between all sister kinetochores (Cane et al., 2013).

It has been further shown that upon stable K-MT binding an increase in intra-kinetochore stretch is observed in conjunction with bipolar K-MT attachments. This separation between the inner and outer kinetochore was correlated with SAC satisfaction (Maresca and Salmon, 2009; Uchida et al., 2009), suggesting that intra-kinetochore tension may, in fact, be the key to SAC silencing. The requirements for SAC satisfaction are discussed further in Chapter 3.

The transition from SAC activation to SAC satisfaction coincides with decreased phosphorylation of ABK kinetochore substrates. Bi-oriented sister kinetochore pairs aligned at the metaphase plate exhibit reduced phosphorylation of KNL1, DSN1 (Welburn et al., 2010), and Hec1 (DeLuca et al., 2011) which is typically indicative of stable K-MT binding. Stable attachments are thought to reduce ABK activity by reducing BUB1 recruitment to KNL1 (Caldas et al., 2013) through loss of kinetochore association of MPS1 (Aravamudhan et al., 2015). It has been demonstrated that MPS1 and MTs compete for Hec1 binding such that upon the stable binding of Hec1 to MTs, MPS1 is evicted from kinetochores, resulting in decreased phosphorylation of KNL1 and subsequent eviction of SAC proteins (Hiruma et al., 2015; Ji et al., 2015). Reduction of ABK-mediated phosphorylation at the kinetochore is also attributed to increased activity of the protein phosphatases, PP1 and PP2A. PP1 is recruited to the kinetochore via KNL1. PP2A is recruited, at least in part, by the SAC protein BUBR1. Both phosphatases have been implicated in directly counteracting the kinase activity of ABK enhancing stable K-MT binding (Espert et al., 2014; London et al., 2012; Pinsky et al., 2009; Rosenberg et al., 2011). In addition, the minus-end directed motor dynein is recruited to unattached kinetochores, and upon MT binding, dynein ‘strips’ Mad1 and Mad2 from kinetochores motoring them towards spindle poles along MTs (Howell et al., 2001).

The removal of MCC components from kinetochores causes the cessation of checkpoint signaling. CDC20 associates freely with the APC/C, enabling it to ubiquitinate its key mitotic substrates Securin and Cyclin B, and their subsequent proteolysis ensues (Sudakin et al., 1995). As discussed above, the destruction of

Securin enables Separase to cleave the Cohesin component SCC1 (Nasmyth, 2001). This “opens” the Cohesin complex and allows sister chromatids to separate. However, it is the destruction of Cyclin B that reverses the mitotic program and initiates mitotic exit (Chang et al., 2003). Devoid of Cyclin B, CDK1 undergoes a conformational change rendering its kinase activity inactive (Jeffrey et al., 1995). In the absence of CDK1 activity, counteracting phosphatases dephosphorylate mitosis-promoting substrates. Chromosome decondensation and nuclear formation are clear indication of cells that have progressed through mitosis (Sullivan and Morgan, 2007). Finally, cleavage furrow formation and the relocation of INCENP/ABK to the spindle midzone occurs and promotes cytokinesis (Pereira and Schiebel, 2003; Peters, 2006). These highly regulated steps through mitosis ensure segregation of duplicated chromosomes with high fidelity.

1.7 Significance

Despite the regulation and careful monitoring of K-MT attachments, errors in mitosis do occur. Chromosome mis-segregation leads to aneuploidy, a situation whereby daughter cells have the incorrect number of chromosomes and one that is a hallmark of all human solid tumors and some birth defects. Mis-segregations can involve chromosomes encoding for tumor suppressor genes and proto-oncogenes. The down-regulation of the former (Kops et al., 2005b) or the up-regulation of the latter (Chial, 2008) can lead to unmitigated cell growth definitive of many cancers. Both of these scenarios can occur through errors in cell division. Further, segregation errors early in development can lead to birth defects. Errors can occur at almost every step of

mitosis including problems in cohesion of sister kinetochores, centrosomal defects (Kops et al., 2005b), or persistent K-MT attachment errors (Cimini and Degrassi, 2005). The regulation of K-MT attachments by Aurora B Kinase phosphorylation of the Hec1 tail was investigated to gain some insight into how errors avoid detection by the SAC. This was done by preventing phosphorylation on the Hec1 tail through incorporation of alanine substitutions at specific ABK target sites. It was demonstrated that the very fine control over K-MT binding requires at least 7 ABK sites be available for wild-type level of regulation. Preventing ABK phosphorylation in as few as two sites resulted in hyperstable K-MT attachments and a deficiency in chromosome alignment. We performed these experiments to test our hypothesis that we could identify the minimum requirements of the SAC if the error-correcting ability of ABK was reduced. Further, based on observations of cells expressing hyper-stable K-MT attachments, we hypothesized that K-MT attachment is the parameter evaluated by the SAC.

However, it is of greater consequence to understand why the errors in K-MT attachment are not detected by the SAC. Erroneous K-MT attachments do not have cellular or human health consequences until a cell is allowed to complete mitosis-to divide with erroneous attachments. Through understanding what the SAC is ‘reading’ at kinetochores to allow anaphase onset, we can explain how errors occur. Elucidating the parameters evaluated by the SAC can lead to treatment targets and drug designs to minimize risks and maximize therapies for cancers. Throught the studies described here, we gained a deeper understanding of changes that occur within the kinetochore concurrent with SAC satisfaction by implementing a non-phosphorylatable, mutant

version of Hec1 that stabilized K-MT attachments in the absence of any microtubule pulling forces, and with minimal manipulation to cells (Tauchman et al., 2015).

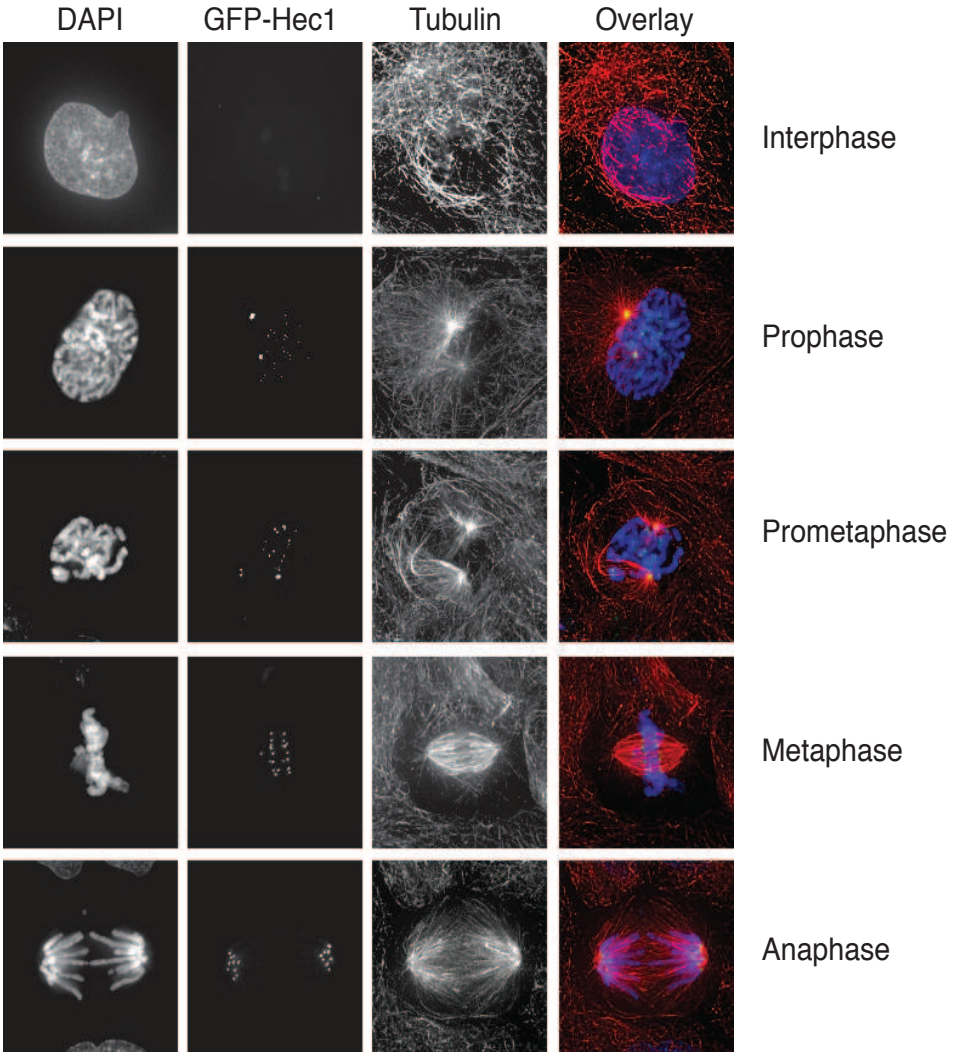

Figure 1: The stages of the cell cycle. Ptk1 cells are shown. DNA is DAPI stained (blue) in the overlay. The condensed mitotic chromosomes have a thread-like appearance. The β-subunit of tubulin is antibody labeled (red). Kinetochore component Hec1 is GFP-labeled (green). Note the attachment of Hec1 to microtubules following nuclear envelope breakdown.

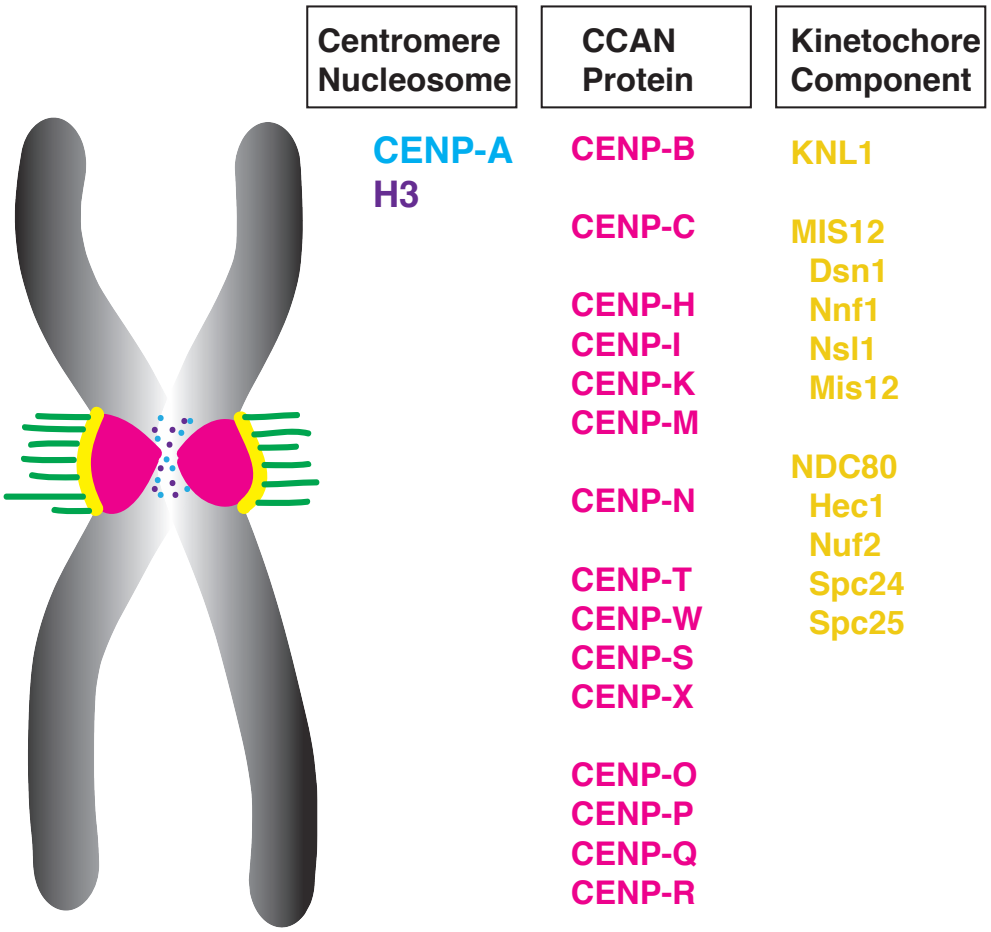

Figure 2: Diagrammatic representation of sister kinetochores showing the association of the CCAN to centromeric chromatin. The chromatin contains both canonical H3 (shown only at centromere) and a histone H3 variant, CENP-A, shown in purple and blue, respectively. The CCAN (pink) is assembled on sites of centromeric chromatin constitutively throughout the cell cyle. They are listed from inner to outer position and grouped by their complex formation. Just prior to mitosis, the KMN complex (yellow) accociates with CCAN components, and during mitosis the KMN complex binds to spindle microtubules (green). Modified from A. Musacchio http://www.mpi-dortmund.mpg.de/9310/Mechanistische_Zellbiologie

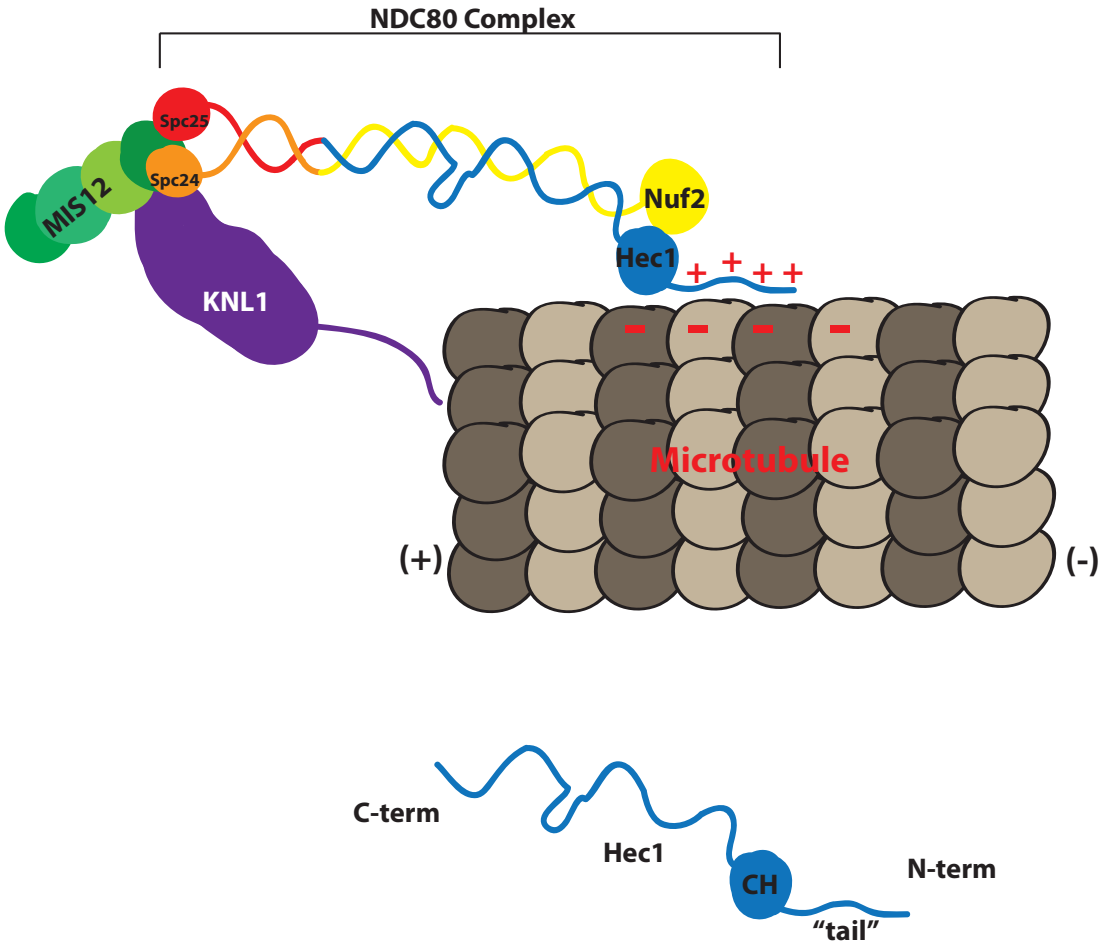

Figure 3: The KMN network serves as the bridge between the centromere and spindle microtubules. The KMN network is anchored to the CCAN by the four protein MIS12 complex (green). The four protein NDC80 complex contains the primary microtubule binding protein Hec1 (blue). The electrostatic interaction between Hec1 and a microtubule is indicated. Nuf2 (yellow) is required for the stabilization of Hec1 and may also play a role in the formation of stable kinetochore-microtubule attachments. The Spc24 (orange)/Spc25 (red) dimer anchors Hec1/Nuf2 to the kinetochore. KNL1 (purple) has intrinsic microtubule binding activity, although the physiological role of this binding is unclear. A microtubule is shown in brown, its polarity indicated. Hec1 is shown below indicating C- and N-termini as well as the CH domain and the unstructured "tail".

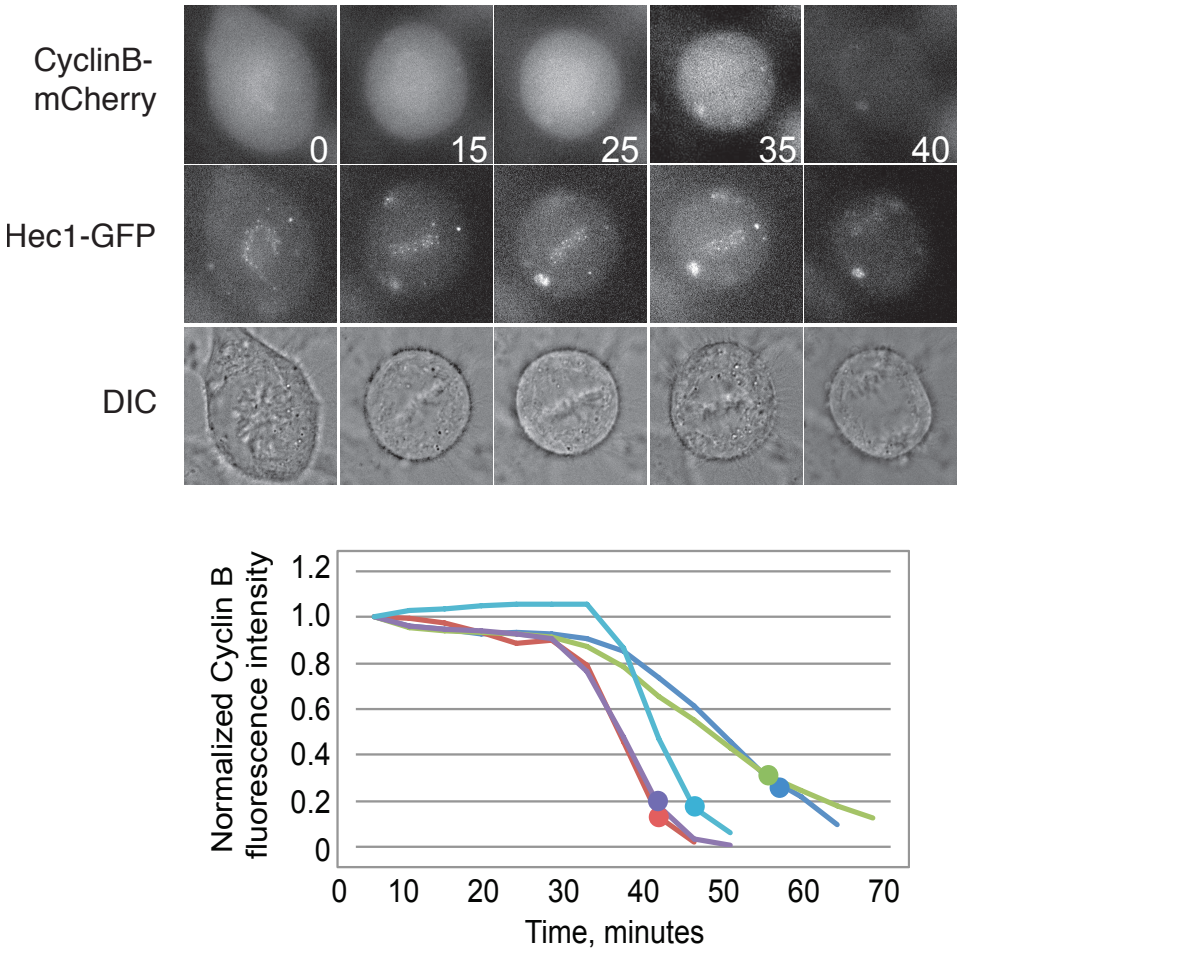

Figure 4: Cyclin B levels increase as cells enter mitosis and rapidly decline to allow anaphase onset. The representative HeLa cell pictured is inducibly expressing Hec1-GFP and transiently transfected with Cyclin B-mCherry. DIC images of the cell are also shown. Time 0 indicates mitotic entry and minutes after are labeled. The graph below represents the whole-cell fluorescence intensity, each cell normalized to intensity at mitotic onset and correct for photo-bleaching, of Cyclin B for 5 representative cells. Dots indicate anaphase onset.

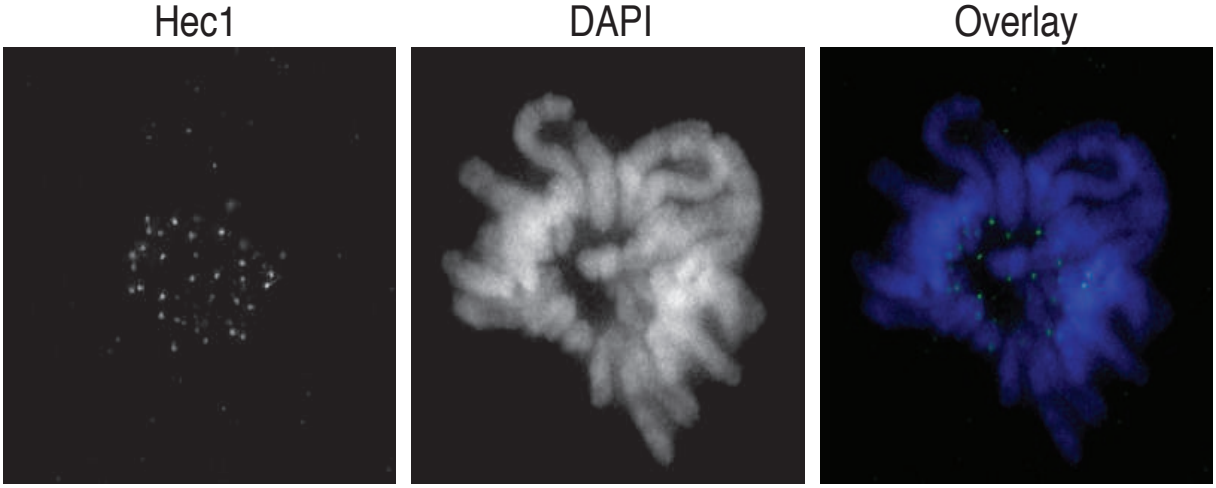

Figure 5: Ptk1 cell in Prometaphase. DNA is stained with DAPI (blue). Hec1 is antibody labeled (green). Notice the ring shape of the kinetochores marked by Hec1. The area in the center of the ring is devoid of chromosomes due to chromosome arms being pushed to the periphery of the ring. This configuration facilitates K-MT interactions leading to stable attachments.

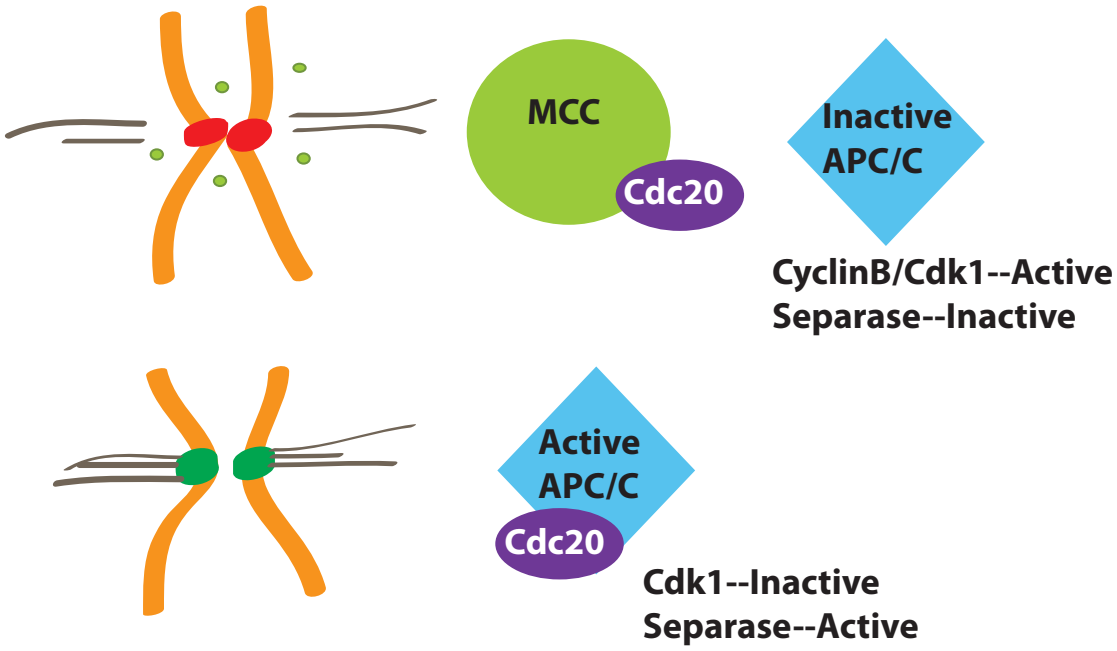

Figure 6: The Spindle Assembly Checkpoint. Mitosis begins by activation of Cyclin B/Cdk1. Unattached kinetochores perpetuate the 'wait anaphase' signal by MCC generation. The MCC binds Cdc20 maintaining inactive APC/C allowing Cdk1 and Separase to remain active maintaining the mitotic state. Stable kinetochore-microtubule attachments satisfy the Spindle Assembly Checkpoint halting MCC generation. The APC/C becomes active through binding free Cdc20, and this E3 ubiquitin ligase ubiquitinates Securin and Cyclin B. This activates Separase and inactivates Cdk1 permitting exit from mitosis.

Chapter 2: Phospho-Regulation of Hec1 in Kinetochore-Microtubule Attachments

2.1 Introduction

Post-translational modifications allow control over cellular function through the alteration of protein structure, interaction, activity, and location. Phosphorylation of proteins is a prevalent post-translational modification for cell regulation that frequently occurs in unstructured regions of proteins (Nishi et al., 2011; Olsen et al., 2006). Variable levels of phosphorylation to these unstructured domains are a common regulatory mechanism and cells are rife with examples.

The carboxy-terminal domain of RNA polymerase II possesses many sites for modification via repeated phosphorylation domains that can alter the polymerase association with proteins enhancing or reducing chromatin accessibility and mRNA processing enzymes (Schüller et al., 2016; Suh et al., 2016). Critical to developmental gene expression and cytokine expression is the protein NFAT1. The multiple phosphorylation sites on NFAT1 need sufficient phosphorylation to reach a threshold for its activation (Salazar and Höfer, 2003). Transcription activation by Ets-1, however, is diminished by increasing phosphorylation. Its DNA binding activity is gradually reduced to inhibition through multiple phosphorylation events that cause it to fold, obscuring binding sites (Pufall et al., 2005). The unstructured domain of PC4 transcription coactivator is able to bind single-strand DNA after a single phosphate is attached, and begins losing DNA unwinding and transcription activator binding ability after a second phosphate is added. Both of these capabilities are reduced further after subsequent phosphorylation (Jonker et al., 2006). The affinity of kinetochore-microtubule binding is also reduced in a graded manner through phosphorylation of members of the KMN

network. KNL1, Dsn1, and Hec1 are all phosphorylated by ABK, and these phosphorylation events reduce K-MT attachment strength to varying degrees as evidenced through phosphomimetic substitution (Cheeseman et al., 2006; Ciferri et al., 2008; DeLuca et al., 2006; Guimaraes et al., 2008; Sarangapani et al., 2013). Amino acid substitutions that prevent ABK-mediated phosphorylation of Dsn1 and KNL1 also reduce MT binding of KMN *in vitro*, but the phenotypes are less severe than those in Hec1 phospho-deficient mutants (Welburn et al., 2010).

Cells depleted of Hec1 are unable to form stable K-MT attachments. This phenotype is not rescued by Hec1 lacking the 80 amino acid, unstructured tail (Guimaraes et al., 2008). The microtubule binding ability of this basic, positively-charged region has been suggested to result from electrostatic interaction with acidic, negatively-charged tails on tubulin (Ciferri et al., 2008; Miller et al., 2008). Phosphorylation would disrupt the electrostatic interaction allowing the release of K-MT attachments (Cheeseman et al., 2002; DeLuca et al., 2006; Pinsky et al., 2006). Experiments *in vitro* show mutation of seven Hec1 tail phosphorylation sites to aspartic acid reduces the pulling forces needed to detach it from microtubules (Sarangapani et al., 2013). Further, rescue of Hec1 depletion with a mutant of Hec1 that has aspartic acid substitutions at each of the nine phosphorylation sites is unable to stably bind microtubules (Guimaraes et al., 2008). While constitutive phosphorylation of Hec1 is detrimental to cellular health, complete obstruction of it is equally disastrous. Microinjection of an antibody against the Hec1 N-terminus (the MT-binding region) suppresses MT turnover at kinetochores. Injected cells with hyperstable K-MT attachments fail to properly align chromosomes to metaphase plate, exhibit increased

centromere stretch, and have segregation errors. Mutation of six ABK phosphorylation sites on the Hec1 tail to non-phosphorylatable alanine closely mimics these results (DeLuca et al., 2006) as does rendering all nine non-phosphorylatable (Guimaraes et al., 2008).

It is important to fully understand the regulation of K-MT attachments because it is so critical to proper chromosome segregation. We sought to determine how many of the nine ABK phosphorylation sites on the Hec1 tail are required for proper K-MT attachment regulation. Several quantifiable parameters, described below, can be used as a readout for K-MT attachment, and these can be readily compared for their evaluation.

The tension that kinetochores can withstand due to microtubule pulling forces declines with phosphorylation, or phosphomimetic substitutions, of the Hec1 tail (Cheeseman et al., 2006; Sarangapani et al., 2013). The reduced ability to hold microtubules under tension corresponds to smaller distances between sister kinetochores (Guimaraes et al., 2008). Kinetochores unable to be phosphorylated or unable to release K-MT binding through antibody interference have hyperstable K-MT attachments and exhibit increased distance between sister kinetochores (DeLuca et al., 2006). Both the introduction of phosphomimetic substitutions and decreasing the ability of ABK to phosphorylate its Hec1 substrate result in reduced ability of cells to align chromosomes to the metaphase plate (DeLuca et al., 2006; Guimaraes et al., 2008). K-MT attachment stability was evaluated in cells expressing a battery of phospho-restricted Hec1 mutants by measuring inter-kinetochore distances and assessing chromosome alignment capability. Measuring the response of cells with limited

opportunity for Hec1 phosphorylation-mediated K-MT attachment regulation provided insight into the mechanism of that regulation. First, the cellular response to this phospho-limitation indicates whether all nine phospho-sites on the Hec1 tail are needed or if redundancy exits. Redundancy is indicated if cells expressing mutants are still able to exhibit wild-type phenotypes with regard to inter-kinetochore distance measures and chromosome alignment in spite of phospho-site limitations imparted to the Hec1 tail. Additionally, variation of the cellular response to the position of the mutated phospho-site was investigated by engineering mutations to the Hec1 tail that maintain similar number of alanine mutations, but at different residue positions. These were examined to determine if the location of the site on the Hec1 tail is important to K-MT attachment regulation.

2.2 Results

To understand how many phosphorylation sites on the Hec1 tail are needed to regulate K-MT attachments, the number of sites available for Ptk1 cells to phosphorylate was reduced. Ptk1 cells were chosen because they round up less than human cells when they enter mitosis which eases imaging of them. Non-phosphorylatable alanine mutations made by Jeanne Mick (6A-Hec1 from J. DeLuca) were introduced to the Hec1 tail at different positions and combinations (Figure 7a; DeLuca et al., 2006). Ptk1 cells were depleted of endogenous Hec1 through siRNA treatment. The depletion was rescued by transfection of GFP-fusion proteins containing the human Hec1 mutants shown in Figure 7a. To characterize the effects in cells with reduced numbers of residues for ABK phosphorylation on the Hec1 tail, inter-

kinetochore distances were measured between GFP-labeled sister kinetochores. The inter-kinetochore distance is reflective of K-MT attachment strength (DeLuca et al., 2006). These distances were compared to controls WT-GFP-Hec1, all ABK targets on the Hec1 tail left as wild-type) and 9A-Hec1-GFP (all ABK targets on the Hec1 tail mutated to alanine) to evaluate the stability of attachments in phospho-limited substitutions. An increase of inter-kinetochore distance relative to WT-Hec1 indicates hyperstability of K-MT attachments, while distance smaller than those exhibited by cells expressing 9A-Hec1 demonstrate at least some level of regulation of K-MT attachments. It has been demonstrated that small changes in K-MT attachment stability can be resolved by measuring inter-kinetochore distances (Zaytsev et al., 2014).

To measure the effects of mutations to Hec1, wild-type Hec1 fused to GFP was transfected and expressed in cells providing for control measures of K-MT attachment stability. Imparting only two alanine mutations to the Hec1 tail (15,44A) resulted in increased attachment stability, but addition of a third mutation had no additional impact (15,44,55A). However, when the third site was move from residue 15 to residue 69 (44,55,69A), a further increase in inter-kinetochore distance was observed. Introducing an additional alanine mutation to Ser15 (15,44,55,69A) did not result in further expansion of inter-kinetochore distance. Hec1 mutants with six and with all nine alanine mutations increased inter-kinetochore distances further still but to an equivalent extent (Figure 7b).

Alignment of kinetochores to the metaphase plate was quantified as another readout for attachment stability. Although both K-MT destabilization and hyper-stabilization cause the inability of chromosomes to align in cells, the increased inter-

kinetochore distances resulting from expression of Hec1 mutants examined indicate these mutants are stabilizing K-MT attachments. To quantify alignment, kinetochore pairs were scored as “mostly aligned” (0-2 kinetochore pairs off the metaphase plate), “partially aligned” (3-6 pairs off the metaphase plate), or “mostly unaligned” (>6 pairs off the metaphase plate). Kinetochores were identified by the Hec1-GFP signal. The data are shown in Figure 7c. The general trend of these data recapitulates the inter-kinetochore distance measures. None of the cells with alanine mutations are able to align chromosomes to the metaphase plate as well as wild-type-expressing cells. However, the 2A-, 3A-, and 4A-Hec1 mutant-expressing cells appear to have similar difficulties in chromosome alignment that are not as severe as the two, more extreme mutants, 6A- and 9A-Hec1 (Figure 7c).

2.3 Discussion

These experiments suggest that all nine phosphorylation sites on the Hec1 tail need to be available to ABK phosphorylation for rigorous K-MT attachment regulation. The increased inter-kinetochore distances resulting from even two of the nine sites being replaced by non-phosphorylatable alanine indicates hyperstable K-MT attachments are formed. This hyper-stability of K-MT attachment measured by increased inter-kinetochore distances are reflected in cells’ inability to align chromosomes. Inter-kinetochore distances and diminished ability to align chromosomes are each exacerbated by greater reduction in Hec1 phospho-site availability. In the future, it will be valuable to determine if a single alanine substitution has measurable consequences in terms of kinetochore-microtubule attachment regulation. Regardless, the alanine substitutions on the Hec1 tail evaluated thus far cause increased stability of

K-MT attachments that could lead to premature silencing of the SAC and chromosome segregation errors at anaphase.

Additionally, a varied response due to the position of the alanine substitutions is suggested by the data. In particular, the two 3A-Hec1 mutants have different levels of hyperstable attachments shown by inter-kinetochore distance measures. In both instances Ser44 and Ser55 are mutated to alanine, but the additional mutation of Ser69 has more a severe impact than Ser15. Further, increasing 3A- to 4A-Hec1 by mutation of Ser15 does not increase inter-kinetochore distance. This is in accord with data that show phosphomimetic substitutions of aspartic acid to ABK-targeted residues have a more severe phenotype when imparted to the C-terminal half of the Hec1 tail relative to those imparted to the N-terminal half. The relative importance of N- versus C-terminal Hec1 tail regions was quantified through *in vitro* microtubule pelleting assays and chromosome alignment evaluation (Alushin et al., 2012). The data generated here support this idea that the C-terminal region of the Hec1 tail is more influential in K-MT binding regulation.

Proper K-MT attachment relies on the cell's ability to finely tune the affinity of Hec1 for microtubules. This is accomplished by altering electrostatic interaction via phosphorylation. Limiting phosphorylation site opportunity through alanine mutations demonstrated that multiple sites are required as even two alanine substitutions disrupted K-MT that interaction regulation. Those data also show that some sites are potentially more influential than others (Figure 7b,c).

2.4 Future Direction

It is of interest, and would further our understanding of K-MT binding regulation to know which sites exert more influence on K-MT binding (DeLuca and Musacchio, 2012). DNA constructs have been engineered to determine the relative impact of phosphorylation by ABK on single sites on the Hec1 tail. Beginning with the 9A-Hec1 clone, nine DNA constructs were made such that each had a single ABK phosphorylation site returned to the wild-type phosphorylation site (1WT8A-Hec1-GFP; Figure 8a). Cells depleted of endogenous Hec1 will be rescued with these DNA constructs and inter-kinetochore distances and chromosome alignment phenotypes evaluated. Perhaps even more informatively, the chromosome oscillation behavior in these transfected cells will be quantified.

While images of metaphase cells depict chromosomes aligned to the equatorial plate, those chromosomes are in fact not static. When that snapshot is observed in real time, the chromosomes are seen to oscillate over the plate when they are attached to microtubules emanating from centrosomes. During these oscillations, chromosomes switch between poleward and antipoleward motions (Skibbens et al., 1993). Though mechanistically not fully understood, these oscillations are inherent to cells able to align and properly segregate chromosomes (Maiato et al., 2004). Parameters of chromosome oscillations can be quantified to characterize K-MT interaction (Wan et al., 2012; Waters et al., 1996).

Critical to normal chromosome oscillation is the ability of ABK to phosphorylate the Hec1 tail. Alanine substitutions to all nine ABK phosphorylation sites (9A-Hec1) severely dampen oscillation behavior (DeLuca et al., 2011). However, further work from

this lab demonstrated that replacing any one of those alanines of 9A-Hec1 with an aspartic acid restored wild-type chromosome oscillations (Zaytsev et al., 2014). This provided the rationale for engineering the 1WT8A-Hec1-GFP DNA clones. If the wild-type residue is phosphorylated, the negatively charged phospho-serine should be able to rescue oscillations as the aspartic acid does.

The nine 1WT8A-Hec1-GFP clones have been transfected into cells depleted of endogenous Hec1 and demonstrated to localize to kinetochores. Further, immuno-staining with phospho-specific antibodies to the Hec1 tail residues (DeLuca et al., 2011) show that the wild-type phosphorylation sites are phosphorylated *in vivo* (Figure 9a). However, it is noteworthy that the phosphorylation levels of aligned kinetochores, those that are evaluated for inter-kinetochore distance and chromosome oscillations, is reduced relative that of unaligned kinetochores (Figure 9b). In the absence of full phosphorylation, it is possible the 1WT8A-Hec1-GFP mutants will not mimic the single aspartic acid substitutions of Zaytsev et al. (2014). However, they additionally showed that three aspartic acid substitutions to the 9A-Hec1 mutant rescued wild-type spindle pole separation rates. Separation of centrosomes occurs early in mitosis when phosphorylation levels are at a maximum. To determine if critical phosphorylation sites exist on the Hec1 tail, mutants were engineered such that three wild-type sites were availed to ABK phosphorylation while the other five were left alanine (Figure 8b). These 3WT5A-Hec1-GFP mutants were created to see which would mimic aspartic acid substitutions indicating their import in K-MT attachment regulation. It is possible that cells transfected with 3WT5A-Hec1-GFP will more closely mimic aspartic acid substitution early in mitosis due to higher levels of phosphorylation.

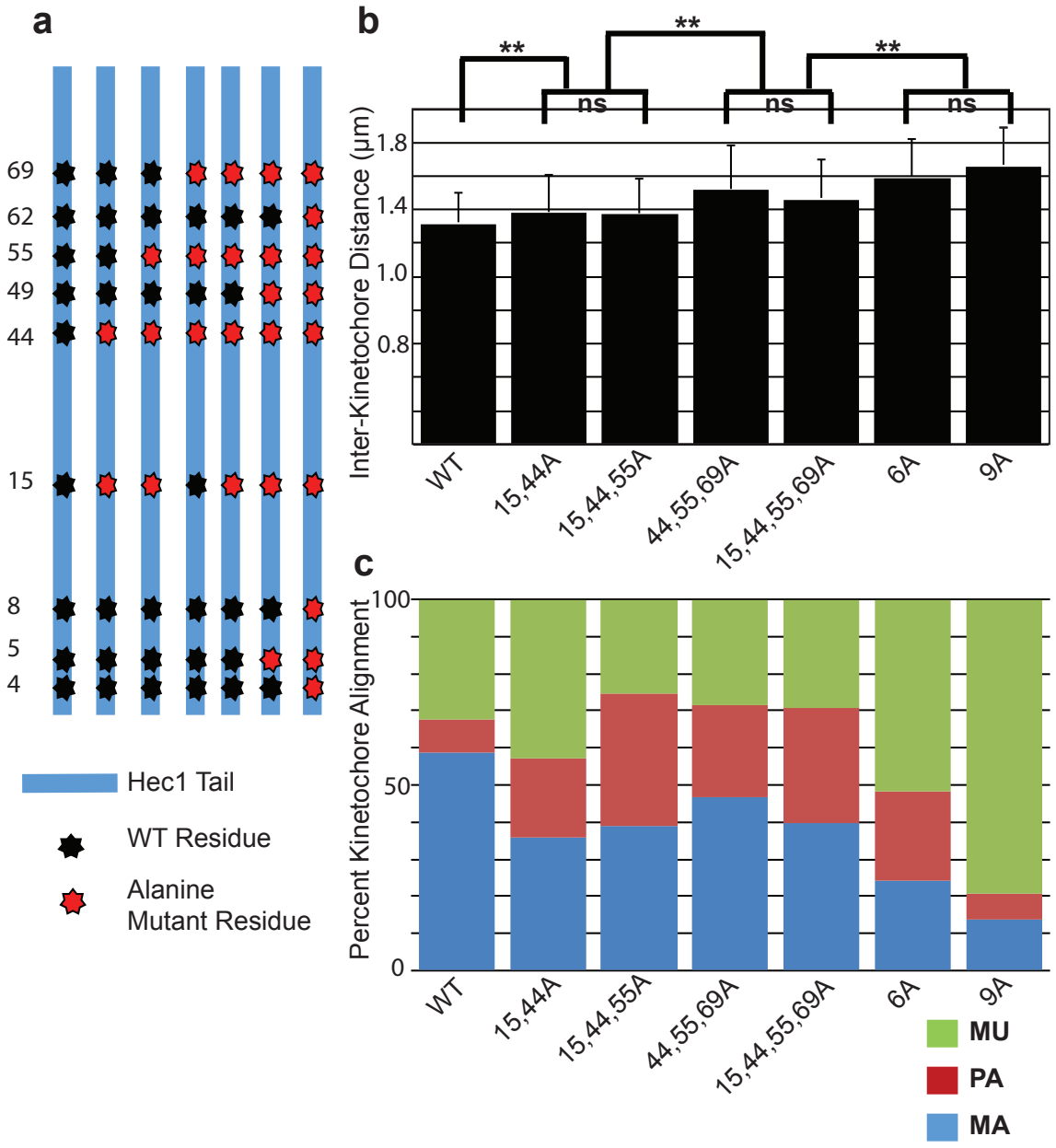

Figure 7: Inter-kinetochore distances and alignment defects from limited Hec1 phospho-site availability. A) Schematic depicting alanine mutations (red stars) imparted on wild-type (WT) Hec1 phosphorylation sites (black stars). Residue numbers are indicated at the left. DNA constructs made by Jeanne Mick. B) Inter-kinetochore distances measured in Ptk1 cells after siRNA depletion of Hec1 and GFP-Hec1 fusion protein rescue. ns--not statistically significant. **--p=<0.01 by Student's t-test. n=125, 133, 115, 227, 126, 196, and 84 kinetochores respectively from at least 3 experiments. C) Graph showing percent of kinetochores aligned to metaphase plate. Blue: Mostly Aligned (0-2 pairs off the plate), red: Partially Aligned (3-6 pairs off plate), green: Mostly Unaligned (>6 pairs off plate).

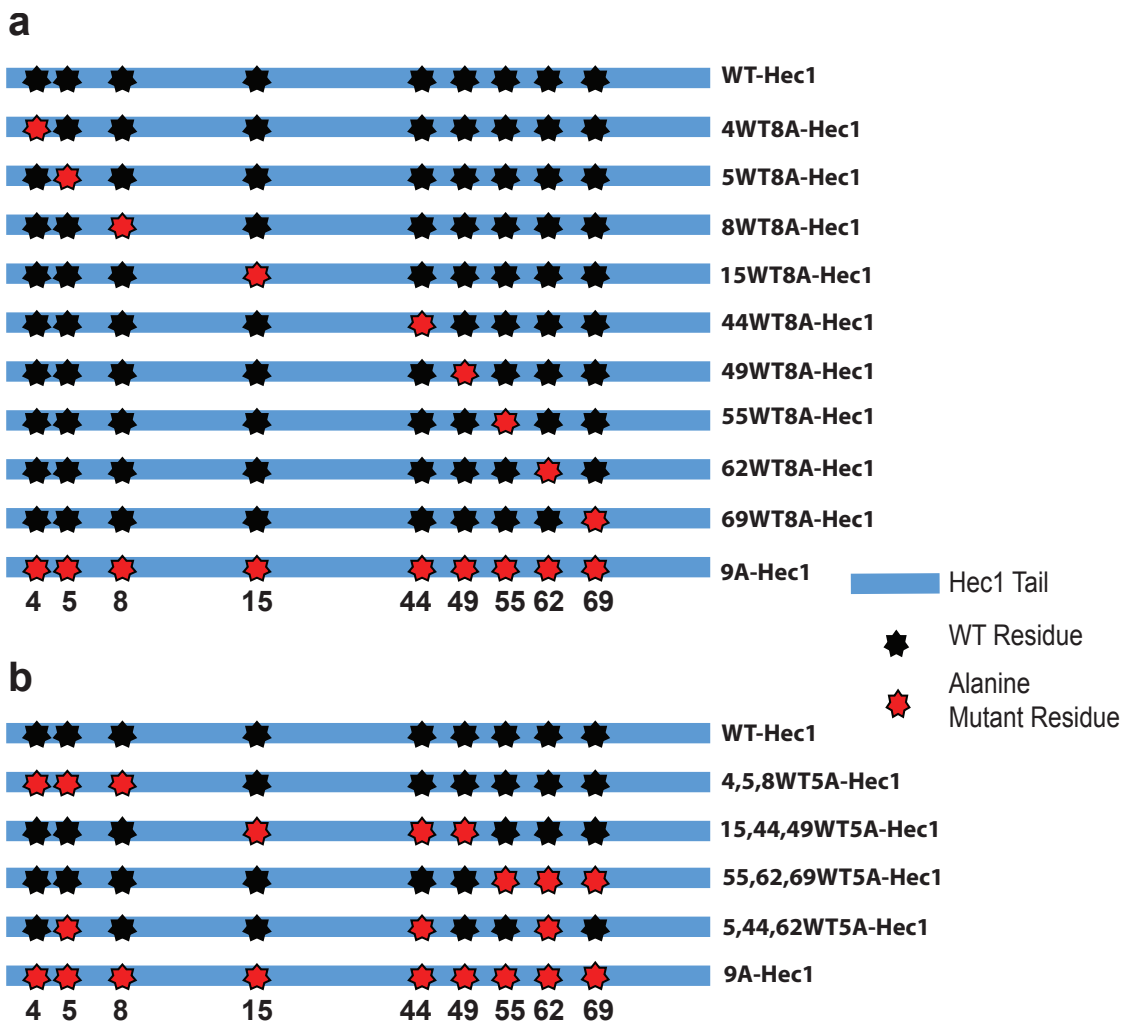

Figure 8: Schematic representation of Hec1 mutants to be used to determine the importance of ABK phosphorylation site location. A) Depiction of 1WT8A-Hec1-GFP mutants. Blue bars represent Hec1 tail. Black stars indicate wild-type (WT) residues, red stars indicate alanine mutated residues. Residue numbers indicated below. B) Depiction of 3WT5A-Hec1-GFP mutants. Blue bars represent Hec1 tail. Black stars indicate wild-type residues; red stars indicate alanine mutated residues. Residue numbers indicated below.

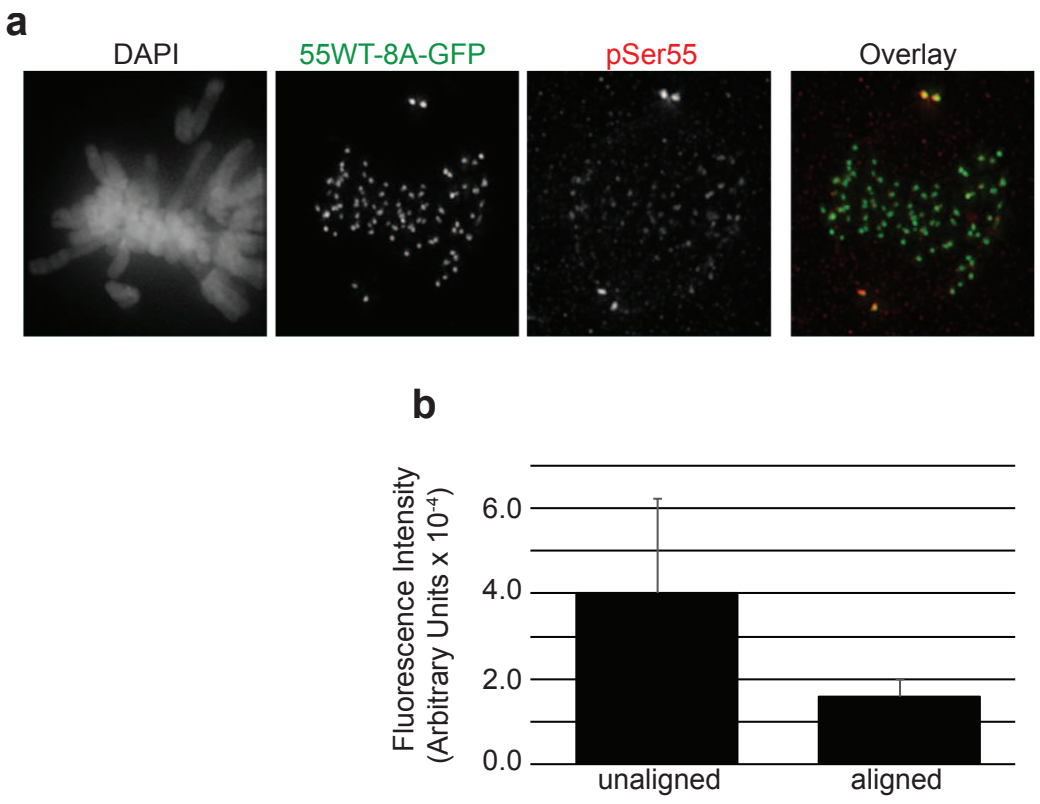

Figure 9: Representative Ptk1 cell expressing a WT8A-Hec1-GFP plasmid. A) Ptk1 depleted of endogenous Hec1 expressing 55WT-8A-GFP. Cell is fixed and labeled with antibody for phosphorylated serine 55. B) Fluorescence intensity of pSer55 is quantified showing the decline in the phosphorylated residue when aligned to the metaphase plate. It is these aligned kinetochores that are evaluated for oscillation behavior and inter-kinetochore distances.

Chapter 3: Stable Kinetochore-Microtubule Attachment is Sufficient to Silence the Spindle Assembly Checkpoint in Human Cells[1]

3.1 Brief Introduction

During mitosis, duplicated sister chromatids attach to microtubules emanating from opposing sides of the bipolar spindle through large protein complexes called kinetochores. In the absence of stable kinetochore–microtubule attachments, a cell surveillance mechanism known as the spindle assembly checkpoint (SAC) produces an inhibitory signal that prevents anaphase onset. Precisely how the inhibitory SAC signal is extinguished in response to microtubule attachment remains unresolved. To address this, we induced formation of hyper-stable kinetochore–microtubule attachments in human cells using a non- phosphorylatable version of the protein Hec1, a core component of the attachment machinery. We find that stable attachments are sufficient to silence the SAC in the absence of sister kinetochore bi-orientation and strikingly in the absence of detectable microtubule pulling forces or tension. Furthermore, we find

[1] The work presented in this chapter was published as a research article in 2015 under the same title. Figures presented in the original manuscript as supplementary figures, due to length constraints, are shown in this chapter as main figures and supplementary movies are not referenced.

J.G.D and I conceived the idea for the project, designed the experiments, analyzed the data and prepared the manuscript. I conducted the experiments. Frederick J. Boehm performed statistical modeling and hypothesis testing of kinetochore distance measures.

Tauchman, E.C., Boehm, F.J., and DeLuca, J.G. (2015) Stable kinetochore-microtubule attachment is sufficient to satisfy the spindle assembly checkpoint in human cells. *Nature Communications*. 6:10036

that SAC satisfaction occurs despite the absence of large changes in intra-kinetochore distance, suggesting that substantial kinetochore stretching is not required for quenching the SAC signal.

3.2 Introduction

Accurate segregation of duplicated chromosomes in mitosis is critical for the viability of daughter cells and for the maintenance of genomic integrity. Incorrect chromosome segregation can result in aneuploidy, a condition associated with tumorigenesis and developmental defects (Holland and Cleveland, 2009). On mitotic entry, dynamic microtubules form a bipolar spindle, which is responsible for capturing and congressing mitotic chromosomes. These events require proper attachment between spindle microtubule plus ends and kinetochores, large protein structures built on centromeric chromatin (Santaguida and Musacchio, 2009; Westhorpe and Straight, 2013). In order for cells to successfully complete mitosis, chromosomes must congress to the spindle equator and generate amphitelic kinetochore attachments, in which each sister kinetochore is connected to microtubules from each of the two opposite poles. In the absence of such attachments the cell will delay mitotic exit.

The mechanism that monitors and responds to kinetochore–microtubule attachment is called the spindle assembly checkpoint (SAC). In the presence of unattached kinetochores, SAC proteins form a complex that inhibits the anaphase promoting complex/cyclosome by binding to its activator, Cdc20 (Foley and Kapoor, 2013; Jia et al., 2013; Lara-Gonzalez et al., 2012; Musacchio, 2011). Precisely how the inhibitory SAC signal is extinguished in response to microtubule binding remains unresolved, although both the physical engagement of microtubules with core

kinetochore–microtubule attachment factors and the ensuing tension that follows are considered to be important aspects of the signaling process (Kops and Shah, 2012; Maresca and Salmon, 2010).

In the case of correctly attached bi-oriented sister kinetochore pairs, kinetochore microtubules are stabilized, at least in part, in response to a decrease in Aurora B kinase phosphorylation of outer kinetochore substrates including Hec1/Ndc80 and KNL1 (DeLuca et al., 2011; Welburn et al., 2010). Decreased phosphorylation of these substrates results in kinetochore–microtubule stabilization, development of inter-kinetochore tension, and SAC silencing (Foley and Kapoor, 2013; Funabiki and Wynne, 2013; van der Horst and Lens, 2014; Musacchio, 2011). Although it is well-accepted that kinetochore tension develops after formation of bi-oriented kinetochore–microtubule attachments, there is also evidence that tension itself can impact kinetochore–microtubule stability (Sarangapani and Asbury, 2014). Classic experiments in grasshopper spermatocytes demonstrated that pulling on kinetochores with a microneedle resulted in kinetochore–microtubule stabilization (Li and Nicklas, 1995). More recently it was shown that syntelic kinetochore–microtubule attachments can be stabilized in Drosophila cells by experimentally increasing polar ejection forces, and thereby increasing kinetochore tension (Cane et al., 2013). Finally, application of tension to purified budding yeast kinetochores has been shown to activate a ‘catch-bond’ mechanism that directly stabilizes microtubule attachment (Akiyoshi et al., 2010). It is clear that kinetochore–microtubule attachments can be stabilized by changes in kinetochore kinase activity and by application of tension, and in cells, these two mechanisms likely work together to increase kinetochore–microtubule stability

(Sarangapani and Asbury, 2014). An issue that still remains unresolved, however, is whether the presence of stable kinetochore microtubules is sufficient to induce changes in the kinetochore that lead to SAC silencing, or if kinetochore tension is additionally required. This issue has been difficult to address, since on chromosome bi-orientation and formation of correct kinetochore–microtubule attachments the development of kinetochore tension is a consequence. Despite this, there is evidence that microtubule attachment itself is sufficient for SAC silencing. In a landmark study by the Rieder lab using PtK1 cells, a single remaining unattached kinetochore was laser ablated, which resulted in silencing the SAC and entry into anaphase (Rieder et al., 1995). In this case, tension between the two sister kinetochores (typically monitored by the distance between kinetochores) was surely lost, pointing to stable microtubule attachment as the critical parameter monitored by the SAC. However, it is likely that the remaining kinetochore was still under tension, resulting from pulling forces produced by the attached microtubules and pushing forces produced from polar (Cane et al., 2013; Khodjakov and Pines, 2010; Nezi and Musacchio, 2009) ejection forces . A later study demonstrated that the addition of taxol, which resulted in loss of inter-kinetochore tension, but retention of stable kinetochore–microtubule attachment, resulted in eviction of the SAC protein Mad2 from kinetochores in PtK1 cells (Waters et al., 1998), providing further support for the idea that stable attachment is sufficient to silence the SAC. Similar to the laser ablation study, it is likely that in the presence of taxol, individual kinetochores remained under tension (McEwen and Dong, 2009). This is important to consider, since recent studies have suggested that tension within individual kinetochores, detected by displacement of outer kinetochore components from the inner

kinetochore (referred to as ‘intra-kinetochore stretching’), on microtubule attachment is the signal detected by the SAC machinery to silence the checkpoint and initiate anaphase (Maresca and Salmon, 2009; Uchida et al., 2009). Although intra-kinetochore distance increases on microtubule attachment and is indeed correlated to SAC satisfaction (Maresca and Salmon, 2009; Suzuki et al., 2014; Uchida et al., 2009), it remains to be determined if intra-kinetochore stretching serves as the critical signal for SAC silencing. Alternatively, increased intra-kinetochore distances may result from changes in kinetochore architecture that are a consequence of stable kinetochore–microtubule attachment, which ultimately signals to quench SAC activation (Khodjakov and Pines, 2010; Nezi and Musacchio, 2009).

Here we investigate how hyper-stabilization of kinetochore–microtubule attachment affects progression through mitosis and SAC satisfaction in the absence of chromosome bi-orientation. To induce kinetochore–microtubule hyper-stabilization, we used a mutant version of the kinetochore–microtubule attachment factor Hec1 that is unable to be phosphorylated by Aurora B kinase: 9A-Hec1, in which nine identified Aurora B target sites were mutated to alanine (9A) (DeLuca et al., 2011). Our previous studies demonstrated that cells depleted of endogenous Hec1 and rescued with 9A-Hec1-GFP harbour hyper-stable kinetochore microtubules and exhibit an increased number of erroneous attachments (DeLuca et al., 2011; Zaytsev et al., 2014). Here we find that the hyper-stable kinetochore–microtubule attachments in cells expressing 9A-Hec1-GFP are sufficient to silence the SAC, even in the absence of chromosome bi-orientation or experimentally induced tension. In addition, we find that SAC silencing

occurs in the absence of large changes in intra-kinetochore distance, suggesting that substantial intra-kinetochore stretching is not required for quenching the SAC signal.

3.3 Results

9A-Hec1 Cells With Unaligned Chromosomes Satisfy the SAC

The kinetochore protein Hec1/Ndc80 directly links kinetochores to microtubules in metazoans (Alushin et al., 2010; Cheeseman et al., 2006). We previously demonstrated that cultured vertebrate cells expressing a mutant Hec1 that cannot be phosphorylated by Aurora B kinase on its disordered 'tail' domain (9A-Hec1) generate hyper-stable kinetochore– microtubule attachments as evidenced by: (i) increased inter-kinetochore distances, (ii) thicker kinetochore fibres and (iii) an accumulation of syntelic attachments, in which both sister kinetochores of a pair are attached to a single pole (DeLuca et al., 2006, 2011; Guimaraes et al., 2008; Zaytsev et al., 2014). To determine if these latter incorrect attachments are sufficient to satisfy the SAC, we time-lapse imaged HeLa cells inducibly expressing GFP-labelled 9A-Hec1 or wild-type (WT)-Hec1 (Figure 10a). Indeed, the majority of cells expressing 9A-Hec1 entered anaphase in the presence of one or more pole-associated, syntelically attached chromosomes (Figure 11a–c).

To determine if 9A-Hec1-expressing cells enter anaphase as a consequence of SAC defects, we quantified SAC protein levels at kinetochores following nocodazole-mediated microtubule depolymerization. Cells expressing 9A-Hec1 recruited equivalent levels of Mad1 and BubR1 to kinetochores as WT cells (Figure 11d,e). Furthermore, 9A-Hec1-expressing cells exhibited a robust mitotic arrest after incubation in 5 μM

nocodazole that was indistinguishable from cells expressing WT-Hec1 (Figure 12b,c). We repeated these experiments under conditions in which endogenous Hec1 was depleted by RNAi and found identical results (Figure 10b and 12b,d).

We next determined whether the kinetics of SAC satisfaction were similar in 9A-Hec1 and WT-Hec1- expressing cells in the absence of microtubules. For this experiment, we treated cells expressing either WT- or 9A-Hec1 with nocodazole to depolymerize all microtubules and subsequently incubated cells in reversine, a small molecule inhibitor of Mps1, which is known to induce rapid SAC abrogation (Santaguida et al., 2010). As shown in Figure 12, the kinetics of mitotic exit on reversine treatment between the two cell lines were indistinguishable. We conclude from these experiments that 9A-Hec1-expressing cells are not defective in SAC signaling, but progress through mitosis with pole-associated chromosomes as a consequence of SAC satisfaction.

Stable Kinetochore–Microtubule Attachment Silences the SAC

To further investigate the link between SAC satisfaction and stable kinetochore–microtubule attachment in the absence of pulling forces from chromosome bi-orientation, we created conditions whereby cells entirely lack proper kinetochore-microtubule attachments. Cells with monopolar spindles, generated by inhibition of Eg5 with S-trityl-L-cysteine (STLC), contain a large number of monotelic and syntelic attachments (Kapoor et al., 2000; Mayer et al., 1999; Ogo et al., 2007). Consequently, cells mount a mitotic arrest due to the activity of the Aurora B kinase-mediated error-correction machinery, which destabilizes incorrectly attached microtubules (Kapoor et al., 2000; Mayer et al., 1999). STLC-treated cells expressing WT-Hec1 largely arrested

in mitosis owing to the presence of a large number of unattached kinetochores, as evidenced by retention of Mad1 on kinetochores (Figure 13).

In contrast, 9A-Hec1-expressing cells treated with STLC formed stable attachments as evidenced by formation of robust kinetochore–microtubule bundles and loss of kinetochore Mad1, and subsequently exited mitosis (Figure 13). This result suggests that stabilized kinetochore–microtubule attachments, even in the absence of chromosome bi-orientation, are sufficient to satisfy the SAC and promote mitotic exit. We repeated these experiments in WT- and 9A-Hec1-expressing cells depleted of endogenous Hec1, which produced the same result (Figure 14). Furthermore, addition of ZM447439 to inhibit Aurora B kinase, which serves to destabilize kinetochore–microtubule attachments (Cimini et al., 2006; Ditchfield et al., 2003) (and also may contribute to SAC signaling by synergizing with other SAC proteins) (Santaguida et al., 2011), resulted in gradual SAC satisfaction and mitotic exit (Supplementary Figure 15). Consistent with our finding that 9A-Hec1-expressing cells satisfy rather than abrogate the SAC, the kinetics of mitotic exit in 9A-Hec1-expressing cells were similar to ZM447439-treated host (parental) HeLa cells, but not to host cells treated with 10 mM reversine, which results in rapid SAC abrogation and subsequent mitotic exit (Santaguida et al., 2010) (Figure 15). Finally, to test if the mitotic exit observed in 9A-Hec1-expressing cells was indeed due to SAC satisfaction and not mitotic slippage, we expressed an mCherry-tagged version of Cyclin B in cells stably expressing 9A- and WT-Hec1 and measured loss of Cyclin B fluorescence over time (Figure 16). In all cells, loss of Cyclin B preceded mitotic exit, suggesting that mitotic slippage was not responsible for the observed exit from mitosis in cells expressing 9A-Hec1-GFP.

Stable MTs Induce Small Changes in Kinetochore Architecture

A current model for SAC satisfaction posits that 'stretching' of individual kinetochores, in which the outer kinetochore is pulled away from the inner kinetochore, is the critical event detected by the SAC-silencing machinery (Maresca and Salmon, 2009; Uchida et al., 2009). Using super-resolution co-localization microscopy (Figure 17), we therefore tested if kinetochores on pole-proximal chromosomes in 9A-Hec1-expressing cells (Figure 11a) experienced such stretching before mitotic exit. We first measured intra-kinetochore distances on kinetochores of bi-oriented chromosomes to establish the 'full' stretch level. In 9A-Hec1-expressing cells, the average distance from CENP-C (an inner kinetochore marker) to the C-terminal GFP tag on Hec1 on bi-oriented kinetochores was ~46nm, which was slightly larger than the distance measured in WT-Hec1-expressing cells (~40 nm; Figure 18 and Table 1) (Wan et al., 2009). We then measured intra-kinetochore distances in cells treated with 5 μM nocodazole to establish the 'rest length'. Under these conditions, the average CENP-C to Hec1-C-term distance was similar (~14nm) in both WT- and 9A-Hec1-expressing cells (Figure 18c and Table 1). In the case of kinetochores on pole-proximal chromosomes in 9A-Hec1-expressing cells, the intra-kinetochore distances were slightly larger than the measured rest length (~28 versus ~14nm; Figure 18c and Table 1). These results suggest that stable kinetochore–microtubule attachments in the absence of chromosome bi-orientation generate a rearrangement of kinetochore proteins that produces a small, but significant, displacement of the outer kinetochore from the inner kinetochore.

Consistent with this finding, the average intra-kinetochore distance in 9A-Hec1-expressing cells treated with STLC was ~29nm, compared with ~20nm in cells

expressing WT-Hec1 (Figure 18c and Table 1). These results demonstrate that SAC satisfaction occurs in cells that form stable kinetochore–microtubule attachments in the absence of large-scale intra-kinetochore ‘stretch.’ Nevertheless, microtubule binding to kinetochores, even in cells that lack bi-oriented chromosomes, results in small, but measurable changes in kinetochore architecture. MT attachment silences the SAC in the absence of tension. On the basis of these results, we formulated two hypotheses. In the first hypothesis, SAC silencing in STLC-treated 9A-Hec1- expressing cells results from kinetochore tension produced via pulling forces from the attached microtubules. Support for this comes from a recent study, which found that syntelically attached kinetochores were competent to silence the SAC in Drosophila S2 cells, but only after polar ejection forces were experimentally increased (Cane et al., 2013). In this case, tension arises from the opposition of kinetochore–microtubule poleward forces and chromosome-arm-mediated anti-poleward forces. In the second hypothesis, the accumulation of stable microtubules bound to the core kinetochore–microtubule attachment molecules signals for SAC satisfaction independently of the tension that results from external pulling or pushing forces. To differentiate between these two possibilities, we set out to generate conditions in which kinetochores are stably bound to microtubules in the absence of spindle pole-dependent pushing or pulling forces. We achieved this by treating cells expressing either 9A- or WT-Hec1 with a moderately low dose (300 nM) of nocodazole, which resulted in the loss of all non-kinetochore spindle microtubules but retention of kinetochore–microtubule ‘tufts,’ which were comprised

Table 1: Summary of mean values of inter- and intra-kinetochore distances measured in HeLa cells expressing WT- or 9A-Hec1-GFP.

		Inter-kinetochore distance, μm	Intra-kinetochore distance, nm	N kinetochores/N cells
WT-Hec1	Aligned	1.17 (0.08)	40.2 (4.9)	450/30
9A-Hec1	Aligned	1.34 (0.11)	46.2 (5.6)	414/30
9A-Hec1	Polar	0.95 (0.05)	28.9 (10.2)	21/14
WT-Hec1	5 μM noco	0.73 (0.04)	15.1 (5.6)	101/15
9A-Hec1	5 μM noco	0.73 (0.04)	13.2 (6.0)	104/15
WT-Hec1	5 μM STLC	0.81 (0.08)	20.0 (7.0)	194/30
9A-Hec1	5 μM STLC	0.93 (0.08)	29.4 (6.8)	258/30
WT-Hec1	300 nM noco	0.71 (0.05)	12.6 (8.7)	214/30
9A-Hec1	300 nM noco	0.73 (0.08)	20.0 (10.4)	163/30

Values indicate mean distances; numbers in parentheses indicate s.e.m. The first three rows display mean inter- and intra-kinetochore distances of aligned sister kinetochore pairs in cells expressing either WT- or 9A-Hec1-GFP with no drug treatment and pole-proximal kinetochore pairs in cells expressing 9A-Hec1-GFP with no drug treatment. All other conditions are indicated.

of short microtubule bundles attached to kinetochores (Figure 19a). As expected, cells expressing WT-Hec1 arrested in mitosis in response to 300 nM nocodazole treatment. Strikingly, similarly treated cells expressing 9A-Hec1 exited mitosis after a delay (Figure 19b,c). Mitotic exit resulted as a consequence of SAC satisfaction as evidenced by a significant decrease in Mad1-positive kinetochores (Figure 19d). We then tested if occupancy of kinetochore-microtubule-binding sites resulted in architectural changes in kinetochores in cells treated with 300 nM nocodazole. Under these conditions, the average distance between CENP-C and Hec1-C-term in 9A-Hec1-expressing cells was ~20 nm, whereas the distance in WT-Hec1-expressing cells was ~13 nm, which is equivalent to the rest length (Figure 19e and Table 1). Together, these results suggest that stable kinetochore–microtubule-binding signals for SAC satisfaction independent of tension, and furthermore, that microtubule occupancy at kinetochores results in small, but detectable changes in kinetochore protein architecture.

3.4 Discussion

It is well-established that formation of stable, end-on kinetochore–microtubule attachments quenches the 'wait-anaphase' signal generated by the SAC. Although it is not yet clear how microtubule attachment turns the SAC off, recent studies have suggested that pulling forces provided by end-on attached microtubules 'stretch' individual kinetochores, which leads to SAC satisfaction (Maresca and Salmon, 2009; Uchida et al., 2009). How might intra-kinetochore stretching promote SAC silencing? The prevailing model is that increasing the distance between outer kinetochore components and centromere-localized Aurora B prevents their phosphorylation (Lampson and Cheeseman, 2011; Liu et al., 2009; Maresca and Salmon, 2010). This in turn, is predicted to promote to SAC silencing by tipping the balance towards kinetochore phosphatases such as PP1, whose increased kinetochore localization and activity promotes the delocalization of key checkpoint proteins, leading to SAC satisfaction (Foley and Kapoor, 2013; Funabiki and Wynne, 2013; London and Biggins, 2014; Sacristan and Kops, 2015).

In this study, we find that stable kinetochore–microtubule attachment is sufficient to silence the SAC in the absence of large- scale changes in either inter-kinetochore or intra-kinetochore distance. Our data argue that tension, per se, is not a parameter read by the checkpoint machinery. How does the SAC detect and respond to stable kinetochore–microtubule attachment in the absence of 'stretching' or tension? Two recent studies have demonstrated that end-on microtubule binding to the NDC80 complex promotes displacement of the SAC protein kinase Mps1 from kinetochores (Hiruma et al., 2015; Ji et al., 2015). Mps1 phosphorylates the kinetochore scaffold

protein KNL1 to recruit, either directly or indirectly, a suite of checkpoint proteins including Bub1, BubR1, Bub3, Mad1 and Mad2 (Caldas and DeLuca, 2014; Sacristan and Kops, 2015), thus eviction of Mps1 leads to delocalization of these SAC components and subsequent SAC satisfaction. In addition, stable microtubule attachment has been shown to promote dissociation of SAC proteins through the minus-end directed dynein motor, which 'strips' SAC components off kinetochores along spindle microtubules, thereby contributing to checkpoint silencing (Kops and Shah, 2012). Finally, it is possible that stable microtubule occupancy results in biochemical and/or conformational changes in kinetochore proteins that promote the dissociation of SAC-promoting proteins such as Aurora B kinase or the SAC proteins themselves, or alternatively, in the recruitment of SAC-silencing proteins such as the phosphatase PP1 (Caldas and DeLuca, 2014; Foley and Kapoor, 2013; Funabiki and Wynne, 2013; Sacristan and Kops, 2015; Stukenberg and Burke, 2015).

Here we established experimental conditions that prevented chromosome bi-orientation and the generation of opposing pulling forces on sister kinetochores. In one scenario, cells were treated with STLC to generate monopolar spindles in which chromosomes were either syntelically or monotelically oriented. In another, cells were treated with 300nM nocodazole to create conditions in which most spindle microtubules were depolymerized and very short kinetochore fibres were retained. In both cases, 9A-Hec1-expressing cells were able to satisfy the SAC and exit mitosis. On average, the time to mitotic exit after nuclear envelope breakdown in the presence of STLC was significantly longer than in untreated cells. We predict that the increased time required to silence the SAC results from a gradual accumulation of stable kinetochore–

microtubule attachments. The relatively large distribution of times required for SAC satisfaction likely reflects a graded response of the SAC (Collin et al., 2013), in which the rate of formation of stable kinetochore–microtubule attachments correlates to the time required for SAC silencing. It is also important to note that intra-kinetochore distances were measured in a population of fixed cells that spent a variable amount of time arrested in mitosis (that is, some cells had just entered mitosis, while others were arrested for up to several hours), which in part explains the large distribution of distances. Nevertheless, these measurements revealed a very small (~10 nm), but statistically significant, difference in the average distance between CENP-C (an inner kinetochore protein) and the C-terminus of NDC80 (an outer kinetochore protein) in 9A- versus WT-Hec1-expressing cells. It is formally possible that this small increase in intra-kinetochore distance triggers SAC silencing. However, it is difficult to envision a scenario in which moving the outer kinetochore away from the inner kinetochore by such a small distance is sufficient to limit the access of Aurora B kinase, which is proposed to emanate as a gradient from the centromere, to outer kinetochore substrates. We propose instead that the small change in intra-kinetochore distance results from alterations in overall kinetochore architecture that are a consequence of stable microtubule binding. In support of this notion, a recent study from the Salmon lab demonstrated in HeLa cells that intra-kinetochore distances increased by ~10 nm on average from late prometaphase to metaphase, which represents the transition from SAC activation to SAC silencing (Suzuki et al., 2014). Interestingly, in this study, the authors demonstrated that the major drop in Aurora B kinase activity, measured using phospho-specific Hec1 antibodies, occurred at this transition from late prometaphase to

metaphase (Suzuki et al., 2014). Thus, the large decrease in Aurora B kinase activity at kinetochores does not coincide with a large-scale change in intra-kinetochore distance. This suggests, together with the findings from our study, that the SAC is not silenced by intra-kinetochore stretch and the spatial re-positioning of outer kinetochore components in relation to the inner kinetochore. Instead, it is likely that SAC silencing occurs owing to a cascade of biochemical and conformational changes within kinetochore proteins and protein complexes that are triggered by stable, end-on microtubule binding that lead to SAC protein eviction. How stable attachment signals such architectural changes that ultimately silence the SAC is not known, but likely involves conformational changes within both inner and outer kinetochore proteins, including CENP-C, CENP-T, KNL1 and the NDC80 complex (Ault and Nicklas, 1989; Dumont et al., 2012; Suzuki et al., 2011, 2014; Wan et al., 2009).

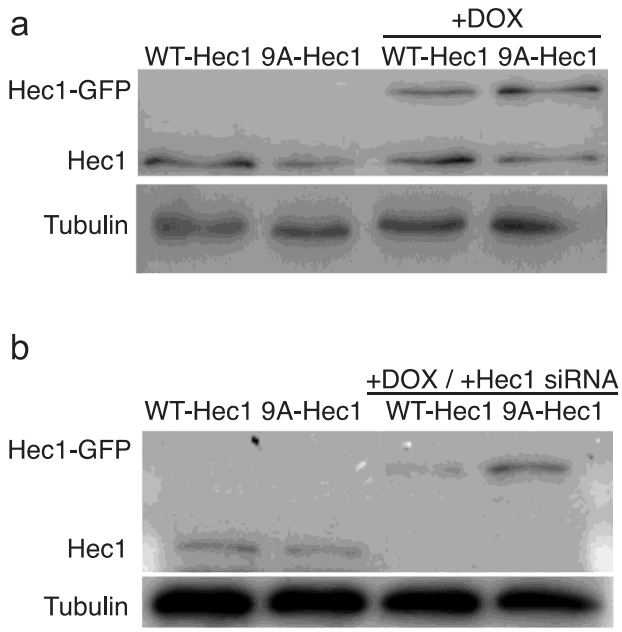

Figure 10: Western blot analysis of HeLa cells stably expressing WT- and 9A-Hec1-GFP. (a) Western blot showing endogenous Hec1 and exogenous WT- and 9A-Hec1-GFP in HeLa Flp-In cell lines. The first two lanes contain clarified cell lysates from uninduced cells; the last two lanes contain lysates from cells induced with doxycycline to express WT- or 9A-Hec1-GFP. Band intensities were quantified and averaged over three experiments. In doxycyline-treated cells, exogenous WT-Hec1-GFP expression levels were ~92% of endogenous Hec1 levels, and exogenous 9A-Hec1-GFP expression levels were ~106% of endogenous Hec1. Comparison of the expression levels of doxycyline-treated cells revealed that WT-Hec1-GFP levels were ~82% of 9A-Hec1-GFP levels over the entire cell population. By analyzing individual cells, we determined that, on average, a higher percentage of the doxycycline-induced 9A-Hec1-GFP cells were expressing the construct compared to the WT population. However, kinetochore fluorescence intensity measurements revealed nearly identical levels of kinetochore-associated WT- and 9A-Hec1-GFP. (b) Western blot showing endogenous Hec1 and exogenous WT- and 9A-Hec1-GFP in HeLa Flp-In cell lines treated with Hec1 siRNA. The first two lanes contain clarified cell lysates from uninduced cells; the last two lanes contain lysates from cells treated with doxycycline to induce expression of WT- or 9A-Hec1-GFP and depleted of endogenous Hec1. For these “knock-out / knock-in” experiments, similar to those above, we found that a higher percentage of the doxycycline- induced 9A-Hec1-GFP cells were expressing the stable construct compared to the WT population, however, kinetochore fluorescence intensity measurements revealed nearly identical levels of kinetochore-associated WT- and 9A-Hec1-GFP in individual cells.

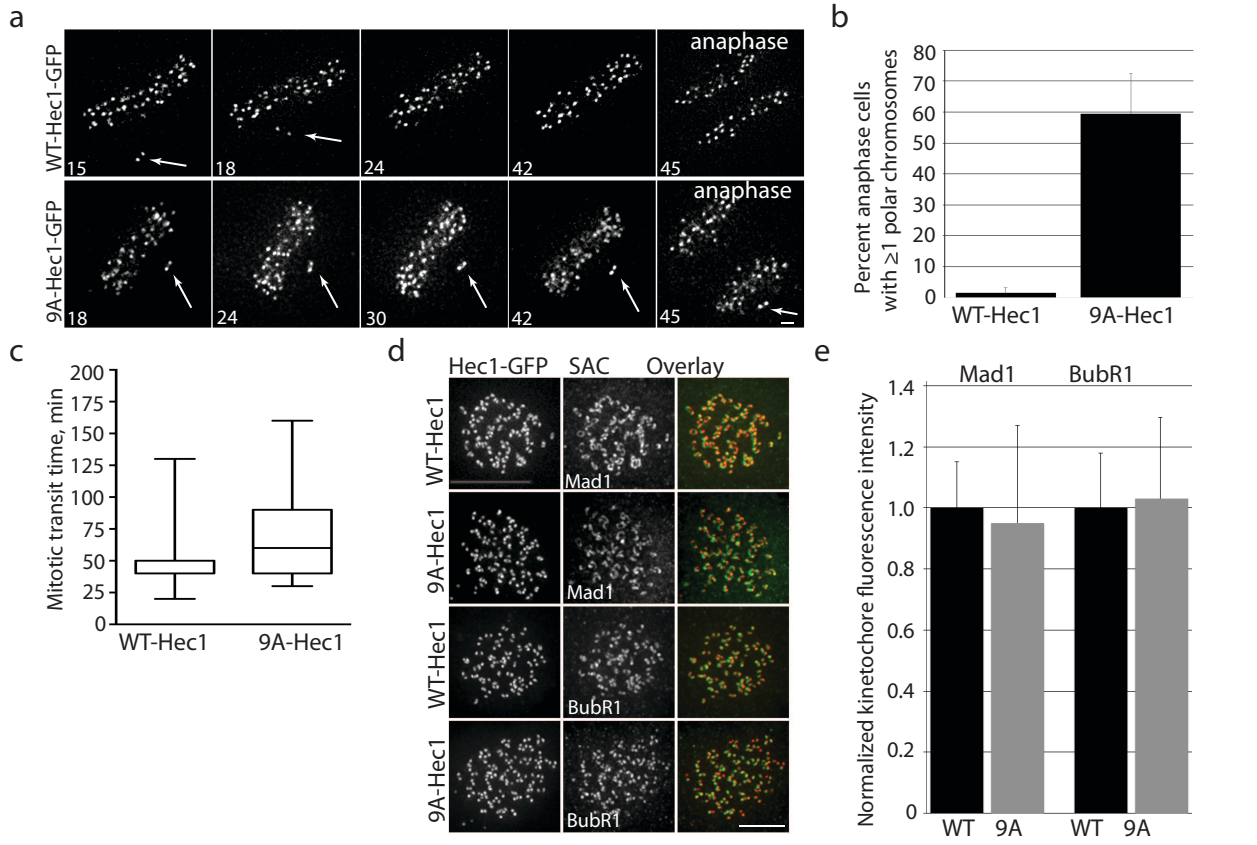

Figure 11: Cells expressing 9A-Hec1 satisfy the SAC and enter anaphase with pole-proximal chromosomes. (a) Time-lapse images of HeLa cells expressing WT- or 9A-Hec1-GFP. Cells expressing WT-Hec1-GFP enter anaphase only after all chromosomes are properly aligned at the metaphase plate. Cells expressing 9A-Hec1-GFP enter anaphase in the presence of polar, unaligned chromosomes. Arrows point to pole-proximal chromosomes. In the WT-Hec1-GFP-expressing cell shown, the pole-proximal chromosome eventually migrates to the metaphase plate. In the 9A-Hec1-GFP-expressing cell, the pole-proximal chromosome remains at the spindle pole, even after anaphase onset. Time, post-nuclear envelope breakdown, is shown in minutes. Scale bar, 5 μm. (b) Frequency of anaphase onset with pole-proximal chromosomes in WT- and 9A-Hec1-GFP-expressing cells. In all, 109 and 60 cells were scored, respectively, from three independent experiments. (c) Mitotic durations for WT- and 9A-Hec1-GFP-expressing cells. Mitotic duration was scored from cell rounding to cell cleavage. Average time in minutes is shown. n=100 cells for each condition. (d) Immuno-fluorescence images and (e) quantification of kinetochore fluorescence intensities of Mad1 (n=438 kinetochores for WT-Hec1-GFP-expressing cells; n=444 kinetochores for 9A-Hec1-GFP-expressing cells) and BubR1 (n=414 kinetochores for WT- and n=416 kinetochores for 9A-Hec1-GFP-expressing cells) from three independent experiments. Cells were treated with 5 μM nocodazole for 5 h. Error bars indicate standard deviation. NS=not significantly different, P=0.01, as evaluated by Student's t-test (Mad1, P=0.66, BubR1, P=0.92).

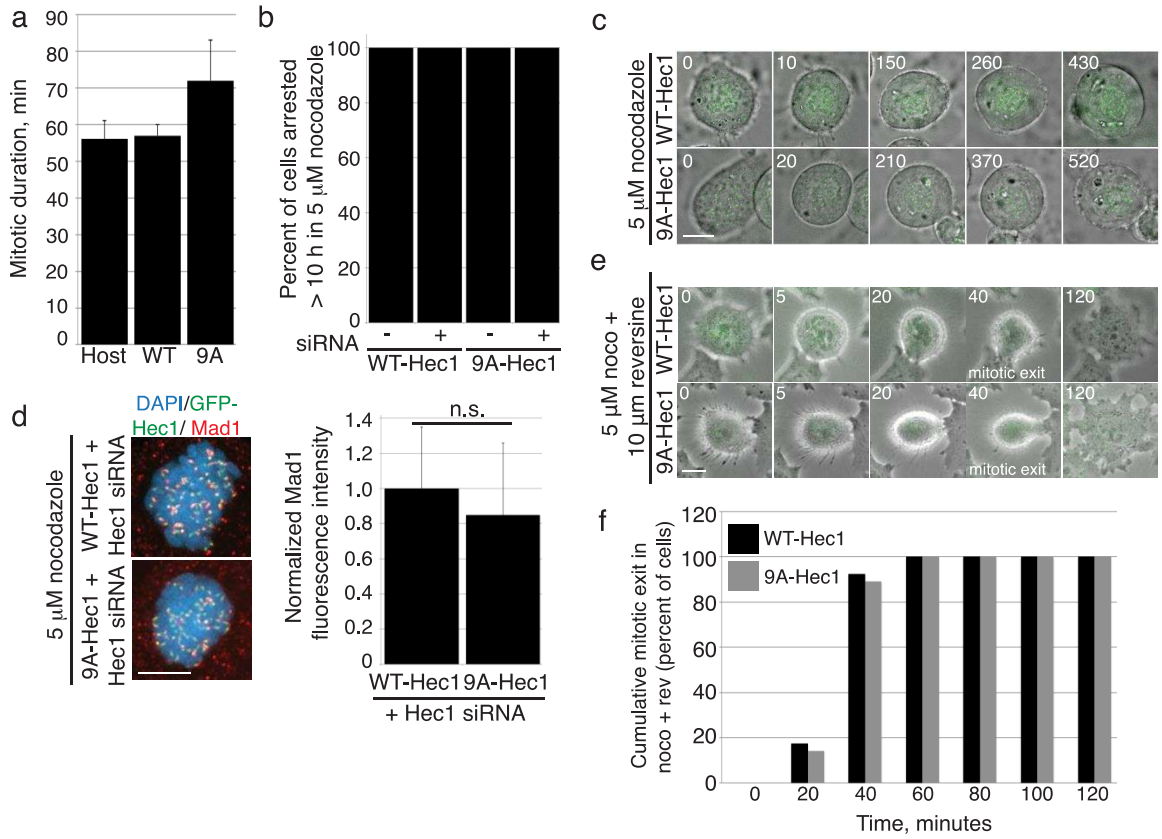

Figure 12: SAC signaling is functional in cells expressing WT- and 9A- Hec1-GFP. (a) Graph indicating mitotic transit times for the host HeLa cell line, WT-Hec1-GFP expressing cells, and 9A-Hec1-GFP expressing cells. Mitotic transit time was scored from cell rounding to anaphase onset. Bars indicate standard deviation. n=100 cells per condition. (b) Graph indicating the percent of cells arrested for greater than 10 hours in 5 μM nocodazole. For all cell lines shown, no cells were observed to exit mitosis. n=100 cells for WT/no siRNA; n=49 cells for WT/siRNA; n=100 cells for 9A/no siRNA; n=47 cells for 9A/siRNA. (c) Stills from time-lapse imaging of WT- and 9A-Hec1-GFP expressing cells treated with 5 μM nocodazole. Shown are overlays of phase-contrast and GFP images. Time is indicated in minutes. Scale bar is 10 μm. (d) Immuno-fluorescence images and quantification of kinetochore fluorescence intensities of Mad1 in WT- and 9A-Hec1-GFP-expressing cells depleted of endogenous Hec1. Error bars indicate standard deviation. For each cell line, 3 experiments were performed. n=299 kinetochores for WT- and n=291 kinetochores for 9A-Hec1-GFP expressing cells. Scale bar is 5 μm. n.s.=not significantly different, p=0.15, as evaluated by Student's t-test. (e) Representative images from time-lapse movies of WT- and 9A-Hec1-GFP expressing cells treated with nocodazole and reversine. Shown are overlays of phase-contrast and GFP images. Time is indicated in minutes. Scale bar is 10 μm. (f) Quantification of mitotic exit for the indicated cell lines treated with 5 μm nocodazole and 10 μm reversine. Bars indicate cumulative mitotic exit at the indicated time point. Shown is one representative experiment, n=50 cells for WT- and n=21 cells for 9A-Hec1-GFP expressing cells.

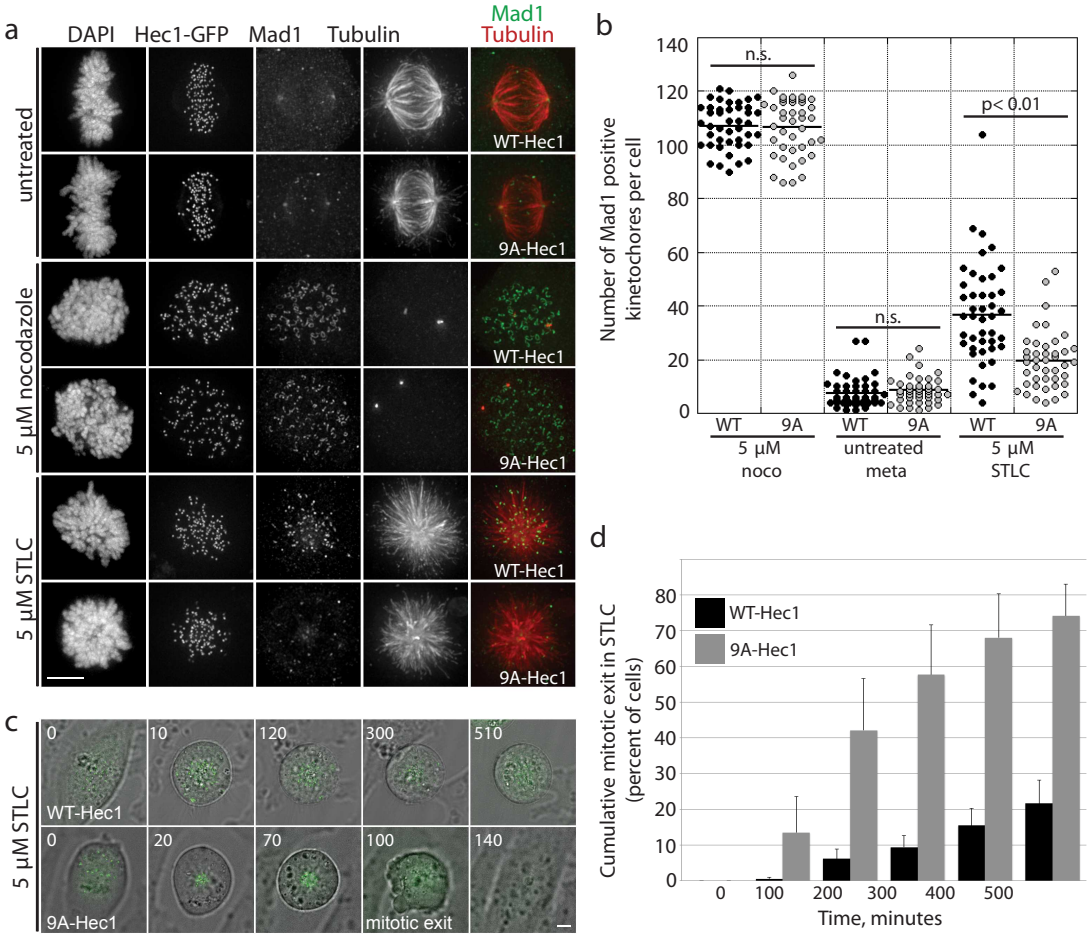

Figure 13: Stable kinetochore–microtubule attachment is sufficient to satisfy the SAC in the absence of chromosome bi-orientation. (a) Immunofluorescence images of cells expressing either WT- or 9A-Hec1-GFP, treated as indicated. Scale bars are 5 μm. (b) Quantification of Mad1-positive kinetochore staining. For the untreated (no drug) condition, only metaphase cells were scored. NS=not significantly different, P=0.01, as evaluated by Student's t-test (5 μM nocodazole-treated cells, P=0.88; untreated cells, P=0.39). For each condition, at least 41 cells were scored from three experiments. (c) Stills from time-lapse imaging of STLC-treated WT- and 9A-Hec1-GFP-expressing cells. Shown are overlays of phase contrast and GFP images. Time is indicated in minutes, and the time of mitotic exit (as evidenced by membrane blebbing and chromosome decondensation) is also indicated. Scale bar, 5 μm. (d) Quantification of mitotic exit time for WT- and 9A-Hec1-GFP-expressing cells. Graph indicates cumulative mitotic exit at the indicated time point. Data from three independent experiments are included, n=345 cells for WT- and n=212 cells for 9A-Hec1-GFP-expressing cells. Error bars indicate s.d.

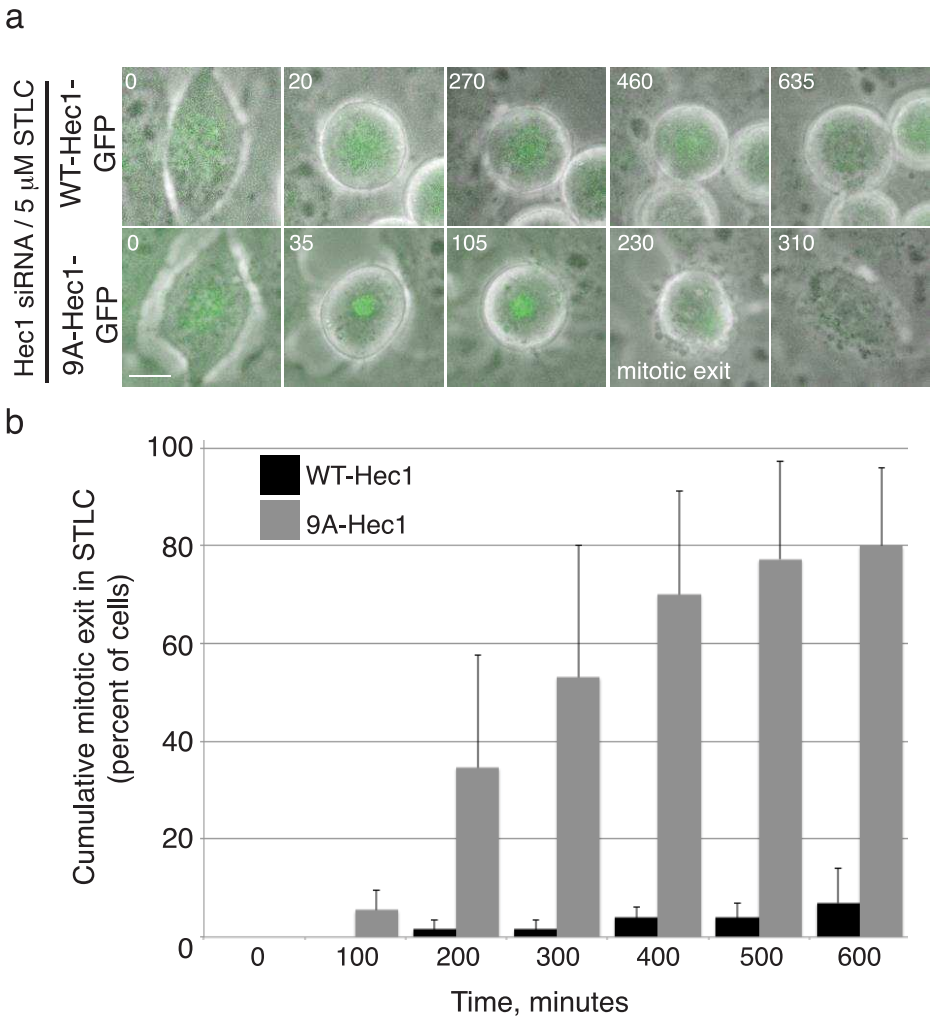

Figure 14: Stable kinetochore-microtubule attachment is sufficient to satisfy the SAC in cells expressing 9A-Hec1-GFP and depleted of endogenous Hec1. (a) Stills from time-lapse imaging of STLC-treated WT- and 9A-Hec1-GFP expressing cells depleted of endogenous Hec1. Shown are overlays of phase-contrast and GFP images. Time is indicated in minutes. Scale bar is 10 μm. (b) Quantification of mitotic exit for WT- and 9A-Hec1-GFP expressing cells depleted of endogenous Hec1. Graph indicates cumulative mitotic exit at the indicated time point. Data from two independent experiments are included, n=111 for WT- and n=85 for 9A-Hec1-GFP expressing cells. Error bars indicate standard deviation.

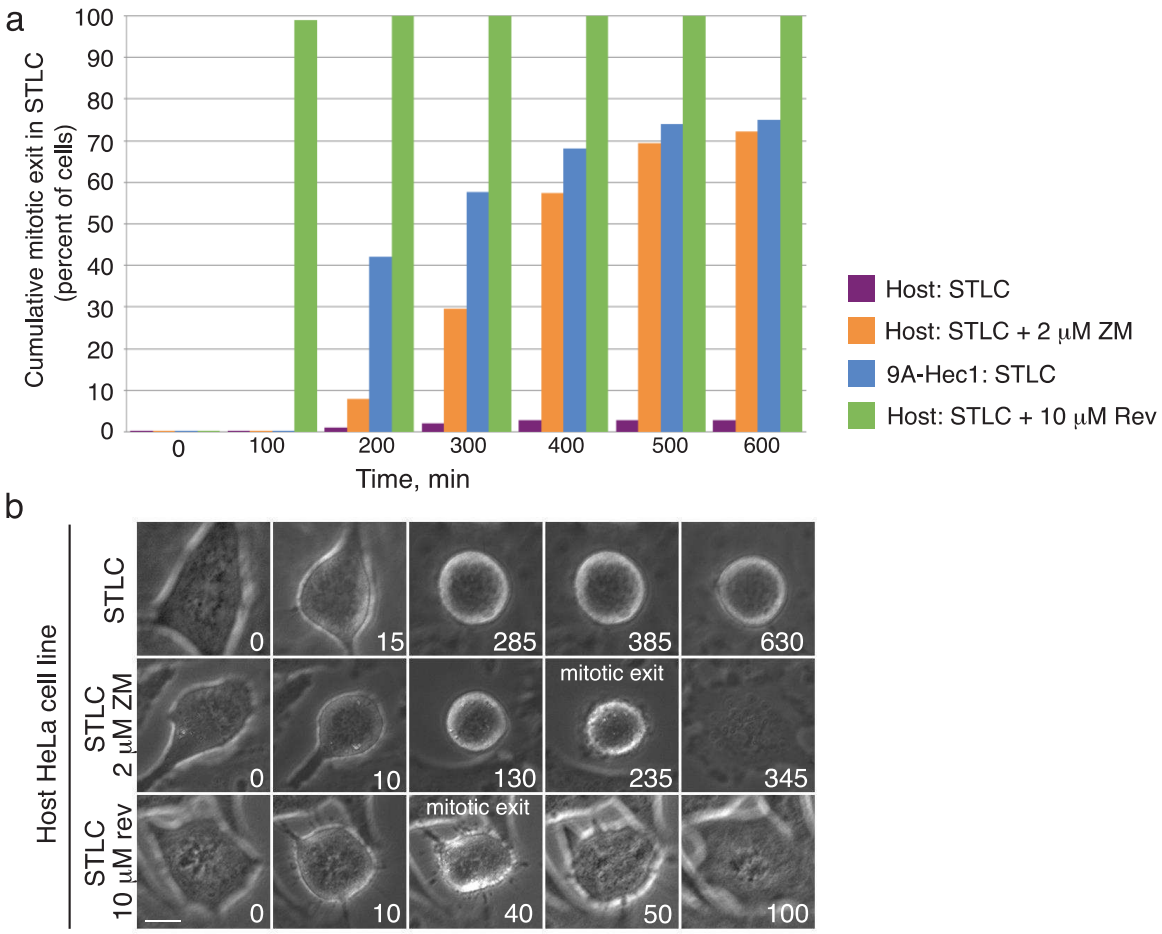

Figure 15: Formation of hyper-stable kinetochore-microtubule attachments results in SAC silencing, not SAC abrogation. (a) Quantification of mitotic exit for the indicated cell lines. Bars indicate cumulative mitotic exit at the indicated time point. Shown is one representative experiment in which 100 cells were measured per condition. (b) Representative images from time-lapse movies. Time is indicated in minutes. Scale bar is 10 μm.

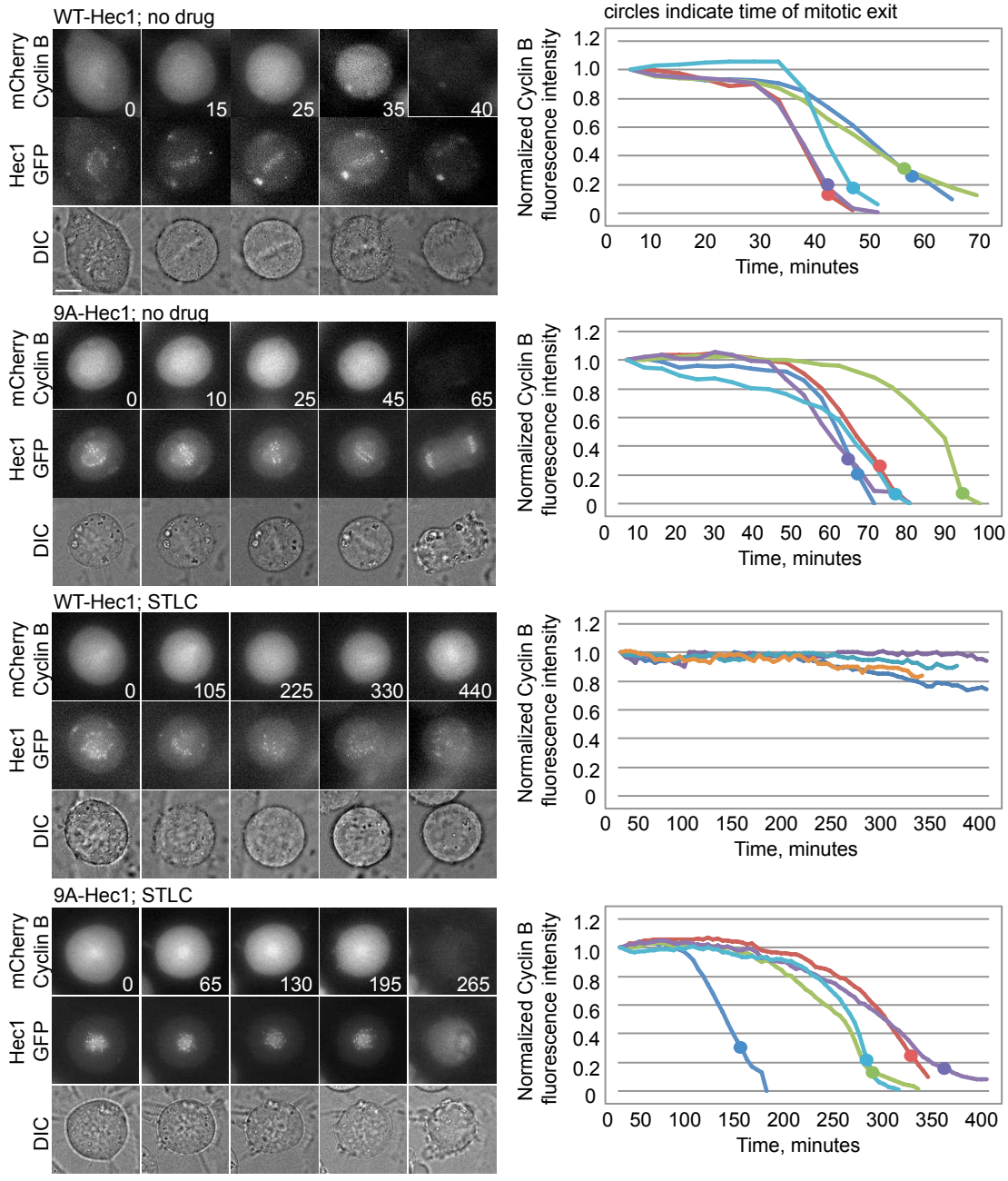

Figure 16: Mitotic exit in STLC-treated, 9A-Hec1-GFP expressing cells is not due to mitotic slippage. The indicated cells were transfected with mCherry-Cyclin B and imaged over time. Stills from time-lapses are shown on the left. Time is indicated in minutes. Scale bar is 10 μm. Shown on the right are graphs indicating normalized mCherry-Cyclin B whole-cell fluorescence intensity over time. Lines indicate representative individual cells. At least 12 cells were analyzed for each condition. Mitotic exit times are indicated by filled circles. In all cells, mitotic exit only occurred after loss of mCherry-Cyclin B fluorescence.

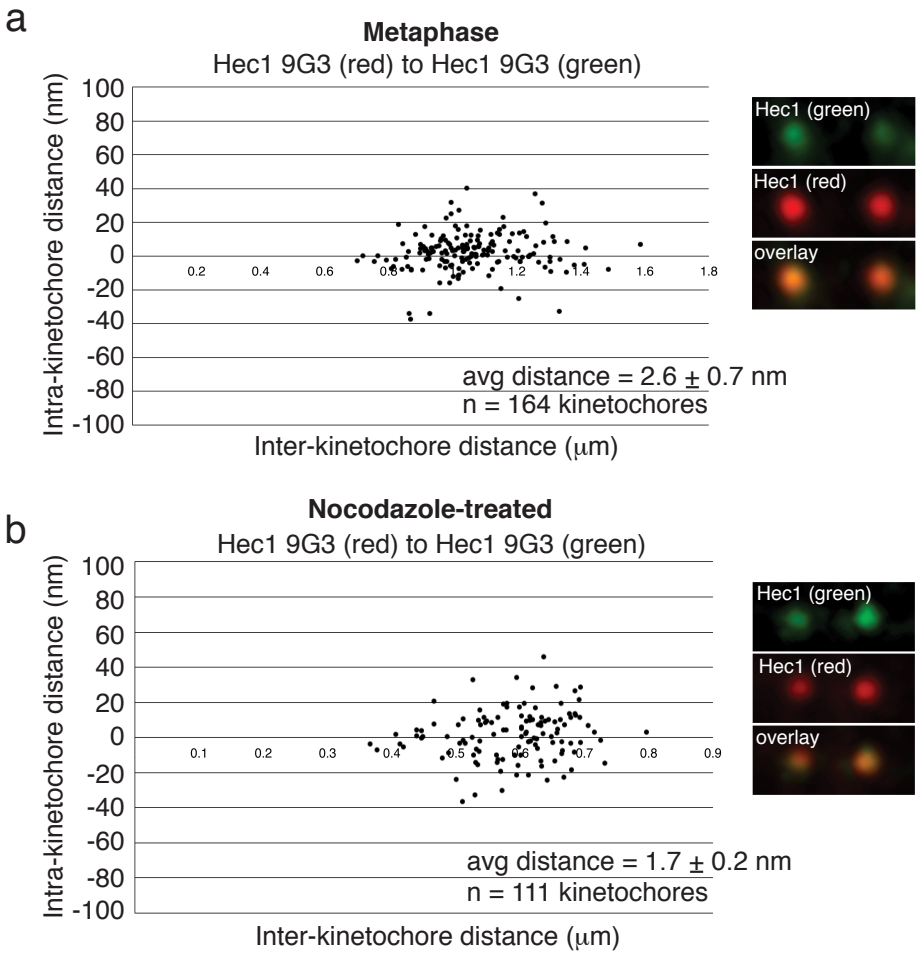

Figure 17: Intra-kinetochore distance measurements. Cells were fixed and incubated with primary antibodies directed against Hec1 (Hec1 9G3) followed by incubation with two secondary antibodies: donkey anti-mouse-Alexa488 and donkey anti-mouse- Alexa568. Intra-kinetochore distances were measured in both untreated metaphase cells (a) and nocodazole-treated cells (b) n values are shown on the graphs; data are from 3 independent experiments.

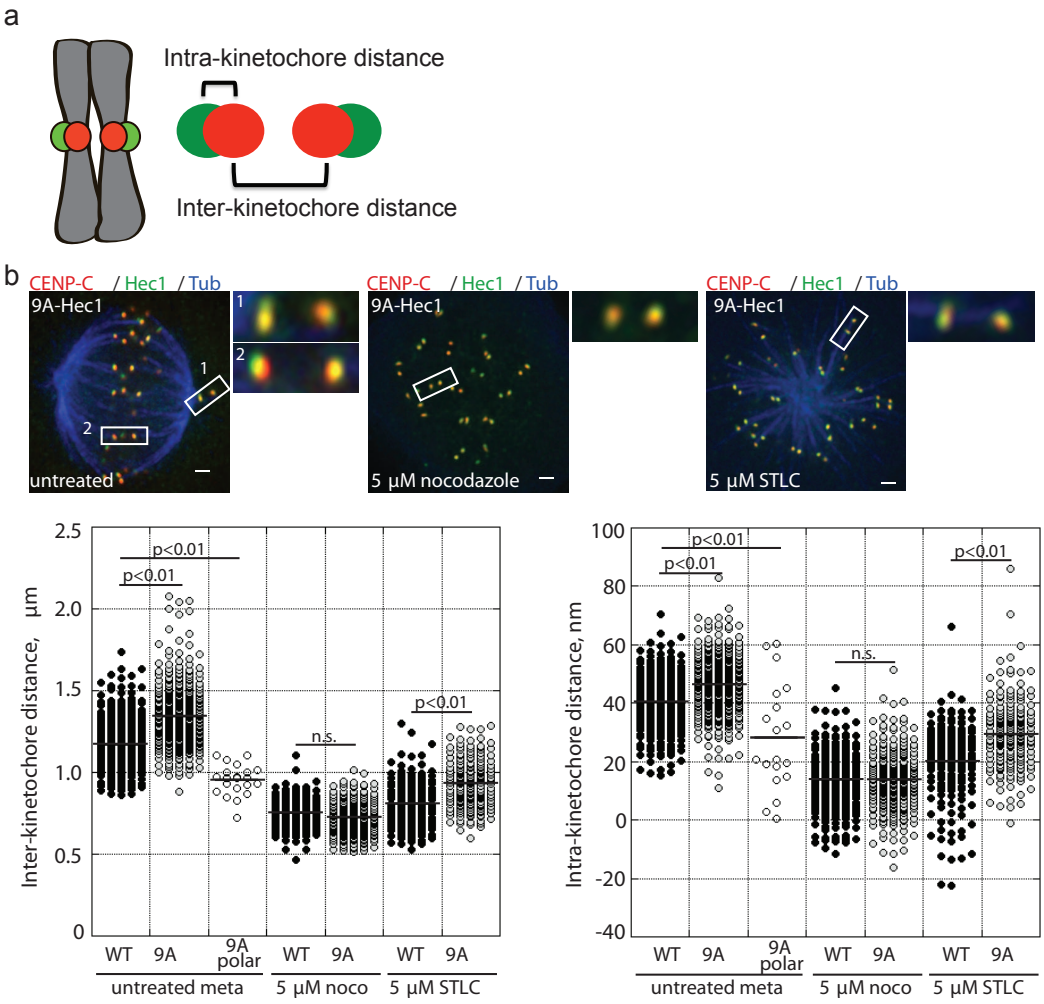

Figure 18: Stable attachments do not induce large-scale changes in intra-kinetochore distance in STLC-treated cells. (a) Cartoon depiction of inter- and intra-kinetochore distances. (b) Immunofluorescence images of 9A-Hec1-GFP-expressing cells. Scale bar, 5 μm. Left: untreated cell in metaphase. Boxed insets show examples of a (1) pole-proximal and (2) bi-oriented kinetochore pair. Middle: cell treated with 5 μM nocodazole. Right: cell treated with 5 μM STLC. In the insets, Hec1-GFP is shown in green, and CENP-C staining is shown in red. Scale bars are 1 μm. (c) Inter-kinetochore and intra-kinetochore distance measurements. Each circle represents a measured inter- or intra-kinetochore distance for a pair of sister chromatids. n values are listed in Table 1. NS=not significantly different, P=0.01, as evaluated by Welch's two-sample t-tests (inter-kinetochore distances, P=0.52; intra-kinetochore distances, P=0.90).

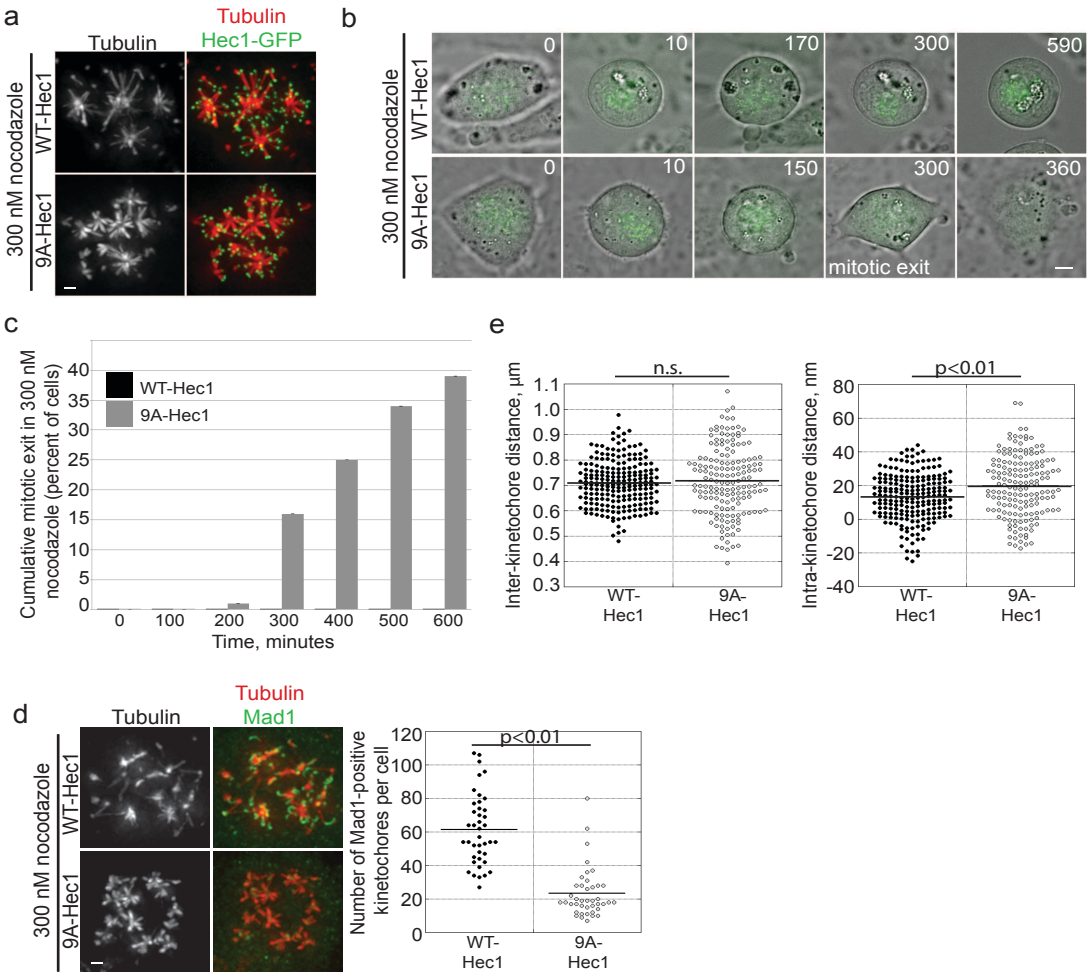

Figure 19: Stable kinetochore–microtubule attachment silences the SAC in the absence of spindle pole-mediated pushing or pulling forces. (a) Immuno-fluorescence images showing formation of kinetochore-associated microtubule 'tufts' in WT- and 9A-Hec1-GFP-expressing cells. Scale bar, 5 mm. (b) Stills from time-lapse imaging of WT- and 9A-Hec1-GFP-expressing cells treated with 300 nM nocodazole. Shown are overlays of phase contrast and GFP images. Time is indicated in minutes, and the time of mitotic exit initiation is also indicated. Scale bar, 5 μm. (c) Quantification of mitotic exit in WT- and 9A-Hec1-GFP-expressing cells. Graph indicates cumulative mitotic exit at the indicated time point. Data from three independent experiments are included, n=156 for WT- and n=141 for 9A-Hec1-expressing cells. Error bars indicate s.d. (d) Immunofluorescence images of WT- and 9A-Hec1-GFP- expressing cells stained for Mad1. Quantification of Mad1-positive kinetochores is shown on the right. P value determined by Student's t-test. For each cell line, 41 cells were scored from three experiments. (e) Inter- and intra-kinetochore distance measurements for WT- and 9A-Hec1-GFP-expressing cells treated with 300 nM nocodazole. Each circle represents a measured inter- or intra-kinetochore distance for a pair of sister chromatids. n values are listed in Table 1. P values were determined from Welch's two-sample t-tests. NS=not significantly different, P=0.40.

Chapter 4: Methods

4.1 Cell Culture, Transfections and Generation of Cell Lines

Stable cell lines expressing inducible WT-Hec1-GFP or 9A-Hec1-GFP were generated from a FlpIn T-REx HeLa host cell line (a gift from Stephen Taylor, University of Manchester, Manchester, England). Cells were grown to 50% confluence in DMEM supplemented with 10% fetal bovine serum (FBS), 1% penicillin/streptomycin, and 2 mM L-glutamine at 37 °C in 5% CO_2. Cells were grown to 50% confluence in $10cm^2$ dishes and transfected with 2.4 μg pOG44 recombinase-containing plasmid and 0.3 μg pcDNA5.FRT.TO-WT- or 9A-Hec1-GFP containing plasmids with Fugene HD (Promega). The pcDNA5.FRT.TO-Hec1 plasmids were generated through PCR amplification of WT- and 9A-Hec1-GFP fragments and cloned into a pcDNA5.FRT.TO vector through In-Fusion cloning. After 48 h, cells were switched to media containing 100 μg/ml hygromycin (EMD Millipore) and grown in this selection media for 2 weeks. Hygromycin-resistant foci were expanded and examined for inducible Hec1-GFP expression . Gene expression was induced with 1 mg/ml doxycycline (Sigma-Aldrich) for 30 h. For silence and rescue experiments in which endogenous Hec1 was depleted, 7 μl of a 20 μM stock solution of Cy-5-labelled, human-specific Hec1 siRNA targeted to the 5' UTR (5'-CCCUGGGUCGUGUCAGGAA-3') was added to 150 μl of OptiMem (Invitrogen). Concurrently, 6 μl of Oligofectamine (Invitrogen) was added to 150 μl of OptiMem. Samples were incubated in 1.7 ml microfuge tubes at room temperature for 5 min. Contents of the two tubes were combined and incubated for an additional 20 min before adding to each well of a 6-well dish containing 50% confluent HeLa cells in 1 ml

OptiMem plus 10% FBS. The following day an additional 1 ml OptiMem/FBS plus 2 μg/ml doxycycline was added to each well. Coverslips were processed at 48 h. mCherry-Cyclin B (Pines, 2010) was transiently expressed using Fugene 6 Transfection Reagent (Promega) lipid transfection agent. Fugene (5 μl) was added to 95 μl of OptiMEM for each well of a 6-well dish. Following a 5 min incubation at room temperature, 750 ng mCherry-Cyclin B (a gift from Jonathon Pines, The Gurdon Institute, Cambridge, UK) was added. After 20 min at room temperature, the solution was added dropwise to 2 ml Optimem plus 10% FBS. Cells were imaged at 24 h post transfection.

4.2 DNA Clone Engineering

Point mutagenesis was done to create the 1WT8A-Hec1-GFP clones. Primer pairs were ordered (Integrated DNA Technologies) that base paired with 9A-Hec1-GFP (from Jeanne Mick) except at a single target triplet codon. The indicated phospho-site (serine or threonine) was mutated to Alanine using the following primer pairs.

4WT8A-Hec1
5'-GAGCTCATGAAGCGCAGTGCAGTTTCCGCCGGT-3'
3'-ACCGGCGGAAACTGCACTGCGCTTCATGAGCTC-5'

5WT8A-Hec1
5'-CTCATGAAGCGCGCTTCAGTTTCCGCCGGTGGT-3'
3'-ACCACCGGCGGAAACTGAAGCGCGCTTCATGAG-5'

8WT8A-Hec1
5'-CGCTGCAGTTTCCAGCGGTGGTGCTGGC-3'
3'-GCCAGCACCACCGCTGGAAACTGCAGCG-5'

15WT8A-Hec1
5'-GGTGCTGGCCGCCTCTCCATGCAGGAGTTAAGA-3'
3'-TCTTAACTCCTGCATGGAGAGGCGGCCAGCACC-5'

44WT8A-Hec1

5’-CCAACCTTTGGAAAGTTGAGTATAAACAAACCGGCATCTGAAAGAAAAGTC-3’
3’-GACTTTTCTTTCAGATGCCGGTTTGTTTATACTCAACTTTCCAAAGGTTGG-5’

49WT8A-Hec1
5’-GTTGGCTATAAACAAACCGACATCTGAAAGAAAAGTCGCGC-3’
3’-GCGCGACTTTTCTTTCAGATGTCGGTTTGTTTATAGCCAAC-5’

55WT8A-Hec1
5’-GGCATCTGAAAGAAAAGTCTCGCTATTTGGCAAAAGAACTGC-3’
3’-GCAGTTCTTTTGCCAAATAGCGAGACTTTTCTTTCAGATGCC-5’

62WT8A-Hec1
5’-TTTGGCAAAAGAACTAGTGGACATGGATCCCGG-3’
3’-CCGGGATCCATGTCCACTAGTTCTTTTGCCAAA-5’

69WT8A-Hec1
5’-GCTGGACATGGATCCCGGAATAGTCAACTTGGTATATTTTCCAGTTC-3’
3’-GAACTGGAAAATATACCAAGTTGACTATTCCGGGATCCATGTCCAGC-5’

Each 50 μl PCR reaction in 1X PFU Turbo reaction buffer contained 200 μM of each forward and reverse primer, 200 μM dNTPs, and 2.5 U of PFU Turbo DNA polymerase (Agilent). 50 ng of 9A-Hec1-GFP was used as PCR template. Reactions were thermocycled on a Techne (TC-3000) thermocycler. Competent *E. coli* (DH5α, 0.6 optical density) were transformed through heat shock. Amplified plasmids with point mutations were recovered through Qiagen Maxi-Prep kit as per manufacturer instruction.

4.3 Western Blotting and Quantification

To determine Hec1 protein expression levels, cells were grown in 25 cm^2 flasks to 80% confluency. Cells were collected from the flasks with trypsin, pelleted in a tabletop centrifuge and resuspended in cold 1X PBS (140 mM NaCl, 2.5 mM KCl, 1.6 mM KH_2PO_4, 15 mM Na_2HPO_4, pH 7.0), 2 mM dithiothreitol and protease inhibitor cocktail (Thermo). Cells were sonicated on ice (Ultra Sonic Device) and lysates were

clarified by centrifugation. Lysate protein concentrations were quantified by Bradford Assay and then boiled for 1 min with 1X SDS Sample Buffer. Protein samples (30 μg) were run on 12% SDS-polyacrylamide gels and transferred to polyvinylidene difluoride membrane (Millipore). Blots were probed for Hec1 with mouse anti-Hec1 antibodies (Novus Biologicals, GTX70268) at a dilution of 1:2,000. Anti-α-tubulin antibodies (Sigma, T6199) were used at a dilution of 1:6,000 for a loading control. Primary antibodies were detected using horseradish peroxidase-conjugated-anti-mouse secondary antibody at a dilution of 1:10,000 (Gene Script Corp., A00160) and visualized via chemiluminescence (Thermo Scientific). Chemiluminescent images were obtained on an ImageQuant LAS 500 imager. Bands were background subtracted and quantified using Metamorph software.

4.4 Immunofluorescence

Before fixation and lysis, cells were rinsed in PHEM Buffer (60 mM PIPES, 25 mM HEPES, 10 mM EGTA, 8 mM $MgSO_4$, pH 7.0) pre-warmed to 37 °C. For fixed-cell analysis of inter- and intra-kinetochore distance measurements, cells were fixed in 4% paraformaldehyde at 37 °C for 20 min and subsequently lysed in PHEM buffer + 0.5% Triton X-100 at 37 °C for 5 min. For all other immunofluorescence experiments, cells were lysed in PHEM buffer + 0.5% Triton X-100 at 37 °C for 5 min, followed by fixation in 4% paraformaldehyde at 37 °C for 20 min. Cells were then rinsed 3 x 15 min in PHEM + 0.05% Triton X-100 and blocked for 1 h at room temperature with 10% boiled donkey serum (BDS) in PHEM. Primary antibodies were diluted in 5% BDS in PHEM as follows: mouse anti-Hec1-9G3, 1:2,500 (Novus Biologicals, GTX70268), rabbit anti-

Mad1, 1:200 (GeneTex, GTX109519), rabbit anti-CENP-A, 1:400 (Cell Signaling, 2186S), guinea pig anti-CENP-C, 1:1,000 (Medical and Biological Laboratories, PD030), rabbit anti-GFP, 1:500 (Invitrogen, A6455), mouse anti-a-tubulin, 1:300 (Sigma, T6199) and mouse anti-BubR1, 1:200 (Millipore, MAB3612). Cells were incubated with primary antibodies overnight at 4 °C, and then rinsed 3 x 15 min in PHEM + 0.05% Triton X-100. Cells were incubated with secondary antibodies conjugated to Alexa488 or Alexa647 (Jackson ImmunoResearch Laboratories, 715-545-150 and 715-605-150 respectively) or Alexa568 (Abcam, 175470) diluted 1:300 in 5% BDS in PHEM for 45 min at room temperature. Cells were rinsed 3 x 5 min in PHEM + 0.05% Triton X-100 and subsequently incubated in 4,6-diamidino-2-phenylindole diluted to 2ng/ml for 1min at room temperature. Cells were rinsed with PHEM + 0.05% Triton X-100 4 x 5 min, rinsed once with PHEM, and mounted onto slides using the following mounting media: 20 mM Tris, pH 8.0, 0.5% N-propyl gallate, and 90% glycerol. Coverslips were sealed to the slides using nail polish. Before fixation cells were treated as indicated with 5 μM STLC (Tocris) or with 5 μM or 300 nM nocodazole (Tocris).

4.5 Image Acquisition and Analysis

Images were acquired on a DeltaVision Personal DV (Applied Precision) imaging system equipped with a CoolSNAP HQ2 (Photometrics/Roper Scientific) camera with a 60X/1.42 NA PlanApochromat objective and SoftWorx acquisition software (Applied Precision). Images for fixed-cell experiments were acquired as z-stacks at 200 nm intervals. Kinetochores were identified by Hec1-GFP position, and fluorescence intensities of proteins of interest were determined using custom MATLAB software ('Speckle Tracker'; Mathworks, Natlick, MA) written by Drs Xiaohou Wan and Ted

Salmon. Fluorescence intensities were normalized to the level of GFP-fusion protein expression using the GFP fluorescence intensity. To determine the number of Mad1-positive kinetochores, kinetochore signals were identified by GFP-Hec1 localization and scored from deconvolved images. Inter- and intra-kinetochore distance measurements were performed on sister kinetochore pairs that resided in a single focal plane. The centroids of GFP-Hec1 and antibody-labelled CENP-C were determined by custom-written MATLAB software (provided by Drs Xiaohou Wan and Ted Salmon). Inter-kinetochore distances were calculated using the centroids of the GFP signal (C-terminal GFP-Hec1, labelled with anti-GFP antibodies to increase fluorescence signal) on each of the two kinetochores in a sister kinetochore pair. Intra-kinetochore distances (Hec1-GFP to CENP-C) were calculated as one-half the difference of the distance between outer kinetochore centroids (Hec1-GFP) and inner kinetochore centroids (CENP-C) (Wan et al., 2009). Before carrying out these measurements, we carried out control experiments, in which inter- and intra-kinetochore distances were measured from kinetochores stained with Hec1-9G3 antibodies followed by simultaneous staining with Alexa488 and Alexa568 secondary antibodies (Supplementary Fig. 6). Live cell images were acquired on the DeltaVision imaging system described above using a 60X/1.42 NA PlanApochromat or a 40X/0.75NA UPlanFL objective. Cells were imaged in a

37 °C environmental chamber in Leibovitz's L-15 media (Gibco) supplemented with 10% FBS, 7 mM HEPES and 4.5 g/l D-glucose (pH 7.0). As indicated in the text, live cell experiments were carried out using the following drug concentrations: 5 μM STLC (Tocris), 5 μM or 300 nM nocodazole (Tocris), 2 μM ZM447439 (Tocris) and 10 μM reversine (Sigma-Aldrich). For determining mitotic transit time, cells were scored only if

they entered mitosis during imaging. To determine if cells underwent mitotic slippage, HeLa cells stably expressing WT- or 9A-Hec1-GFP were transfected with an mCherry-Cyclin B expression vector (Gavet and Pines, 2010). Cells were time-lapse imaged and total mCherry cell fluorescence was measured over time using SoftWorx® analysis software.

4.6 Statistical Analysis

Most statistical comparisons were made using two-tailed Student's t-tests, as indicated in the figure legends. Normality was determined through Anderson–Darling tests for normality. Kinetochore distance measurements were compared using Welch's two-sample t-tests. In addition, linear mixed effects models, appropriate for nested data (kinetochore pairs within cells, within experiments) were used for kinetochore distance comparisons. The experimental data were analysed in the R statistical computing environment (2015; Wickham, 2014). Restricted maximum likelihood methods were used, as implemented in the R package lme4 (Bates et al., 2014) to fit the models. Fitted values, standard deviations, and standard errors were calculated based on the mixed effects models including omission of random effects. The values obtained from this analysis are shown in Table 2.

Table 2: Inter- and intra-kinetochore distances measured in HeLa cells expressing WT- or 9A-Hec1-GFP displayed as fitted values determined by a linear mixed effects model. Values indicate fitted distances calculated using a linear mixed effects model, which is appropriate for nested data, such as kinetochore pairs within cells, within experiments (see Methods). Numbers in parentheses indicate standard error of the mean. The first three rows display calculated inter- and intra-kinetochore distances of aligned sister kinetochore pairs in cells expressing either WT- or 9A-Hec1-GFP with no drug treatment and pole-proximal kinetochore pairs in cells expressing 9A-Hec1-GFP with no drug treatment. All other conditions are indicated.

		Inter-kinetochore distance (μm)		Intra-kinetochore distance (nm)		N kinetochores/ N cells
WT-Hec1	aligned	1.16	(0.01)	39.9	(0.4)	450/30
9A-Hec1	aligned	1.34	(0.01)	45.9	(0.4)	414/30
9A-Hec1	polar	0.92	(0.01)	28.1	(2.0)	21/14
WT-Hec1	5 μM noco	0.73	(0.01)	14.7	(0.7)	101/15
9A-Hec1	5 μM noco	0.73	(0.01)	12.9	(0.7)	104/15
WT-Hec1	5 μM STLC	0.80	(0.01)	19.8	(0.5)	194/30
9A-Hec1	5 μM STLC	0.93	(0.01)	29.2	(0.5)	258/30
WT-Hec1	300 nM noco	0.71	(0.01)	12.8	(0.5)	214/30
9A-Hec1	300 nM noco	0.72	(0.01)	19.7	(0.6)	163/30

Chapter 5: Conclusions and Future Directions

5.1 Hec1 Tail Phosphorylation

Regulation of K-MT attachments is heavily reliant on ABK phosphorylation of the Hec1 tail for release of incorrect attachments. Cells expressing the non-phosphorylatable, mutant version of Hec1, 9A-Hec1, illustrate the necessity of this release. The reduced ability of these cells to release K-MT attachments manifests through an inability to align chromosomes and the generation of segregation errors (Figure 7c; DeLuca et al., 2011). Chromosome alignment deficiency and segregation errors persist to nearly the same degree in cells expressing 6A-Hec1 where there is some opportunity (3WT sites on the Hec1 tail) for K-MT attachment regulation by ABK (Figure 7c; DeLuca et al., 2006). Further, the nine phosphorylation sites are likely all be required for proper regulation of K-MT attachments as mutations of even two sites to alanine generates hyper-stable attachments and chromosome alignment deficiency (Figure 7). It will be interesting in the future to determine if single alanine mutations to a Hec1 tail phosphorylation site impart measurable indications of hyper-stability to confirm all nine truly are required. Additionally, testing single alanine mutations at each site could elucidate a site that is not required, or one that exerts greater influence on K-MT binding stability.

Experiments limiting the number of Hec1 phosphorylation sites available to ABK indicate that some of those sites are more influential than others. This is shown by the greater impact of alanine mutation to Ser69 than Ser15 (Figure 7). While this appears to contrast the finding demonstrating an aspartic acid substitution at any site rescues 9A-Hec1 chromosome oscillations (Zaytsev et al., 2014), it is more likely indicative of the

idea that it is not merely the location of the charge alteration on Hec1 through phosphate addition, but the activity level of ABK on the site. Immuno-staining cells transfected with 1WT8A-Hec1-GFP using phospho-specific antibodies generated by this lab (DeLuca et al. 2011) confirms these wild-type sites are phosphorylated. However, the wild-type sites display reduced phosphorylation upon alignment to the metaphase plate (Figure 9). These data are in accord with the findings of DeLuca et al., 2011 demonstrating decreased ABK substrate phosphorylation in later mitosis. Proper K-MT attachment regulation at this stage requires this low level of phosphorylation on all nine Hec1 ABK phosphorylation sites (at least 8) which enables wild-type metaphase inter-kinetochore distances and oscillations. The single aspartic acid substitutions of Zaytsev et al., 2014 indicate rescue to wild-type could be obtained through maximal phosphorylation of a single site, but cells depend on low-levels of phosphorylation at all nine sites because they appear to be inhibited from, or otherwise unable to compensate with full phosphorylation at a single site.

5.2 Satisfaction of the Spindle Assembly Checkpoint

SAC satisfaction has been attributed to tension between sister kinetochores generated from MT pulling forces (Biggins and Murray, 2001; Li and Nicklas, 1995). More recently, SAC satisfaction was attributed to separation between inner and outer kinetochore proteins, intra-kinetochore stretch. *Drosophila* S2 cells treated with taxol did not acquire increased inter-kinetochore distance, but did have increased intra-kinetochore distances of ~100nm (CENP-A-GFP to Hec1 N-terminus). These cells were able to satisfy the checkpoint and exit mitosis (Maresca and Salmon, 2009). Further, HeLa cells treated with low doses of nocodazole (7nM) were able to form and maintain

K-MT attachments that did not increase inter-kinetochore distance. These cells displayed a similar 100nm intra-kinetochore stretch from mCherry-Mis12 to GFP-CENP-A on kinetochores that Mad2 had vacated, indicating satisfaction of the checkpoint (Uchida et al., 2009).

During the study of Hec1 tail phospho-site requirements mutant 9A-Hec1 cells were observed exiting mitosis with polar-oriented chromosomes that fail to align to the metaphase plate. These unaligned kinetochore pairs did not exhibit the increase in inter-kinetochore tension observed in aligned kinetochores (Figure 18b). Our observations of 9A-Hec1 polar chromosomes led us to hypothesize that bipolar attachments were not necessary for SAC satisfaction. We found that cells expressing 9A-Hec1 treated with 5 μM STLC were able to satisfy the SAC and exit mitosis. Analyses of kinetochore distance measures indicated that substantial change in intra-kinetochore distance was not requisite for SAC satisfaction as we only observed a ~10nm increase. There was, however, a slight but statistically significant increase in inter-kinetochore distance in the STLC-treated cells. To rule this inter-kinetochore distance increase out as the parameter evaluated by the SAC, the 'MT Tuft Assay' was developed. Treatment of cells with 300nM nocodazole created numerous tufts of MTs rather than a single spindle pole as in STLC treated cells that eliminated the increase in inter-kinetochore distance. These cells were still able to satisfy the SAC and retained the ~10nm increase in intra-kinetochore distance. We suggest this is an architectural shift or conformational change of the kinetochore proteins upon binding MTs rather than an actual stretch within the kinetochore. This is supported by the fact that bipolar attachments, where pulling forces are generated, are unnecessary for checkpoint

satisfaction. These results clearly demonstrate stable kinetochore-microtubule binding is sufficient for SAC satisfaction.

Offering further confirmation that stable K-MT attachments are the parameter evaluated by the SAC, strikingly similar research results were co-submitted and concurrently published. This work also demonstrated an increase of ~10nm associated with K-MT attachment (Etemad et al., 2015). They reported this distance to be statistically irrelevant, however. The differing interpretation of such similar results is interesting. While both groups convincingly show and attest the requirement for SAC satisfaction is stable attachment, each recognizes the architectural change at the kinetochore may, or may not, be relevant. An even more recent publication (Magidson et al., 2016) supports the finding that K-MT attachment is the requirement for SAC satisfaction. They show loss of K-MT attachments is the cause of arrest in taxol-treated human cells. Further, cells satisfying the checkpoint when treated with taxol do so with less intra-kinetochore stretch than untreated, metaphase cells. However, they do not establish a baseline, unattached, measure to determine whether or not they observe an architectural change associate with stable K-MT attachment.

5.3 Mechanism of Hec1 Tail Phosphorylation

The spatial positioning model arose from observations that sister kinetochore pairs are not under tension early in mitosis and are thus near the CPC-containing centromere. This is also when phosphorylation levels of ABK substrates is highest. As bipolar K-MT attachments are formed, kinetochores are pulled away from from the source of phosphorylation. The model posits this separation of kinase and substrates

prohibits K-MT attachment destabilizing activity of ABK (Lampson and Cheeseman, 2011; Tanaka et al., 2002). The model was supported by experiments that tethered ABK to the outer kinetochore. This relocation of ABK resulted in persistent phosphorylation of kinetochore substrates (Liu et al., 2009). The spatial positioning model explained observations of SAC satisfaction while separation of sister kinetochores was thought to be required for SAC satisfaction. Spatial positioning remained a tenable model while intra-kinetochore stretching of ~40 nm was thought to be required for SAC satisfaction. The observation that SAC satisfaction can occur with only 10 nm of outer kinetochore movement away from the centromere (Etemad et al., 2015; Tauchman et al., 2015) makes it is difficult to envision an ABK activity gradient functioning on such a small scale (Krenn and Musacchio, 2015). This lends further skepticism to the model called into question by DeLuca et al., 2011 by uncovering of a population of ABK at kinetochores. Caldas et al. (2013) iterated these findings demonstrating activity of ABK at the outer kinetochore is dependent on the outer kinetochore protein KNL1. A population of ABK at the kinetochore makes it even less likely that a kinase substrate could pull away from the influence of ABK in only 10 nm. This strongly suggests that phosphorylation of Hec1 tail substrates is regulated not by position, but by kinase activity or kinase-phophatase balance.

5.4 Therapeutic Potential and Follow-Up Studies

The response of 9A-Hec1 expressing cells to the spindle poisons STLC and nocodazole is illustrative of the variable nature of chemotherapeutic success. Cells expressing this mutant protein exhibit hyper-stable K-MT attachments and are less

susceptible to microtubule poisons. This is critical to human health as a large class of anti-cancer drugs is anti-mitotic. Cells expressing 9A-Hec1 demonstrate decreased response to these drugs in terms of halting mitotic progression due to increase stability of K-MT attachments. K-MT attachment stability is also shown by work in this lab to influence susceptibility to depletion of the SAC protein, BubR1 (Ding et al., 2013). In that instance, cells with smaller inter-kinetochore distances, an indication of reduced K-MT attachment stability, were susceptible to the depletion while other cells were not (Herman et al., 2015). This finding further illustrates differences in cell lethality correlated with K-MT attachment. These differences could be exploited to develop therapies that are cancer-cell lethal while harmless to healthy cells. To illustrate, the kinetochore protein, BugZ (*Bu*b3 interacting *G*LEBS and *Z*inc finger domain containing protein), was found in a cancer lethal screen, and was demonstrated to be required for glioblastoma cells, but not healthy neural cells (Toledo et al., 2014). These findings indicate the potential of implementing assays to determine differences between cancerous and heathy cells, such as K-MT attachment stability measurements, to predict tumor response to various therapies.

Additionally, defining the protein or proteins responsive to microtubule binding at the kinetochore would offer targets for robust mitotic inhibition. Interfering directly with the signal the SAC reads at the kinetochore-microtubule interface would halt cell cycle progression. This would provide an invaluable tool in cancer therapy. This would be particularly effective if therapies could distinguish between healthy and cancerous cells. Studies of kinetochore protein distribution and relative positions offer clues to that target. Immuno-EM images of kinetochore proteins show the distribution of CENP-C,

CENP-T, and CENP-R (Figure 2) changes similarly in cells treated with nocodazole versus MG132 indicating a response to K-MT attachment (Suzuki et al., 2011). Further, Wan et al. (2009) described compliant linkage proteins. These proteins were labeled as compliant because they diminished in length from N- to C-termini after metaphase tension was reduced by the application of taxol. They observed this characteristic in CENP-C, CENP-I, and CENP-T, the Dsn1 subunit of MIS12, and KNL1. Also, KNL1 supports Bub1 binding and its ABK activation early in mitosis before stable K-MT attachments are made. Following stable K-MT binding Bub1 interaction with KNL-1 ceases, leading to reduction in ABK activity (Caldas et al., 2013). It is possible KNL1 undergoes a conformational change on MT binding . This conformational change could disrupt Bub1 binding which influences the SAC.

We now know the SAC is satisfied by stable K-MT attachment. Concurrent with these attachments is a change in the molecular architecture of the kinetochore. The aforementioned proteins that respond to K-MT attachment offer clues as to what those protein(s) may be. Future research will identify the protein(s) responsible for the transition from SAC activation to its satisfaction and will likely provide powerful mitotic arrest therapeutic agents. The aforementioned proteins that respond to K-MT attachment offer clues as to what those protein(s) may be.

References

Abe, S., Nagasaka, K., Hirayama, Y., Kozuka-Hata, H., Oyama, M., Aoyagi, Y., Obuse, C., and Hirota, T. (2011). The initial phase of chromosome condensation requires Cdk1-mediated phosphorylation of the CAP-D3 subunit of condensin II. Genes Dev. 25, 863–874.

Akiyoshi, B., Sarangapani, K.K., Powers, A.F., Nelson, C.R., Reichow, S.L., Arellano-Santoyo, H., Gonen, T., Ranish, J.A., Asbury, C.L., and Biggins, S. (2010). Tension directly stabilizes reconstituted kinetochore-microtubule attachments. Nature 468, 576–579.

Alushin, G.M., Ramey, V.H., Pasqualato, S., Ball, D.A., Grigorieff, N., Musacchio, A., and Nogales, E. (2010). The Ndc80 kinetochore complex forms oligomeric arrays along microtubules. Nature 467, 805–810.

Alushin, G.M., Musinipally, V., Matson, D., Tooley, J., Stukenberg, P.T., and Nogales, E. (2012). Multimodal microtubule binding by the Ndc80 kinetochore complex. Nat. Struct. Mol. Biol. 19, 1161–1167.

Alushin, G.M., Lander, G.C., Kellogg, E.H., Zhang, R., Baker, D., and Nogales, E. (2014). High-resolution microtubule structures reveal the structural transitions in αβ-tubulin upon GTP hydrolysis. Cell 157, 1117–1129.

Andrews, P.D., Knatko, E., Moore, W.J., and Swedlow, J.R. (2003). Mitotic mechanics: the auroras come into view. Curr. Opin. Cell Biol. 15, 672–683.

Andrews, P.D., Ovechkina, Y., Morrice, N., Wagenbach, M., Duncan, K., Wordeman, L., and Swedlow, J.R. (2004). Aurora B regulates MCAK at the mitotic centromere. Dev. Cell 6, 253–268.

De Antoni, A., Pearson, C.G., Cimini, D., Canman, J.C., Sala, V., Nezi, L., Mapelli, M., Sironi, L., Faretta, M., and Salmon, E.D. (2005). The Mad1/Mad2 complex as a template for Mad2 activation in the spindle assembly checkpoint. Curr. Biol. 15, 214–225.

Aravamudhan, P., Goldfarb, A.A., and Joglekar, A.P. (2015). The kinetochore encodes a mechanical switch to disrupt spindle assembly checkpoint signalling. Nat Cell Biol 17, 868–879.

Ault, J., and Nicklas, R.B. (1989). Tension, microtubule rearrangements, and the proper distribution of chromosomes in mitosis. Chromosoma 98, 33–39.

Barnhart, M.C., Kuich, P.H.J.L., Stellfox, M.E., Ward, J.A., Bassett, E.A., Black, B.E., and Foltz, D.R. (2011). HJURP is a CENP-A chromatin assembly factor sufficient to form a functional de novo kinetochore. J. Cell Biol. 194, 229–243.

Bates, D., Mächler, M., Bolker, B., and Walker, S. (2014). Fitting linear mixed-effects models using lme4. arXiv Prepr. arXiv1406.5823.

Bharadwaj, R., Qi, W., and Yu, H. (2004). Identification of two novel components of the human NDC80 kinetochore complex. J. Biol. Chem. 279, 13076–13085.

Biggins, S., and Murray, A.W. (2001). The budding yeast protein kinase Ipl1/Aurora allows the absence of tension to activate the spindle checkpoint. Genes Dev. 15, 3118–3129.

Biggins, S., Severin, F.F., Bhalla, N., Sassoon, I., Hyman, A.A., and Murray, A.W. (1999). The conserved protein kinase Ipl1 regulates microtubule binding to kinetochores in budding yeast. Genes Dev. 13, 532–544.

Caldas, G., and DeLuca, J. (2014). KNL1: bringing order to the kinetochore. Chromosoma 123, 169–181.

Caldas, G. V, DeLuca, K.F., and DeLuca, J.G. (2013). KNL1 facilitates phosphorylation of outer kinetochore proteins by promoting Aurora B kinase activity. J. Cell Biol. 203, 957–969.

Cane, S., Ye, A.A., Luks-Morgan, S.J., and Maresca, T.J. (2013). Elevated polar ejection forces stabilize kinetochore–microtubule attachments. J. Cell Biol. 200, 203–218.

Chang, D.C., Xu, N., and Luo, K.Q. (2003). Degradation of cyclin B is required for the onset of anaphase in mammalian cells. J. Biol. Chem. 278, 37865–37873.

Cheeseman, I.M., and Desai, A. (2008). Molecular architecture of the kinetochore–microtubule interface. Nat. Rev. Mol. Cell Biol. 9, 33–46.

Cheeseman, I.M., Anderson, S., Jwa, M., Green, E.M., Kang, J., Yates, J.R., Chan, C.S.M., Drubin, D.G., and Barnes, G. (2002). Phospho-regulation of kinetochore-microtubule attachments by the Aurora kinase Ipl1p. Cell 111, 163–172.

Cheeseman, I.M., Niessen, S., Anderson, S., Hyndman, F., Yates, J.R., Oegema, K., and Desai, A. (2004). A conserved protein network controls assembly of the outer kinetochore and its ability to sustain tension. Genes Dev. 18, 2255–2268.

Cheeseman, I.M., Chappie, J.S., Wilson-Kubalek, E.M., and Desai, A. (2006). The Conserved KMN Network Constitutes the Core Microtubule-Binding Site of the Kinetochore. Cell 127, 983–997.

Cheeseman, I.M., Hori, T., Fukagawa, T., and Desai, A. (2008). KNL1 and the CENP-H/I/K complex coordinately direct kinetochore assembly in vertebrates. Mol. Biol. Cell 19, 587–594.

Chial, H. (2008). Proto-oncogenes to oncogenes to cancer. Nat. Educ. 1, 33.

Ciferri, C., De Luca, J., Monzani, S., Ferrari, K.J., Ristic, D., Wyman, C., Stark, H., Kilmartin, J., Salmon, E.D., and Musacchio, A. (2005). Architecture of the human ndc80-hec1 complex, a critical constituent of the outer kinetochore. J. Biol. Chem. 280, 29088–29095.

Ciferri, C., Musacchio, A., and Petrovic, A. (2007). The Ndc80 complex: hub of kinetochore activity. FEBS Lett. 581, 2862–2869.

Ciferri, C., Pasqualato, S., Screpanti, E., Varetti, G., Santaguida, S., Dos Reis, G., Maiolica, A., Polka, J., De Luca, J.G., and De Wulf, P. (2008). Implications for kinetochore-microtubule attachment from the structure of an engineered Ndc80 complex. Cell 133, 427–439.

Cimini, D., and Degrassi, F. (2005). Aneuploidy: a matter of bad connections. Trends Cell Biol. 15, 442–451.

Cimini, D., Wan, X., Hirel, C.B., and Salmon, E.D. (2006). Aurora Kinase Promotes Turnover of Kinetochore Microtubules to Reduce Chromosome Segregation Errors. Curr. Biol. 16, 1711–1718.

Ciosk, R., Shirayama, M., Shevchenko, A., Tanaka, T., Toth, A., Shevchenko, A., and Nasmyth, K. (2000). Cohesin's binding to chromosomes depends on a separate complex consisting of Scc2 and Scc4 proteins. Mol. Cell 5, 243–254.

Clute, P., and Pines, J. (1999). Temporal and spatial control of cyclin B1 destruction in metaphase. Nat Cell Biol 1, 82–87.

Collin, P., Nashchekina, O., Walker, R., and Pines, J. (2013). The spindle assembly checkpoint works like a rheostat rather than a toggle switch. Nat Cell Biol 15, 1378–1385.

DeLuca, J.G., and Musacchio, A. (2012). Structural organization of the kinetochore–microtubule interface. Curr. Opin. Cell Biol. 24, 48–56.

DeLuca, J.G., Dong, Y., Hergert, P., Strauss, J., Hickey, J.M., Salmon, E.D., and McEwen, B.F. (2005). Hec1 and nuf2 are core components of the kinetochore outer plate essential for organizing microtubule attachment sites. Mol. Biol. Cell 16, 519–531.

DeLuca, J.G., Gall, W.E., Ciferri, C., Cimini, D., Musacchio, A., and Salmon, E.D. (2006). Kinetochore Microtubule Dynamics and Attachment Stability Are Regulated by Hec1. Cell 127, 969–982.

DeLuca, K.F., Lens, S.M.A., and DeLuca, J.G. (2011). Temporal changes in Hec1 phosphorylation control kinetochore–microtubule attachment stability during mitosis. J. Cell Sci. 124, 622–634.

Desai, A., and Mitchison, T.J. (1997). Microtubule polymerization dynamics. Annu. Rev. Cell Dev. Biol. 13, 83–117.

Desai, A., Rybina, S., Müller-Reichert, T., Shevchenko, A., Shevchenko, A., Hyman, A., and Oegema, K. (2003). KNL-1 directs assembly of the microtubule-binding interface of the kinetochore in C. elegans. Genes Dev. 17, 2421–2435.

Ding Y., Hubert C.G., Herman J., Corrin P., Toledo C.M., Skutt-Kakaria K., et al. (2013). Cancer-specific requirement for BUB1B/BUBR1 in human brain tumor isolates and genetically transformed cells. Cancer Discov. 3, 198–211.

Ditchfield, C., Johnson, V.L., Tighe, A., Ellston, R., Haworth, C., Johnson, T., Mortlock, A., Keen, N., and Taylor, S.S. (2003). Aurora B couples chromosome alignment with anaphase by targeting BubR1, Mad2, and Cenp-E to kinetochores. J. Cell Biol. 161, 267–280.

Dong, Y., Beldt, K.J. Vanden, Meng, X., Khodjakov, A., and McEwen, B.F. (2007). The outer plate in vertebrate kinetochores is a flexible network with multiple microtubule interactions. Nat. Cell Biol. 9, 516–522.

Dumont, S., Salmon, E.D., and Mitchison, T.J. (2012). Deformations Within Moving Kinetochores Reveal Different Sites of Active and Passive Force Generation. Science 337, 355–358.

Earnshaw, W.C., and Rothfield, N. (1985). Identification of a family of human centromere proteins using autoimmune sera from patients with scleroderma. Chromosoma 91, 313–321.

Espert, A., Uluocak, P., Bastos, R.N., Mangat, D., Graab, P., and Gruneberg, U. (2014). PP2A-B56 opposes Mps1 phosphorylation of KNL1 and thereby promotes spindle assembly checkpoint silencing. J. Cell Biol. 206, 833–842.

Espeut, J., Cheerambathur, D.K., Krenning, L., Oegema, K., and Desai, A. (2012). Microtubule binding by KNL-1 contributes to spindle checkpoint silencing at the kinetochore. J. Cell Biol. 196, 469–482.

Etemad, B., Kuijt, T.E.F., and Kops, G.J.P.L. (2015). Kinetochore-microtubule attachment is sufficient to satisfy the human spindle assembly checkpoint. Nat. Commun. 6.

Euskirchen, G.M. (2002). Nnf1p, Dsn1p, Mtw1p, and Nsl1p: a new group of proteins important for chromosome segregation in Saccharomyces cerevisiae. Eukaryot. Cell 1, 229–240.

Foley, E.A., and Kapoor, T.M. (2013). Microtubule attachment and spindle assembly checkpoint signalling at the kinetochore. Nat Rev Mol Cell Biol 14, 25–37.

Foltz, D.R., Jansen, L.E.T., Bailey, A.O., Yates, J.R., Bassett, E.A., Wood, S., Black, B.E., and Cleveland, D.W. (2009). Centromere-specific assembly of CENP-a nucleosomes is mediated by HJURP. Cell 137, 472–484.

Fourest-Lieuvin, A., Peris, L., Gache, V., Garcia-Saez, I., Juillan-Binard, C., Lantez, V., and Job, D. (2006). Microtubule Regulation in Mitosis: Tubulin Phosphorylation by the Cyclin-dependent Kinase Cdk1. Mol. Biol. Cell 17 , 1041–1050.

Fukagawa, T., and Earnshaw, W.C. (2014). The centromere: chromatin foundation for the kinetochore machinery. Dev. Cell 30, 496–508.

Funabiki, H., and Wynne, D. (2013). Making an effective switch at the kinetochore by phosphorylation and dephosphorylation. Chromosoma 122, 135–158.

Gavet, O., and Pines, J. (2010). Progressive activation of Cyclin B1-Cdk1 coordinates entry to mitosis. Dev. Cell 18, 533–543.

Goshima, G., Kiyomitsu, T., Yoda, K., and Yanagida, M. (2003). Human centromere chromatin protein hMis12, essential for equal segregation, is independent of CENP-A loading pathway. J. Cell Biol. 160, 25–39.

Guimaraes, G.J., Dong, Y., McEwen, B.F., and DeLuca, J.G. (2008). Kinetochore-Microtubule Attachment Relies on the Disordered N-Terminal Tail Domain of Hec1. Curr. Biol. 18, 1778–1784.

van Heesbeen, R.G.H.P., Tanenbaum, M.E., and Medema, R.H. (2014). Balanced Activity of Three Mitotic Motors Is Required for Bipolar Spindle Assembly and Chromosome Segregation. Cell Rep. 8, 948–956.

Herzog, F., Primorac, I., Dube, P., Lenart, P., Sander, B., Mechtler, K., Stark, H., and Peters, J.-M. (2009). Structure of the anaphase-promoting complex/cyclosome interacting with a mitotic checkpoint complex. Science (80-.). 323, 1477–1481.

Hill, T.L. (1985). Theoretical problems related to the attachment of microtubules to kinetochores. Proc. Natl. Acad. Sci. 82, 4404–4408.

Hiruma, Y., Sacristan, C., Pachis, S.T., Adamopoulos, A., Kuijt, T., Ubbink, M., von Castelmur, E., Perrakis, A., and Kops, G.J.P.L. (2015). Competition between MPS1 and microtubules at kinetochores regulates spindle checkpoint signaling. Science (80-.). 348, 1264–1267.

Holland, A.J., and Cleveland, D.W. (2009). Boveri revisited: chromosomal instability, aneuploidy and tumorigenesis. Nat Rev Mol Cell Biol 10, 478–487.

Van Hooser, A.A., Ouspenski, I.I., Gregson, H.C., Starr, D.A., Yen, T.J., Goldberg, M.L., Yokomori, K., Earnshaw, W.C., Sullivan, K.F., and Brinkley, B.R. (2001). Specification of kinetochore-forming chromatin by the histone H3 variant CENP-A. J. Cell Sci. 114, 3529–3542.

van der Horst, A., and Lens, S.A. (2014). Cell division: control of the chromosomal passenger complex in time and space. Chromosoma 123, 25–42.

Howell, B.J., McEwen, B.F., Canman, J.C., Hoffman, D.B., Farrar, E.M., Rieder, C.L., and Salmon, E.D. (2001). Cytoplasmic dynein/dynactin drives kinetochore protein transport to the spindle poles and has a role in mitotic spindle checkpoint inactivation. J. Cell Biol. 155, 1159–1172.

Hudson, D.F., Fowler, K.J., Earle, E., Saffery, R., Kalitsis, P., Trowell, H., Hill, J., Wreford, N.G., de Kretser, D.M., Cancilla, M.R., et al. (1998). Centromere Protein B Null Mice are Mitotically and Meiotically Normal but Have Lower Body and Testis Weights. J. Cell Biol. 141 , 309–319.

Jansen, L.E.T., Black, B.E., Foltz, D.R., and Cleveland, D.W. (2007). Propagation of centromeric chromatin requires exit from mitosis. J. Cell Biol. 176, 795–805.

Jeffrey, P.D., Russo, A.A., Polyak, K., Gibbs, E., Hurwitz, J., Massague, J., and Pavletich, N.P. (1995). Mechanism of CDK activation revealed by the structure of a cyclinA-CDK2 complex. Nature 376, 313–320.

Ji, Z., Gao, H., and Yu, H. (2015). Kinetochore attachment sensed by competitive Mps1 and microtubule binding to Ndc80C. Science (80-.). 348, 1260–1264.

Jia, L., Kim, S., and Yu, H. (2013). Tracking spindle checkpoint signals from kinetochores to APC/C. Trends Biochem. Sci. 38, 302–311.

Joglekar, A.P., and DeLuca, J.G. (2009). Chromosome segregation: Ndc80 can carry the load. Curr. Biol. 19, R404–R407.

Johnston, K., Joglekar, A., Hori, T., Suzuki, A., Fukagawa, T., and Salmon, E.D. (2010). Vertebrate kinetochore protein architecture: protein copy number. J. Cell Biol. 189, 937–943.

Jonker, H.R.A., Wechselberger, R.W., Pinkse, M., Kaptein, R., and Folkers, G.E. (2006). Gradual phosphorylation regulates PC4 coactivator function. FEBS J. 273, 1430–1444.

Kapitein, L.C., Peterman, E.J.G., Kwok, B.H., Kim, J.H., Kapoor, T.M., and Schmidt, C.F. (2005). The bipolar mitotic kinesin Eg5 moves on both microtubules that it crosslinks. Nature 435, 114–118.

Kapoor, T.M., Mayer, T.U., Coughlin, M.L., and Mitchison, T.J. (2000). Probing Spindle Assembly Mechanisms with Monastrol, a Small Molecule Inhibitor of the Mitotic Kinesin, Eg5. J. Cell Biol. 150, 975–988.

Kelly, A.E., Ghenoiu, C., Xue, J.Z., Zierhut, C., Kimura, H., and Funabiki, H. (2010). Survivin reads phosphorylated histone H3 threonine 3 to activate the mitotic kinase Aurora B. Science (80-.). 330, 235–239.

Khodjakov, A., and Pines, J. (2010). Centromere tension: a divisive issue. Nat. Cell Biol. 12, 919–923.

Kim, S., and Yu, H. (2015). Multiple assembly mechanisms anchor the KMN spindle checkpoint platform at human mitotic kinetochores. J. Cell Biol. 208, 181–196.

Kirschner, M., and Mitchison, T. (1986). Beyond self-assembly: From microtubules to morphogenesis. Cell 45, 329–342.

Kitagawa, K., Masumoto, H., Ikeda, M., and Okazaki, T. (1995). Analysis of protein-DNA and protein-protein interactions of centromere protein B (CENP-B) and properties of the DNA-CENP-B complex in the cell cycle. Mol. Cell. Biol. 15, 1602–1612.

Kiyomitsu, T., Obuse, C., and Yanagida, M. (2007). Human Blinkin/AF15q14 is required for chromosome alignment and the mitotic checkpoint through direct interaction with Bub1 and BubR1. Dev. Cell 13, 663–676.

Klare, K., Weir, J.R., Basilico, F., Zimniak, T., Massimiliano, L., Ludwigs, N., Herzog, F., and Musacchio, A. (2015). CENP-C is a blueprint for constitutive centromere–associated network assembly within human kinetochores. J. Cell Biol. 210, 11–22.

Kline-Smith, S.L., Sandall, S., and Desai, A. (2005). Kinetochore–spindle microtubule interactions during mitosis. Curr. Opin. Cell Biol. 17, 35–46.

Kops, G.P.L., and Shah, J. (2012). Connecting up and clearing out: how kinetochore attachment silences the spindle assembly checkpoint. Chromosoma 121, 509–525.

Kops, G.J.P.L., Kim, Y., Weaver, B.A.A., Mao, Y., McLeod, I., Yates, J.R., Tagaya, M., and Cleveland, D.W. (2005a). ZW10 links mitotic checkpoint signaling to the structural kinetochore. J. Cell Biol. 169, 49–60.

Kops, G.J.P.L., Weaver, B.A.A., and Cleveland, D.W. (2005b). On the road to cancer: aneuploidy and the mitotic checkpoint. Nat Rev Cancer 5, 773–785.

Krenn, V., and Musacchio, A. (2015). The Aurora B Kinase in Chromosome Bi-Orientation and Spindle Checkpoint Signaling. Front. Oncol. 5.

Lampson, M.A., and Cheeseman, I.M. (2011). Sensing centromere tension: Aurora B and the regulation of kinetochore function. Trends Cell Biol. 21, 133–140.

Lara-Gonzalez, P., Westhorpe, F.G., and Taylor, S.S. (2012). The Spindle Assembly Checkpoint. Curr. Biol. 22, R966–R980.

Li, X., and Nicklas, R.B. (1995). Mitotic forces control a cell-cycle checkpoint. Nature 373, 630–632.

Lindqvist, A., Rodríguez-Bravo, V., and Medema, R.H. (2009). The decision to enter mitosis: feedback and redundancy in the mitotic entry network. J. Cell Biol. 185 , 193–202.

Liu, D., Vader, G., Vromans, M.J.M., Lampson, M.A., and Lens, S.M.A. (2009). Sensing Chromosome Bi-Orientation by Spatial Separation of Aurora B Kinase from Kinetochore Substrates. Science (80-.). 323, 1350–1353.

Liu, S.-T., Rattner, J.B., Jablonski, S.A., and Yen, T.J. (2006). Mapping the assembly pathways that specify formation of the trilaminar kinetochore plates in human cells. J. Cell Biol. 175, 41–53.

London, N., and Biggins, S. (2014). Signalling dynamics in the spindle checkpoint response. Nat. Rev. Mol. Cell Biol. 15, 736–748.

London, N., Ceto, S., Ranish, J.A., and Biggins, S. (2012). Phosphoregulation of Spc105 by Mps1 and PP1 regulates Bub1 localization to kinetochores. Curr. Biol. 22, 900–906.

Lusk, C.P., Waller, D.D., Makhnevych, T., Dienemann, A., Whiteway, M., Thomas, D.Y., and Wozniak, R.W. (2007). Nup53p is a target of two mitotic kinases, Cdk1p and Hrr25p. Traffic 8, 647–660.

Magidson, V., O'Connell, C.B., Lončarek, J., Paul, R., Mogilner, A., and Khodjakov, A. (2011). The spatial arrangement of chromosomes during prometaphase facilitates spindle assembly. Cell 146, 555–567.

Magidson, V., He, J., Ault, J.G., O'Connell, C.B., Yang, N., Tikhonenko, I., McEwen, B.F., Sui, H., and Khodjakov, A. (2016). Unattached kinetochores rather than intrakinetochore tension arrest mitosis in taxol-treated cells. J. Cell Biol. 212, 307–319.

Maiato, H., DeLuca, J., Salmon, E.D., and Earnshaw, W.C. (2004). The dynamic kinetochore-microtubule interface. J. Cell Sci. 117, 5461–5477.

Maresca, T.J., and Salmon, E.D. (2009). Intrakinetochore stretch is associated with changes in kinetochore phosphorylation and spindle assembly checkpoint activity. J. Cell Biol. 184, 373–381.

Maresca, T.J., and Salmon, E.D. (2010). Welcome to a new kind of tension: translating kinetochore mechanics into a wait-anaphase signal. J. Cell Sci. 123, 825–835.

Marshall, O.J., Chueh, A.C., Wong, L.H., and Choo, K.H.A. (2008). Neocentromeres: new insights into centromere structure, disease development, and karyotype evolution. Am. J. Hum. Genet. 82, 261–282.

Maure, J.-F., Komoto, S., Oku, Y., Mino, A., Pasqualato, S., Natsume, K., Clayton, L., Musacchio, A., and Tanaka, T.U. (2011). The Ndc80 loop region facilitates formation of kinetochore attachment to the dynamic microtubule plus end. Curr. Biol. 21, 207–213.

Mayer, T.U., Kapoor, T.M., Haggarty, S.J., King, R.W., Schreiber, S.L., and Mitchison, T.J. (1999). Small Molecule Inhibitor of Mitotic Spindle Bipolarity Identified in a Phenotype-Based Screen. Science (80-.). 286, 971–974.

McCleland, M.L., Kallio, M.J., Barrett-Wilt, G.A., Kestner, C.A., Shabanowitz, J., Hunt, D.F., Gorbsky, G.J., and Stukenberg, P.T. (2004). The vertebrate Ndc80 complex contains Spc24 and Spc25 homologs, which are required to establish and maintain kinetochore-microtubule attachment. Curr. Biol. 14, 131–137.

McEwen, B.F., and Dong, Y. (2009). Releasing the spindle assembly checkpoint without tension. J. Cell Biol. 184, 355–356.

McKinley, K.L., and Cheeseman, I.M. (2016). The molecular basis for centromere identity and function. Nat Rev Mol Cell Biol 17, 16–29.

Miller, S.A., Johnson, M.L., and Stukenberg, P.T. (2008). Kinetochore attachments require an interaction between unstructured tails on microtubules and Ndc80 Hec1. Curr. Biol. 18, 1785–1791.

Mitchison, T.J., Maddox, P., Gaetz, J., Groen, A., Shirasu, M., Desai, A., Salmon, E.D., and Kapoor, T.M. (2005). Roles of polymerization dynamics, opposed motors, and a tensile element in governing the length of Xenopus extract meiotic spindles. Mol. Biol. Cell 16, 3064–3076.

Murray, A.W., Solomon, M.J., and Kirschner, M.W. (1989). The role of cyclin synthesis and degradation in the control of maturation promoting factor activity. Nature 339, 280–286.

Musacchio, A. (2011). Spindle assembly checkpoint: the third decade. Philos. Trans. R. Soc. London B Biol. Sci. 366, 3595–3604.

Musacchio, A., and Salmon, E.D. (2007). The spindle-assembly checkpoint in space and time. Nat. Rev. Mol. Cell Biol. 8, 379–393.

Nasmyth, K. (2001). Disseminating the genome: joining, resolving, and separating sister chromatids during mitosis and meiosis. Annu. Rev. Genet. 35, 673–745.

Nezi, L., and Musacchio, A. (2009). Sister chromatid tension and the spindle assembly checkpoint. Curr. Opin. Cell Biol. 21, 785–795.

Nicklas, R.B. (1988). The forces that move chromosomes in mitosis. Annu. Rev. Biophys. Biophys. Chem. 17, 431–449.

Nicklas, R.B. (1997). How cells get the right chromosomes. Science (80-.). 275, 632–637.

Nicklas, R.B., and Koch, C.A. (1969). CHROMOSOME MICROMANIPULATION: III. Spindle Fiber Tension and the Reorientation of Mal-Oriented Chromosomes. J. Cell Biol. 43, 40–50.

Nishi, H., Hashimoto, K., and Panchenko, A.R. (2011). Phosphorylation in protein-protein binding: effect on stability and function. Structure 19, 1807–1815.

Nogales, E., Wolf, S.G., and Downing, K.H. (1998). Structure of the [alpha][beta] tubulin dimer by electron crystallography. Nature 391, 199–203.

Nogales, E., Whittaker, M., Milligan, R.A., and Downing, K.H. (1999). High-Resolution Model of the Microtubule. Cell 96, 79–88.

Nousiainen, M., Silljé, H.H.W., Sauer, G., Nigg, E.A., and Körner, R. (2006). Phosphoproteome analysis of the human mitotic spindle. Proc. Natl. Acad. Sci. 103, 5391–5396.

Nurse, P. (1990). Universal control mechanism regulating onset of M-phase. Nature 344, 503–508.

O'Connell, C.B., Lončarek, J., Hergert, P., Kourtidis, A., Conklin, D.S., and Khodjakov, A. (2008). The spindle assembly checkpoint is satisfied in the absence of interkinetochore tension during mitosis with unreplicated genomes. J. Cell Biol. 183, 29–36.

O'Connell, C.B., Khodjakov, A., and McEwen, B.F. (2012). Kinetochore flexibility: creating a dynamic chromosome–spindle interface. Curr. Opin. Cell Biol. 24, 40–47.

Ogo, N., Oishi, S., Matsuno, K., Sawada, J., Fujii, N., and Asai, A. (2007). Synthesis and biological evaluation of l-cysteine derivatives as mitotic kinesin Eg5 inhibitors. Bioorg. Med. Chem. Lett. 17, 3921–3924.

Olsen, J. V, Blagoev, B., Gnad, F., Macek, B., Kumar, C., Mortensen, P., and Mann, M. (2006). Global, in vivo, and site-specific phosphorylation dynamics in signaling networks. Cell 127, 635–648.

Onn, I., Heidinger-Pauli, J.M., Guacci, V., Ünal, E., and Koshland, D.E. (2008). Sister chromatid cohesion: a simple concept with a complex reality. Annu. Rev. Cell Dev. Biol. 24, 105–129.

Park, J.E., Song, H., Kwon, H.J., and Jang, C.-Y. (2016). Ska1 cooperates with DDA3 for spindle dynamics and spindle attachment to kinetochore. Biochem. Biophys. Res. Commun.

Paul, R., Wollman, R., Silkworth, W.T., Nardi, I.K., Cimini, D., and Mogilner, A. (2009). Computer simulations predict that chromosome movements and rotations accelerate mitotic spindle assembly without compromising accuracy. Proc. Natl. Acad. Sci. 106, 15708–15713.

Pereira, G., and Schiebel, E. (2003). Separase regulates INCENP-Aurora B anaphase spindle function through Cdc14. Science (80-.). 302, 2120–2124.

Peter, M., Nakagawa, J., Doree, M., Labbe, J.C., and Nigg, E.A. (1990). In vitro disassembly of the nuclear lamina and M phase-specific phosphorylation of lamins by cdc2 kinase. Cell 61, 591–602.

Peters, J.-M. (2006). The anaphase promoting complex/cyclosome: a machine designed to destroy. Nat. Rev. Mol. Cell Biol. 7, 644–656.

Pinsky, B.A., Kung, C., Shokat, K.M., and Biggins, S. (2006). The Ipl1-Aurora protein kinase activates the spindle checkpoint by creating unattached kinetochores. Nat. Cell Biol. 8, 78–83.

Pinsky, B.A., Nelson, C.R., and Biggins, S. (2009). Protein phosphatase 1 regulates exit from the spindle checkpoint in budding yeast. Curr. Biol. 19, 1182–1187.

Porter, L.A., and Donoghue, D.J. (2003). Cyclin B1 and CDK1: nuclear localization and upstream regulators. Prog. CELL CYCLE Res. 5, 335–348.

Powers, A.F., Franck, A.D., Gestaut, D.R., Cooper, J., Gracyzk, B., Wei, R.R., Wordeman, L., Davis, T.N., and Asbury, C.L. (2009). The Ndc80 kinetochore complex forms load-bearing attachments to dynamic microtubule tips via biased diffusion. Cell 136, 865–875.

Primorac, I., and Musacchio, A. (2013). Panta rhei: the APC/C at steady state. J. Cell Biol. 201, 177–189.

Przewloka, M.R., and Glover, D.M. (2009). The kinetochore and the centromere: a working long distance relationship. Annu. Rev. Genet. 43, 439–465.

Pufall, M.A., Lee, G.M., Nelson, M.L., Kang, H.-S., Velyvis, A., Kay, L.E., McIntosh, L.P., and Graves, B.J. (2005). Variable control of Ets-1 DNA binding by multiple phosphates in an unstructured region. Science (80-.). 309, 142–145.

Rieder, C.L., and Salmon, E.D. (1994). Motile kinetochores and polar ejection forces dictate chromosome position on the vertebrate mitotic spindle. J. Cell Biol. 124 , 223–233.

Rieder, C.L., Cole, R.W., Khodjakov, A., and Sluder, G. (1995). The checkpoint delaying anaphase in response to chromosome monoorientation is mediated by an inhibitory signal produced by unattached kinetochores. J. Cell Biol. 130, 941–948.

Rosenberg, J.S., Cross, F.R., and Funabiki, H. (2011). KNL1/Spc105 recruits PP1 to silence the spindle assembly checkpoint. Curr. Biol. 21, 942–947.

Sacristan, C., and Kops, G.J.P.L. (2015). Joined at the hip: kinetochores, microtubules, and spindle assembly checkpoint signaling. Trends Cell Biol. 25, 21–28.

Salazar, C., and Höfer, T. (2003). Allosteric regulation of the transcription factor NFAT1 by multiple phosphorylation sites: a mathematical analysis. J. Mol. Biol. 327, 31–45.

Santaguida, S., and Musacchio, A. (2009). The life and miracles of kinetochores. EMBO J. 28, 2511–2531.

Santaguida, S., Tighe, A., D'Alise, A.M., Taylor, S.S., and Musacchio, A. (2010). Dissecting the role of MPS1 in chromosome biorientation and the spindle checkpoint through the small molecule inhibitor reversine. J. Cell Biol. 190, 73–87.

Santaguida, S., Vernieri, C., Villa, F., Ciliberto, A., and Musacchio, A. (2011). Evidence that Aurora B is implicated in spindle checkpoint signalling independently of error correction. EMBO J. 30, 1508–1519.

Sarangapani, K.K., and Asbury, C.L. (2014). Catch and release: how do kinetochores hook the right microtubules during mitosis? Trends Genet. 30, 150–159.

Sarangapani, K.K., Akiyoshi, B., Duggan, N.M., Biggins, S., and Asbury, C.L. (2013). Phosphoregulation promotes release of kinetochores from dynamic microtubules via multiple mechanisms. Proc. Natl. Acad. Sci. 110, 7282–7287.

Schleiffer, A., Maier, M., Litos, G., Lampert, F., Hornung, P., Mechtler, K., and Westermann, S. (2012). CENP-T proteins are conserved centromere receptors of the Ndc80 complex. Nat. Cell Biol. 14, 604–613.

Schüller, R., Forné, I., Straub, T., Schreieck, A., Texier, Y., Shah, N., Decker, T.-M., Cramer, P., Imhof, A., and Eick, D. (2016). Heptad-Specific Phosphorylation of RNA Polymerase II CTD. Mol. Cell 61, 305–314.

Screpanti, E., De Antoni, A., Alushin, G.M., Petrovic, A., Melis, T., Nogales, E., and Musacchio, A. (2011). Direct binding of Cenp-C to the Mis12 complex joins the inner and outer kinetochore. Curr. Biol. 21, 391–398.

Shepperd, L.A., Meadows, J.C., Sochaj, A.M., Lancaster, T.C., Zou, J., Buttrick, G.J., Rappsilber, J., Hardwick, K.G., and Millar, J.B.A. (2012). Phosphodependent recruitment of Bub1 and Bub3 to Spc7/KNL1 by Mph1 kinase maintains the spindle checkpoint. Curr. Biol. 22, 891–899.

Silió, V., McAinsh, A.D., and Millar, J.B. (2015). KNL1-Bubs and RZZ Provide Two Separable Pathways for Checkpoint Activation at Human Kinetochores. Dev. Cell 35, 600–613.

Skibbens, R. V, Skeen, V.P., and Salmon, E.D. (1993). Directional instability of kinetochore motility during chromosome congression and segregation in mitotic newt lung cells: a push-pull mechanism. J. Cell Biol. 122, 859–875.

Sonoda, E., Matsusaka, T., Morrison, C., Vagnarelli, P., Hoshi, O., Ushiki, T., Nojima, K., Fukagawa, T., Waizenegger, I.C., and Peters, J.-M. (2001).

Scc1/Rad21/Mcd1 is required for sister chromatid cohesion and kinetochore function in vertebrate cells. Dev. Cell 1, 759–770.

Stukenberg, P.T., and Burke, D. (2015). Connecting the microtubule attachment status of each kinetochore to cell cycle arrest through the spindle assembly checkpoint. Chromosoma 1–18.

Stumpff, J., Von Dassow, G., Wagenbach, M., Asbury, C., and Wordeman, L. (2008). The kinesin-8 motor Kif18A suppresses kinetochore movements to control mitotic chromosome alignment. Dev. Cell 14, 252–262.

Stumpff, J., Wagenbach, M., Franck, A., Asbury, C.L., and Wordeman, L. (2012). Kif18A and chromokinesins confine centromere movements via microtubule growth suppression and spatial control of kinetochore tension. Dev. Cell 22, 1017–1029.

Sudakin, V., Ganoth, D., Dahan, A., Heller, H., Hershko, J., Luca, F.C., Ruderman, J. V, and Hershko, A. (1995). The cyclosome, a large complex containing cyclin-selective ubiquitin ligase activity, targets cyclins for destruction at the end of mitosis. Mol. Biol. Cell 6, 185–197.

Sudakin, V., Chan, G.K.T., and Yen, T.J. (2001). Checkpoint inhibition of the APC/C in HeLa cells is mediated by a complex of BUBR1, BUB3, CDC20, and MAD2. J. Cell Biol. 154, 925–936.

Suh, H., Ficarro, S.B., Kang, U.-B., Chun, Y., Marto, J.A., and Buratowski, S. (2016). Direct Analysis of Phosphorylation Sites on the Rpb1 C-Terminal Domain of RNA Polymerase II. Mol. Cell 61, 297–304.

Sullivan, M., and Morgan, D.O. (2007). Finishing mitosis, one step at a time. Nat. Rev. Mol. Cell Biol. 8, 894–903.

Sundin, L.J.R., and DeLuca, J.G. (2010). Kinetochores: NDC80 toes the line. Curr. Biol. 20, R1083–R1085.

Sundin, L.J.R., Guimaraes, G.J., and DeLuca, J.G. (2011). The NDC80 complex proteins Nuf2 and Hec1 make distinct contributions to kinetochore–microtubule attachment in mitosis. Mol. Biol. Cell 22, 759–768.

Suzuki, A., Hori, T., Nishino, T., Usukura, J., Miyagi, A., Morikawa, K., and Fukagawa, T. (2011). Spindle microtubules generate tension-dependent changes in the distribution of inner kinetochore proteins. J. Cell Biol. 193, 125–140.

Suzuki, A., Badger, B.L., Wan, X., DeLuca, J.G., and Salmon, E.D. (2014). The Architecture of CCAN Proteins Creates a Structural Integrity to Resist Spindle Forces and Achieve Proper Intrakinetochore Stretch. Dev. Cell 30, 717–730.

Suzuki, A., Badger, B.L., and Salmon, E.D. (2015). A quantitative description of Ndc80 complex linkage to human kinetochores. Nat Commun 6.

Tachiwana, H., Müller, S., Blümer, J., Klare, K., Musacchio, A., and Almouzni, G. (2015). HJURP Involvement in De Novo CenH3 CENP-A and CENP-C Recruitment. Cell Rep. 11, 22–32.

Tanaka, T.U., Rachidi, N., Janke, C., Pereira, G., Galova, M., Schiebel, E., Stark, M.J.R., and Nasmyth, K. (2002). Evidence that the Ipl1-Sli15 (Aurora kinase-INCENP) complex promotes chromosome bi-orientation by altering kinetochore-spindle pole connections. Cell 108, 317–329.

Tauchman, E.C., Boehm, F.J., and DeLuca, J.G. (2015). Stable kinetochore-microtubule attachment is sufficient to silence the spindle assembly checkpoint in human cells. Nat Commun 6.

Toledo, C.M., Herman, J.A., Olsen, J.B., Ding, Y., Corrin, P., Girard, E.J., Olson, J.M., Emili, A., DeLuca, J.G., and Paddison, P.J. (2014). BuGZ is required for Bub3 stability, Bub1 kinetochore function, and chromosome alignment. Dev. Cell 28, 282–294.

Tooley, J.G., Miller, S.A., and Stukenberg, P.T. (2011). The Ndc80 complex uses a tripartite attachment point to couple microtubule depolymerization to chromosome movement. Mol. Biol. Cell 22, 1217–1226.

Uchida, K.S.K., Takagaki, K., Kumada, K., Hirayama, Y., Noda, T., and Hirota, T. (2009). Kinetochore stretching inactivates the spindle assembly checkpoint. J. Cell Biol. 184, 383–390.

van der Waal, M.S., Saurin, A.T., Vromans, M.J.M., Vleugel, M., Wurzenberger, C., Gerlich, D.W., Medema, R.H., Kops, G.J.P.L., and Lens, S.M.A. (2012). Mps1 promotes rapid centromere accumulation of Aurora B. EMBO Rep. 13, 847–854.

Wan, X., O'Quinn, R.P., Pierce, H.L., Joglekar, A.P., Gall, W.E., DeLuca, J.G., Carroll, C.W., Liu, S.-T., Yen, T.J., McEwen, B.F., et al. (2009). Protein Architecture of the Human Kinetochore Microtubule Attachment Site. Cell 137, 672–684.

Wan, X., Cimini, D., Cameron, L.A., and Salmon, E.D. (2012). The coupling between sister kinetochore directional instability and oscillations in centromere stretch in metaphase PtK1 cells. Mol. Biol. Cell 23, 1035–1046.

Wang, F., Ulyanova, N.P., van der Waal, M.S., Patnaik, D., Lens, S.M.A., and Higgins, J.M.G. (2011). A positive feedback loop involving Haspin and Aurora B promotes CPC accumulation at centromeres in mitosis. Curr. Biol. 21, 1061–1069.

Wang, H.-W., Long, S., Ciferri, C., Westermann, S., Drubin, D., Barnes, G., and Nogales, E. (2008). Architecture and flexibility of the yeast Ndc80 kinetochore complex. J. Mol. Biol. 383, 894–903.

Waters, J.C., Skibbens, R. V, and Salmon, E.D. (1996). Oscillating mitotic newt lung cell kinetochores are, on average, under tension and rarely push. J. Cell Sci. 109, 2823–2831.

Waters, J.C., Chen, R.-H., Murray, A.W., and Salmon, E.D. (1998). Localization of Mad2 to Kinetochores Depends on Microtubule Attachment, Not Tension. J. Cell Biol. 141, 1181–1191.

Wei, R.R., Sorger, P.K., and Harrison, S.C. (2005). Molecular organization of the Ndc80 complex, an essential kinetochore component. Proc. Natl. Acad. Sci. U. S. A. 102, 5363–5367.

Wei, R.R., Schnell, J.R., Larsen, N.A., Sorger, P.K., Chou, J.J., and Harrison, S.C. (2006). Structure of a central component of the yeast kinetochore: the Spc24p/Spc25p globular domain. Structure 14, 1003–1009.

Welburn, J.P.I., Vleugel, M., Liu, D., Yates Iii, J.R., Lampson, M.A., Fukagawa, T., and Cheeseman, I.M. (2010). Aurora B Phosphorylates Spatially Distinct Targets to Differentially Regulate the Kinetochore-Microtubule Interface. Mol. Cell 38, 383–392.

Westhorpe, F.G., and Straight, A.F. (2013). Functions of the centromere and kinetochore in chromosome segregation. Curr. Opin. Cell Biol. 25, 334–340.

Wickham, H. (2014). Tidy Data. J. Stat. Softw. 59.

Wieser, S., and Pines, J. (2015). The biochemistry of mitosis. Cold Spring Harb. Perspect. Biol. a015776.

Wilson-Kubalek, E.M., Cheeseman, I.M., Yoshioka, C., Desai, A., and Milligan, R.A. (2008). Orientation and structure of the Ndc80 complex on the microtubule lattice. J. Cell Biol. 182, 1055–1061.

Yamagishi, Y., Honda, T., Tanno, Y., and Watanabe, Y. (2010). Two histone marks establish the inner centromere and chromosome bi-orientation. Science (80-.). 330, 239–243.

Yamagishi, Y., Yang, C.-H., Tanno, Y., and Watanabe, Y. (2012). MPS1/Mph1 phosphorylates the kinetochore protein KNL1/Spc7 to recruit SAC components. Nat. Cell Biol. 14, 746–752.

Zaytsev, A. V, Sundin, L.J.R., DeLuca, K.F., Grishchuk, E.L., and DeLuca, J.G. (2014). Accurate phosphoregulation of kinetochore–microtubule affinity requires unconstrained molecular interactions. J. Cell Biol. 206, 45–59.

Zhai, Y., Kronebusch, P.J., and Borisy, G.G. (1995). Kinetochore microtubule dynamics and the metaphase-anaphase transition. J. Cell Biol. 131, 721–734.

Zhang, G., Lischetti, T., Hayward, D.G., and Nilsson, J. (2015). Distinct domains in Bub1 localize RZZ and BubR1 to kinetochores to regulate the checkpoint. Nat. Commun. 6.

(2015). R Core Team. R: A Language and Enviroment for Statistical Computing. Vienna, Austria R Found. Stat. Comput. http//www.R-Project.org.

List of Abbreviations

ABK: Aurora B Kinase

APC/C: Anaphase Promoting Complex/Cyclosome

BUB1/3: Budding Uninhibited in Benzimidazole 1/3

BUBR1: Budding Uninhibited in Benzimidazole 1 Homolog Beta (BUB1B)

CCAN: Constitutive Centromere Associated Network

CDC20: Cell Division Cycle 20

CDK1: Cyclin Dependent Kinase

CENP: Centromere Protein

CPC: Chromosomal Passenger Complex

H2A: Histone H2A

H3: Histone H3

Hec1: Highly Expressed in Cancer

HJURP: Holiday Junction Recognition Protein

INCENP: Inner Centromere Protein

KMN: KNL1-MIS12-NDC80

KNL1: Kinetochore Null 1

K-MT: Kinetochore-Microtubule

Mad1/2: Mitotic Arrest Deficient

MCAK: Mitotic Centromere-Associated Kinesin

MPS1: Monopolar Spindle 1

PEF: Polar Ejection Force

PP1/2A: Protein Phosphatase 1/2A

ROD1: Resistance to o-dinitrobenzene Protein 1

RZZ: ROD1-ZW10-Zwint1

SAC: Spindle Assembly Checkpoint

SCC1/3: Sister Chromatid Cohesion Protein 1/3

SGO1: Shugoshin1

SKA: Spindle and Kinetochore Associated Protein 1

SMC1/3: Structural Maintenance of Chromosomes Protein 1/3

Spc24/25: Kinetochore Protein Species 24/25